Technische Universität München
Fakultät für Chemie

NEDD8 orchestrates active ubiquitylation assembly of cullin-RING E3 ligase

Kheewoong Baek

Vollständiger Abdruck der von der Fakultät für Chemie der Technischen Universität München zur Erlangung des akademischen Grades eines

Doktors der Naturwissenschaften (Dr. rer. nat.)

genehmigten Dissertation.

Vorsitzender: Prof. Dr. Matthias Feige

PrüferInnen der Dissertation:

1. Hon.-Prof. Brenda Schulman, Ph.D
2. Prof. Dr. Michael Sattler
3. Prof. Gary Kleiger, Ph.D

Die Dissertation wurde am 30.05.2022 an der Technischen Universität München eingereicht und durch die Fakultät für Chemie am 26.09.2022 angenommen.

Contents

List of Publications

1) Sebastian Kostrhon, J Rajan Prabu, **Kheewoong Baek**, Daniel Horn-Ghetko, Susanne von Gronau, Maren Klügel, Jérôme Basquin Arno F Alpi, Brenda A Schulman. **CUL5-ARIH2 E3-E3 ubiquitin ligase structure reveals cullin-specific NEDD8 activation**. *Nature Chemical Biology*, DOI: 10.1038/s41589-021-00858-8, 2021

2) **Kheewoong Baek**, Daniel C Scott, Brenda A Schulman. **NEDD8 and ubiquitin ligation by cullin-RING E3 ligases.** *Current Opinion in Structural Biology*, DOI: 10.1016/j.sbi.2020.10.007, 2021

3) Michael Heider, Ruth Eichner, Jacob Stroh, Volker Morath, Anna Kuisl, Jana Zecha, Jannis Lawatscheck, **Kheewoong Baek**, Anne-Kathrin Garz, Martina Rudelius, Friedrich-Christian Deuschle, Ulrich Keller, Simone Lemeer, Mareike Verbeek, Katharina S Götze, Arne Skerra, Wolfgang A Weber, Johannes Buchner, Brenda A Schulman, Bernhard Kuster, Vanesa Fernández-Sáiz, Florian Bassermann. **The IMiD target CRBN determines HSP90 activity toward transmembrane proteins essential in multiple myeloma.** *Molecular Cell*, DOI: 10.1016/j.molcel.2020.12.046, 2021

4) Daniel Horn-Ghetko, David T Krist, J Rajan Prabu, **Kheewoong Baek**, Monique P C Mulder, Maren Klügel, Daniel C Scott, Huib Ovaa, Gary Kleiger, Brenda A Schulman. **Ubiquitin ligation to F-box protein targets by SCF-RBR E3-E3 super-assembly**. *Nature*, DOI: 10.1038/s41586-021-03197-9, 2021

5) Donghyuk Shin, Rukmini Mukherjee, Diana Grewe, Denisa Bojkova, **Kheewoong Baek**, Anshu Bhattacharya, Laura Schulz, Marek Widera, Ahmad Reza Mehdipour, Georg Tascher, Paul P Geurink, Alexander Wilhelm, Gerbrand J van der Heden van Noort, Huib Ovaa, Stefan Müller, Klaus-Peter Knobeloch, Krishnaraj Rajalingam, Brenda A Schulman, Jindrich Cinatl, Gerhard Hummer, Sandra Ciesek, Ivan Dikic. **Papain-like protease regulates SARS-CoV-2 viral spread and innate immunity.** *Nature*, DOI: 10.1038/s41586-020-2601-5, 2020

6) **Kheewoong Baek**, David T. Krist, J. Rajan Prabu, Spencer Hill, Maren Klügel, Lisa-Marie Neumaier, Susanne von Gronau, Gary Kleiger, Brenda A. Schulman. **NEDD8 Nucleates a Multivalent cullin-RING-UBE2D Ubiquitin Ligation Assembly.** *Nature,* DOI: 10.1038/s41586-020-2000-y, 2020
*Thesis contains work from this published paper.

7) **Kheewoong Baek**, Brenda A. Schulman. **Molecular Glue Concept Solidifies**. *Nature Chemical Biology,* DOI: 10.1038/s41589-019-0414-3, 2020

8) Ruth Hüttenhain, Jiewei Xu, Lily A. Burton, David E. Gordon, Judd F. Hultquist, Jeffrey R. Johnson, Laura Satkamp, Joseph Hiatt, David Y. Rhee, **Kheewoong Baek**, David C. Crosby, Alan D. Frankel, Alexander Marson, J. Wade Harper, Arno F. Alpi, Brenda A. Schulman, John D. Gross, Nevan J. Krogan. **ARIH2 Is a Vif-Dependent Regulator of CUL5-Mediated APOBEC3G Degradation in HIV Infection.** *Cell Host & Microbe*, DOI: 10.1016/j.chom.2019.05.008, 2019

9) Jin-Gu Lee, **Kheewoong Baek**, Nia Soetandyo, Yihong Ye. **Reversible inactivation of deubiquitinases by reactive oxygen species in vitro and in cells.** *Nature Communications,* 4:1568, doi: 10.1038/ncomms2532, 2013

10) Qiuyan Wang, Yanfen Liu, Nia Soetandyo, **Kheewoong Baek**, Ramanujan Hegde, Yihong Ye. **A ubiquitin ligase-associated chaperone holdase maintains polypeptides in soluble states for proteosomal degradation.** *Molecular Cell*, 42(6):758-7 70, 2011

Summary

Virtually all eukaryotic processes are regulated by cullin-RING E3 ligase (CRL)-catalyzed protein ubiquitylation, which is exquisitely controlled by cullin modification with the ubiquitin (UB)-like protein NEDD8. However, how CRLs catalyze ubiquitylation, and how this is activated by NEDD8 remain unknown. Here, we elucidate the structural mechanism of neddylated CRL mediated ubiquitylation in action. By the cryo-electron microscopy structure of a chemically-trapped complex representing the ubiquitylation intermediate in which the neddylated CRL1 β-TRCP promotes ubiquitin transfer from the ubiquitin-carrying enzyme UBE2D to its recruited substrate phosphorylated IκBα. The structure reveals that NEDD8 acts as a nexus binding disparate cullin elements along with the RING-activated ubiquitin-linked UBE2D. Concomitant local structural remodeling and large-scale CRL domain movements converge to juxtapose the substrate and ubiquitylation active site for efficient ubiquitylation. The results explain how a distinctive UB-like protein alters the functions of its targets, and show how numerous NEDD8-dependent interprotein interactions and conformational changes synergistically establish a catalytic architecture that is both robust for rapid substrate ubiquitylation and fragile to enable ensuing cullin-RING functions.

ZUMSAMMENFASSUNG

Praktisch alle eukaryotischen Prozesse werden durch die von Cullin-RING-E3-Ligase (CRL) katalysierte Ubiquitinierung von Proteinen reguliert, die durch die Modifikation des Cullins mit dem Ubiquitin (UB)-ähnlichen Protein NEDD8 genauestens kontrolliert wird. Wie CRLs die Ubiquitinierung katalysieren und wie diese durch NEDD8 aktiviert wird, ist jedoch noch unbekannt. Hier erläutern wir den strukturellen Mechanismus der durch neddylierte CRLs vermittelten Ubiquitinierung. Die Kryo-Elektronenmikroskopie-Struktur eines chemisch stabilisierten Komplexes, der den Ubiquitinierungszwischenschritt zeigt, in welchem der neddylierte CRL1 b-TRCP Komplex den Transfer des Ubiquitins von dem Ubiquitin-tragenden Enzym UBE2D auf sein rekrutiertes Substrat, phosphoryliertes IkBa, voranbringt. Die Struktur zeigt, dass NEDD8 als Nexus fungiert, der verschiedene Cullin-Elemente und das RING-aktivierte Ubiquitin-konjugierte UBE2D verbindet. Zeitgleiche lokale strukturelle Umgestaltung und signifikante Verschiebung von CRL-Domänen führen dazu, dass das Substrat und das aktive Zentrum in räumliche Nähe gebracht werden, was eine effiziente Ubiquitinierung erlaubt. Die Ergebnisse erklären, wie ein einzigartiges UB-ähnliches Protein die Funktionen seiner Ziele verändert und zeigen, wie zahlreiche NEDD8-abhängige Protein-Protein-Interaktionen und Konformationsänderung synergetisch eine katalytische Architektur aufbauen, die robust genug ist, um eine schnelle Ubiquitinierung des Substrats zu ermöglichen, aber auch die notwendige Instabilität aufweist, um anschließenden Cullin-RING-Funktionen zu erlauben.

1 Introduction

1.1 Ubiquitylation

Ubiquitylation is a posttranslational modification by a 76 amino acid protein called Ubiquitin (UB) (Swatek and Komander, 2016). Ubiquitylation of a target substrate changes its fate ranging from most famously proteasomal degradation, to changes in protein-protein interactions, assembly and disassembly of complexes, protein trafficking and localization, conformational changes etc (Kirkin and Dikic, 2007).

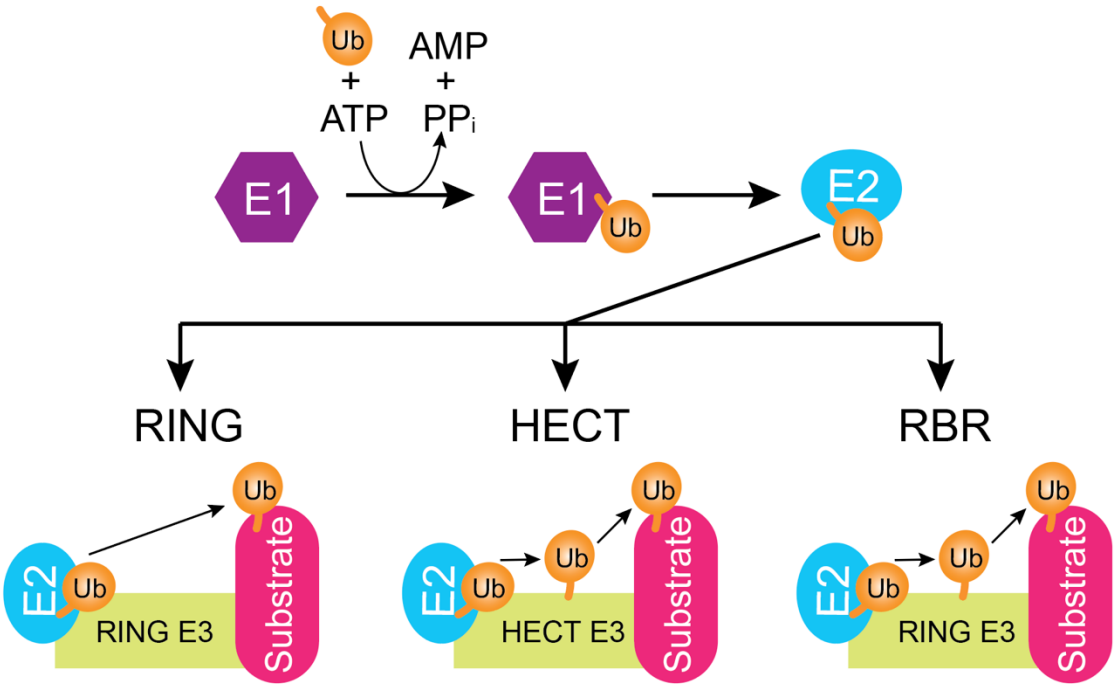

Figure 1.1: The Ubiquitin Cascade.
Ubiquitylation is mediated by series of enzymes E1, E2, and E3 for substrate modification. Ubiquitin E3 ligases are classified into three major families, RING, HECT, and RBR.

This process occurs in a highly regulated manner involving a cascade of enzymes which include the ubiquitin activating enzyme (E1), ubiquitin conjugating enzymes (E2), and ubiquitin ligases (E3) (Cappadocia and Lima, 2018). First, the ubiquitin activating enzyme activates ubiquitin with ATP by adenylating its C-terminus which then forms a thioester bond

between the E1's catalytic cysteine and ubiquitin's C-terminus. The E1 activating enzyme then recruits an E2 conjugating enzyme to transfer its bound ubiquitin to the E2 catalytic cysteine via a transthiolation reaction. Then, the ubiquitin conjugated E2 interacts with an E3 ligase to ultimately modify a recruited substrate. In human, there are two E1s, dozens of E2s, and over 600 E3 ligases that modify thousands of substrates (**Figure 1.1**). Thus, the ubiquitin system is essentially involved in all cellular processes making it a system of great importance to understand.

Furthermore, much like ubiquitin, there are ubiquitin-like (UBL) proteins that very much follow a similar mechanism of modification, including SUMO, ATG12, FAT10, ISG15, UFM1, and NEDD8, which work with their own set of E1, E2, and E3 enzymes, further providing complexity to the system (**Figure 1.2**) (Cappadocia and Lima, 2018; Yau and Rape, 2016).

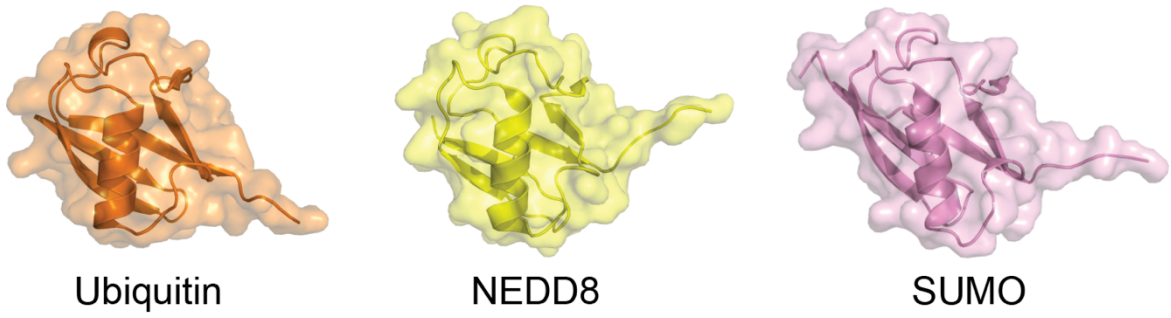

Figure 1.2: Ubiquitin and Ubiquitin-like proteins.
Structures of ubiquitin (shown in orange, PDB ID 1UBQ) and ubiquitin-like proteins NEDD8 (shown in yellow, PDB ID 4P5O) and SUMO (shown in pink, PDB ID 5JNE).

The interconnection of ubiquitin and ubiquitin-like proteins provide the ubiquitin system with infinite combinations and possibilities to create a complex code to modulate numerous cellular processes, which are governed by E3 ligases. Ubiquitin E3 ligases are categorized into three major classes by their functional mechanisms: RING, which recruits an E2~UB ('~' indicates thioester bond) in proximity to a recruited substrate, HECT, which transfers the ubiquitin from the E2~UB onto its own catalytic cysteine for further modification of substrate, and RBR, which is a hybrid of both RING and HECT, where it

harbors RING domains but also contains a catalytic cysteine, transferring ubiquitin from the E2 to its own catalytic cysteine for substrate modification just like HECTs (**Figure 1.1**). Among these E3 ligases, cullin-RING ligases(CRL) are the largest family of E3 ligases with over 250 family members in human, nearly accounting for ~50% of all E3 ligases (Buetow and Huang, 2016).

1.2 Architecture of a cullin-RING ligase

Cullin-RING ligases are modular, multiprotein assemblies that share similar architectural principles and regulatory mechanisms. A CRL comprises of a modular cullin(CUL) protein, a RING protein that forms an intermolecular β-sheet comprised of both the CUL and the N-terminus of an RBX protein in complex at its C-terminal region creating a C/R domain, and an interchangeable substrate adaptor/receptor complex that recruits substrate of interest (Bai et al., 1996; Hao et al., 2007; Schulman et al., 2000; Skowyra et al., 1997; Winston et al., 1999a). The modular cullin protein connects the recruited substrate of interest to catalytic machinery for ubiquitylation (**Figure 1.3**) (Zheng et al., 2002b). The vast size of the CRL family comes from 1) numerous cullins, including CUL1, 2, 3, 4A, 4B, 5, 7, 9, 2) form a complex with either RING proteins RBX1 or RBX2, 3) CUL1-5 are each known to associate interchangeably with numerous substrate-recruiting receptors. For example CUL1 binds to ~70 different human SKP1–F-box protein complexes and CUL4 binds to ~60 different DDB1-DCAF complexes, generating CRL family members denoted CRL1 F-box protein, CRL2/5 SOCS-box protein (CRL2 and CRL5 both utilize the substrate adaptor ElonginB/C complex and its bound SOCS-box protein for substrate recruitment), CRL3 BTB protein, and CRL4 DCAF protein, respectively (Jin et al., 2004; Lee and Zhou, 2007; Willems et al., 2004).

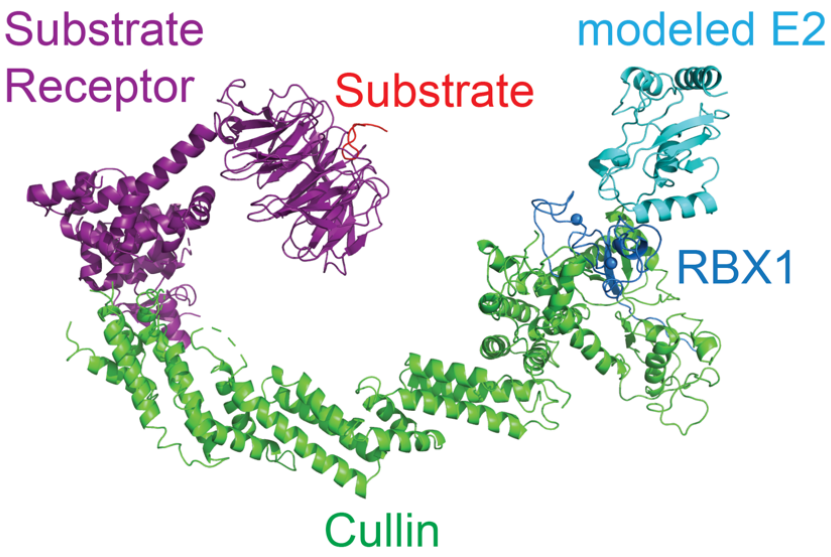

Figure 1.3: Cullin-RING ligase architecture.

A cullin-RING ligase is composed of a cullin scaffold (green), an intermolecular complex of a RING E3 RBX protein (blue), and a substrate receptor complex (purple and red). The RING protein recruits an E2 carrying enzyme (cyan), while the substrate receptor complex recruits substrates (red) to the cullin-RING ligase complex.

1.3 The cullin-RING ligase cycle

CRLs are intricately regulated by several components for accurate and timely ubiquitylation of target substrates (**Figure 1.4**). However, the cellular concentrations of cullins are much lower in comparison to the total amount of substrate receptors available. This discrepancy in the concentrations do not provide access to all substrate receptors simultaneously and limits the occupancy of a given substrate receptor at any given time. In order for the limited number of cullins to accommodate tens of hundreds of substrate receptors to ubiquitylate their thousands of substrates, cullins utilize a CRL assembly factor CAND1 to assemble and disassemble various substrate receptors on demand to its timely necessity. CAND1, originally discovered as an inhibitor of neddylation (Goldenberg et al., 2004; Liu et al., 2002; Zheng et al., 2002a; Zheng et al., 2002b), catalyzes the dissociation of F-box proteins from CUL1 by one million-fold into seconds, normally a complex that would be stable for days. CAND1's ability to provide access to all different substrate receptor complexes to the catalytic cullin-RING complex (Liu et al., 2018; Pierce et al., 2013; Reichermeier et al., 2020; Reitsma et al., 2017; Wu et al., 2013; Zemla et al., 2013).

CRLs are activated through the modification of the cullin itself by a ubiquitin like protein, NEDD8. NEDD8 is conjugated onto a conserved lysine of CRLs at its WHB domain by the E2s UBE2M/UBE2F and a co-E3 ligase DCN (Monda et al., 2013; Scott et al., 2011; Scott et al., 2010; Scott et al., 2014). Neddylation of a CRL is known to induce conformational flexibility and rearrangement of the RING domain of RBX proteins to allow more efficient ubiquitylation of its recruited substrates (Duda et al., 2008; Saha and Deshaies, 2008). Neddylation directly clashes with CAND1, blocking the process by which substrate receptors cycle off and onto a CRL complex and activates the complex for ubiquitylation (Pierce et al., 2013). However, in order for neddylation to occur, CAND1 needs to fall off a CRL prior to/during neddylation, and vice versa (Bornstein et al., 2006).

Once a neddylated CRL efficiently ubiquitylates a recruited substrate via ubiquitin carrying enzymes, which include the canonical UBE2D family E2s (Saha et al., 2011; Wu et al., 2010) or an RBR E3 ligase such as ARIH1/2 (Kelsall et al., 2013, Scott et al., 2016, Hüttenhain et al., 2019). Furthermore, CRLs work with ubiquitin chain forming E2 enzymes such as UBE2R or UBE2G1 to further create its ubiquitin mark for downstream

functionalities such as proteasomal degradation (Kleiger et al., 2009; Lu et al., 2018). When the substrates are marked for degradation, they are recruited to the proteasome for degradation. After the substrate falls off, a CRL gets deneddylated by the deneddylating enzyme CSN (COP9 Signalosome) (Bornstein et al., 2006; Cavadini et al., 2016; Cope et al., 2002; Enchev et al., 2012; Lyapina et al., 2001; Mosadeghi et al., 2016). A deneddylated/unneddylated CRL is now again available for either substrate receptor exchange via CAND1 (Liu et al., 2018; Pierce et al., 2013; Reichermeier et al., 2020; Reitsma et al., 2017) or again for neddylation/activation according to the cellular demand (Lydeard et al., 2013). This entire cycle involving numerous regulatory factors and processes was computationally modeled to occur all within ~90 seconds, which highlights the incredible speed in which cullin-RING ligases and its associated proteins function to mediate cellular processes (Liu et al., 2018).

Neddylated CRLs mediate vast regulation, accounting for ~20% of all ubiquitylation in human cells, controlling transcription, signaling, cell division, immunity, differentiation, development, and more (Soucy et al., 2009). Numerous diseases, including cancers, developmental disorders, and high blood pressure are caused by mutations in CRL subunits. Moreover, CRLs are often hijacked by pathogens during infections. Meanwhile, an inhibitor of neddylation, MLN4924 (Pevonedistat^{TM}) is in anti-cancer clinical trials, and also blocks HIV infectivity by incapacitating ubiquitylation needed by the retrovirus (Soucy et al., 2009; Stanley et al., 2012). CRLs are conserved across eukaryotes and play equally important roles in plants and other organisms. Furthermore, CRLs are one of the most popular platforms for drug discovery as they are used to target substrates that were previously considered undruggable via PROTACs (proteolysis targeting chimeras)(Bekes et al., 2022). Therefore, understanding the mechanism of cullin-RING ligases will aid in tackling numerous diseases.

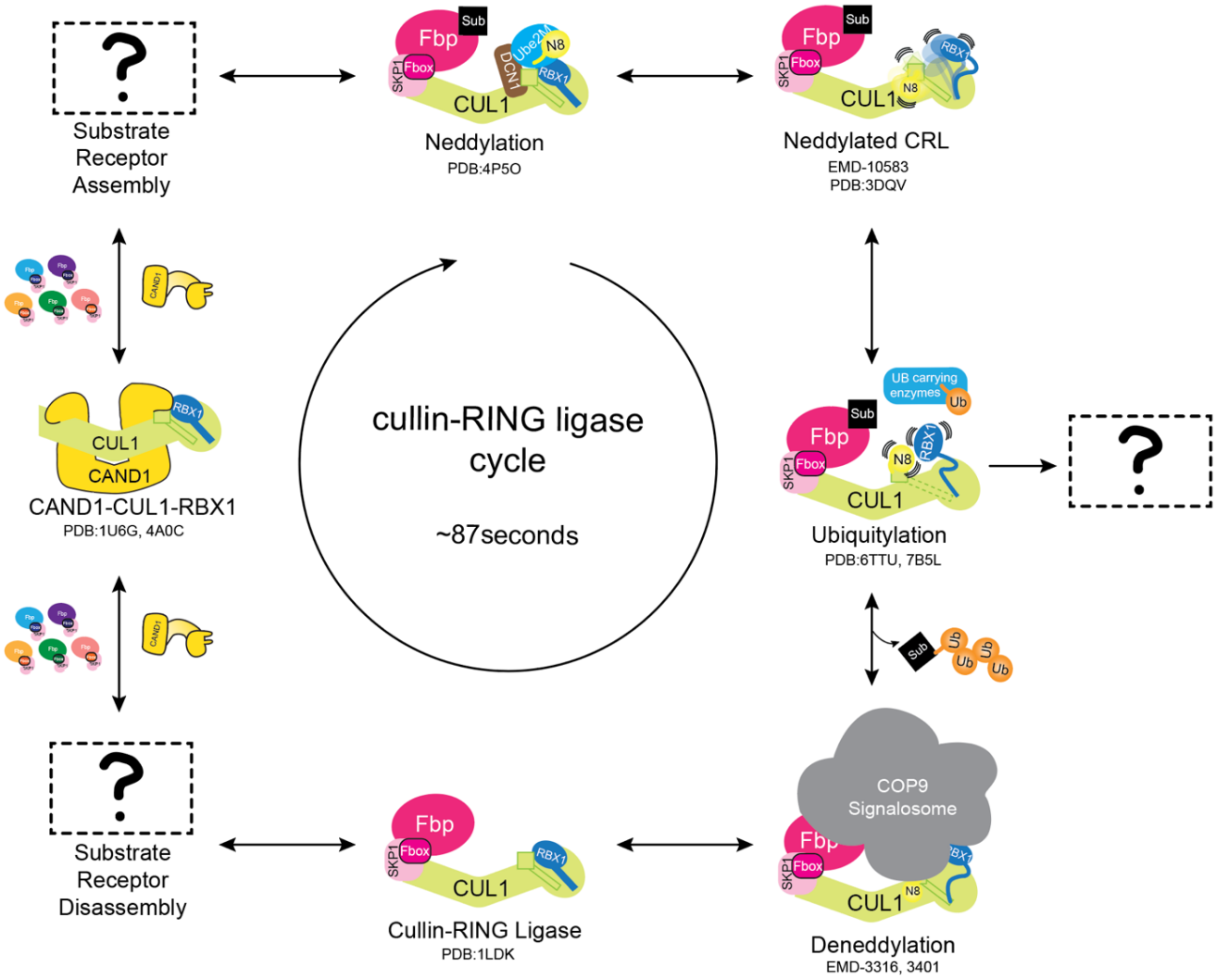

Figure 1.4: The Cullin-RING ligase cycle.

A cullin-RING ligase is tightly regulated by a series of neddylation, substrate ubiquitylation, deneddylation, and substrate receptor exchange that maintains a dynamic equilibrium according to the cellular demand. Structural, cellular, and biochemical studies on numerous parts of the cycle provide mechanistic insight, however several parts of the cycle lack structural information, most importantly including how a neddylated CRL targets substrates for ubiquitylation. Structural information of each step is noted on the bottom of each cartoon with its data codes.

1.4 Mechanism of Ubiquitin Ligation by RING E3s

RING domains themselves lack ubiquitin transferase activity. Rather, RING domains partner with other ubiquitin carrying enzymes, typically E2s, where the active site cysteine is linked to the C-terminus of ubiquitin or a UBL by a covalent but reactive thioester bond (~). Such E2~UB/UBL intermediates are relatively stable on their own and NMR studies provided an explanation to this: the E2 and UB/UBL are flexibly tethered about the thioester bond between them (Brzovic and Klevit, 2006; Brzovic et al., 2006). However, the capacity for UB/UBL to adopt infinitely different orientations relative to the E2 reduces the propensity of properly aligning the E2~UB/UBL active site. Numerous studies discovered that E3 ligase RING domains typically interact with their partner E2~UB/UBL intermediates into a distinct architecture referred to as the so-called 'closed conformation' (**Figure 1.5**) (Branigan et al., 2020; Dou et al., 2012a; Dou et al., 2012b, 2013; Plechanovova et al., 2012; Pruneda et al., 2012; Scott et al., 2014). The RING domain binds both E2 and its linked UB/UBL such that the otherwise flexible UB/UBL C-terminal tail folds and packs against the E2 domain, supported by major contacts between the UB/UBL's hydrophobic patch centered around its residue Ile44 and E2's long central helix. Typically, a RING linchpin residue inserted into the interface between the E2 and UB further stabilizes this 3-way interaction.

Furthermore, an E3 "non-RING priming element" may additionally buttress this activated RING-E2~UB/UBL conformation (Buetow et al., 2015; Dou et al., 2013; Wright et al., 2016). Thus, RING domains stimulate UB/UBL transfer from an E2 to a suitably placed nucleophilic acceptor, such as a lysine residue in a target substrate distally recruited via the E3's substrate receptor domain. In addition, many RING E3 ligases are multifunctional, interacting with various E2s (or other E3s) to modify distinct substrates, transfer ubiquitin or various UBLs, and/or separately initiate and elongate ubiquitin chain formation.

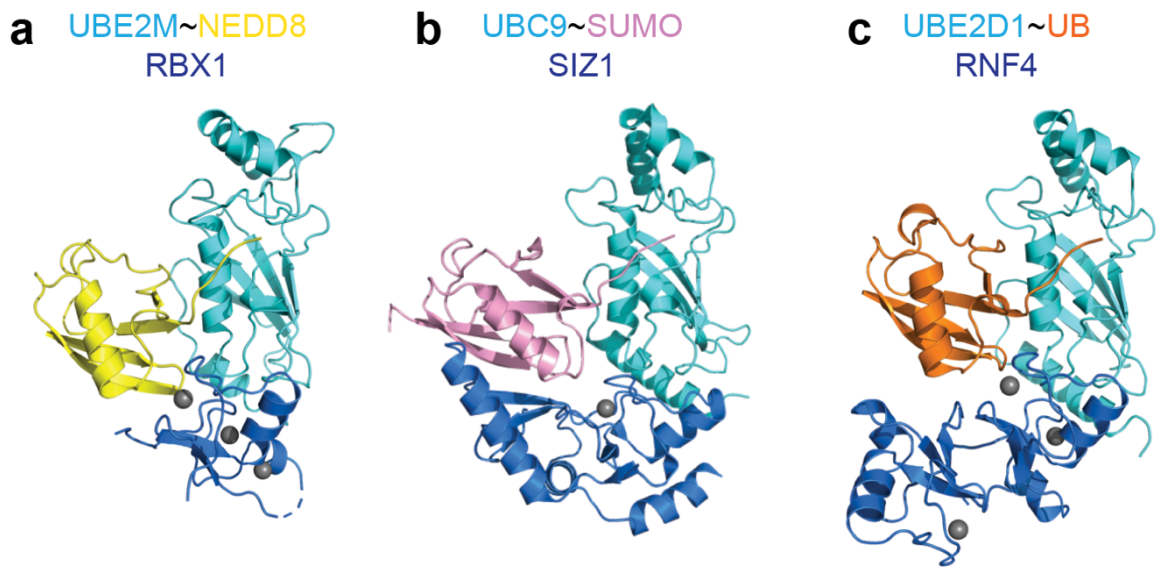

Figure 1.5: Closed conformation of E2~UB/UBL-RING.

a, Closed conformation of E2~UBL-RING shown by ubiquitin-like protein NEDD8, its cognate E2 UBE2M, and RING protein RBX1 (PDB ID 4P5O). **b,** Closed conformation of E2~UBL-RING shown by ubiquitin-like protein SUMO, its cognate E2 UBC9, and RING protein SIZ1 (PDB ID 5JNE). **c,** Closed conformation of E2~UB-RING shown by ubiquitin, E2 UBE2D1, and RING protein RNF4 (PDB ID 4AP4).

1.6 The 20 year mystery

While numerous studies have shed light on understanding of the CRL mechanism to establish the cullin-RING ligase cycle or individual parts of the catalytic components, the question still remains when considered in the context of an active ubiquitylation assembly: how can a recruited E2 carrying enzyme transfer ubiquitin from its catalytic cysteine onto a recruited substrate lysine? With a modeled E2 onto its RBX1 RING, the distance between the recruited substrate to a substrate receptor and a ubiquitin's C-terminal tail bound to a recruited E2 enzyme still required overcoming a 50Å gap. Furthermore, how can the NEDD8 modification to a cullin accelerate this process by thousands of folds? The structure of a neddylated CRL provided some explanation that neddylation of a CRL induces freeing of the RING RBX1 to allow more flexibility and wide range movements, yet did not exactly show how ubiquitylation can occur rapidly in the context of a fully assembled neddylated CRL.

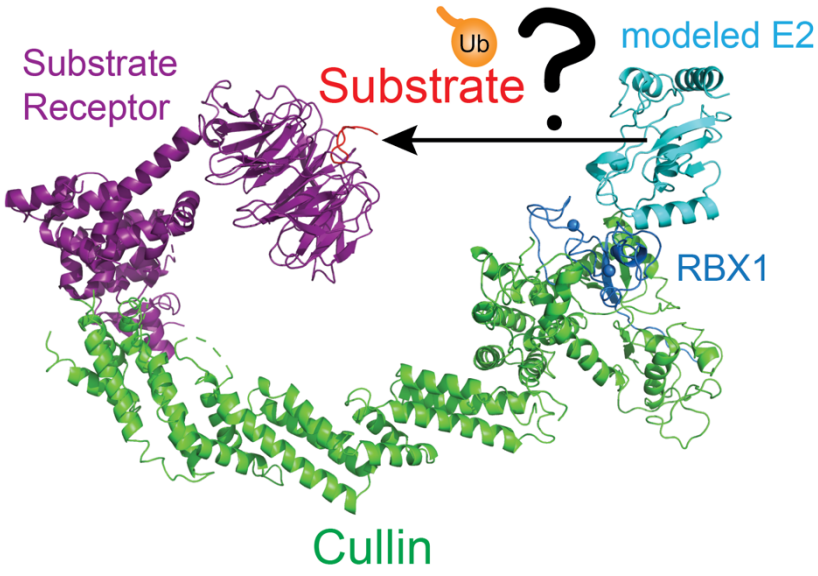

Figure 1.6: Cullin-RING ligase and Ubiquitylation. Previous structural mechanistic studies have yet shown how a cullin-RING ligase overcomes a 20Å gap between the catalytic cysteine of the E2 ubiquitin carrying enzyme to the substrate recruited onto the substrate receptor.

1.6 Aim of this Study

Over the past two decades, numerous structural studies have revealed how E3 ligase substrate receptor domains uniquely recruit their specific protein targets for ubiquitylation (Hao et al., 2007; Kung et al., 2019; Martinez-Zapien et al., 2016; Rusnac et al., 2018). There are also many structures of E3 RING domains bound to stable mimics of their E2~UB/UBL partners (Brown et al., 2015; Brown et al., 2016; Kamadurai et al., 2009; Mabbitt et al., 2020; Reverter and Lima, 2005; Scott et al., 2014; Streich and Lima, 2016). Nonetheless, few high-resolution structures have shown how RING-E2~UB/UBL modules modify specific sites within the distally recruited targets.

To understand how CRLs ubiquitylate their substrates, we focused on a well-defined pathway of significant physiological importance as a model system. Prior studies of the human CRL1 β-TRCP, comprising CUL1-RBX1 and the substrate receptor SKP1–β-TRCP, showed ubiquitin transfer from E2s in the UBE2D family (UBE2D2 and UBE2D3) to diverse substrates, including the β-catenin signaling protein and IκBα, the inhibitor of the NFκB transcription factor, harboring a specific, phosphor-degron (Spencer et al., 1999) (Hart et al., 1999; Jiang and Struhl, 1998; Latres et al., 1999; Orian et al., 2000; Winston et al., 1999b; Wu et al., 2003; Wu et al., 2010; Yaron et al., 1998).

Fundamental roles of NEDD8 in regulating cullin-RING ligase assemblies and its ubiquitylation were defined through pioneering studies of CRL1 β-TRCP (Duda et al., 2008; Liu et al., 2018; Read et al., 2000; Saha and Deshaies, 2008). Moreover, mutations of CRL1 β-TRCP that impair substrate ubiquitylation promote tissue specific tumorigenesis (Frescas and Pagano, 2008); hijacking of CRL1 β-TRCP ubiquitylation mechanism enables HIV evasion of host immunity (Margottin et al., 1998); and NEDD8 Gln40 deamidation by the enteropathogenic and enterohemorrhagic *Escherichia coli* effector proteins such as Cif results in accumulation of the CRL1 β-TRCP substrate IκBα as well as other cullin-RING ligase substrates (Cui et al., 2010; Jubelin et al., 2010; Morikawa et al., 2010). With the underlying biological significance of the CRL β-TRCP system, the central focus of this study is to structurally and biochemically elucidate how an activated cullin-RING ligase assembly ubiquitylates its recruited substrates such as IκBα or β-catenin.

2 Materials and Experimental Methods

2.1 Cloning, Protein Expression, & Purification

All proteins used in this study are sequences derived of human origin, subcloned into expression vectors. Wild type CUL1, RBX1(residues 5-C), SKP1, β-TRCP1 (residues 175-C), β-TRCP2, CUL4A (38-C), CRBN, DDB1, and UBA1 were cloned into pLIB vectors (Weissmann et al., 2016). CUL1 and GST-TEV RBX1, CUL4A(38-C) and GST-TEV-RBX1, His-TEV-β-TRCP2 and SKP1, or His-TEV-DDB1 and CRBN were co-expressed by co-infecting with two baculoviruses. These proteins were expressed in *Trichoplusia ni* High-Five insect cells, purified by either GST or Nickel affinity chromatography, and was relieved from the affinity tag by overnight incubation with TEV protease. The efficiency of TEV protease cleavage was validated by running an SDS-PAGE to monitor migration differences on the gel. If not sufficiently cleaved, the protein was incubated in 16 °C for an extra 2 hours. Once efficient TEV cleavage was confirmed, the proteins were subject to ion exchange for further purification and to separate away from the affinity tag, followed by size exclusion chromatography for final cleanup and buffer exchange into assay buffer containing 25 mM HEPES, 150 mM NaCl, 1 mM DTT, pH 7.5. All variants of CUL1-RBX1 were purified with the same protocol as above. Purification of NEDD8, UBE2M, APPBP1-UBA3, SKP1-FBXW7 (263-C, which deletes the N-terminal region including the dimerization domain of FBXW7), neddylation of CUL1-RBX1, and fluorescent labeling of Ubiquitin by fluoresceine-5-maleimide used for biochemical assays were done as previously described and similar to the protocol described above (Scott et al., 2014). In brief, these proteins were all purified by GST affinity chromatography, cleaved overnight by thrombin or TEV protease, followed by ion exchange and size exclusion chromatography except NEDD8 which skipped ion exchange. For fluorescein-5-maleimide labeling, a construct containing an N-terminal cysteine was purified to utilize as fluorescence labeling. After activating the cysteine with reducing reagents such as DTT or TCEP, protein was initially buffer exchanged into buffer containing no reducing reagents. 4-fold excess fluoresceine-5-maleimide was added immediately and incubated at room temperature for 1 hour. The labeled protein was quenched by adding 20mM DTT, buffer exchanged twice with PD10 desalting columns, and was subject to size exclusion chromatography in assay buffer. β-TRCP1(175-C, N-terminal

deletion including the dimerization domain of β-TRCP1) with an N-terminal His-MBP followed by a TEV cleavage site was cloned into a pRSF Duet vector with SKP1ΔΔ (two internal deletions of residues 38-43 and 71-82) (Schulman et al., 2000). SKP1ΔΔ-β-TRCP1(175-C) was expressed in BL21(DE3) Gold *Escherichia coli* at 18°C and was purified with Nickel affinity chromatography. After overnight TEV cleavage liberating β-TRCP1 from the affinity tag, sample was subject to anion exchange, and size exclusion chromatography. In order to remove excess chaperones binding to the protein, an extra wash step with buffer containing 5mM ATP was included before subjecting the protein to ion exchange chromatography. IKZF1 ZF2 (residues 141-169 harboring mutations K157R K165R) with an introduced lysine at position 140 was cloned into a pGEX-4T1 vector with a N-terminal GST with a 3C-Prescission protease cleavage site and a non-cleavable C-terminal Strep-tag. IKZF1 ZF2 was purified by GST affinity chromatography, 3C-Prescission cleavage overnight, and size exclusion chromatography. UBE2D2 and all of its mutant variants were purified as previous described (Kamadurai et al., 2013), and UBE2D3 and its variants were purified with the same method as UBE2D2, which in brief purification by GST affinity chromatography, followed by TEV cleavage, ion exchange, and size exclusion chromatography. Ubiquitin was expressed in BL21(DE3) RIL as previous described (Kamadurai et al., 2009). All mutant variants of UBE2D2, UBE2D3, UBE2M, RBX1, NEDD8, and UB were cloned using PCR, Quikchange (Agilent), or fragments were synthesized by Twist Biosciences, which were further cloned into expression vectors.

2.2 Peptides

All peptides were synthesized and purified with >95% purity by HPLC. (pX) indicates phosphorylated residues.

Peptides used for enzyme kinetics:
IκBα – KERLLDDRHD(pS)GLD(pS)MRDEERRASY (purchased from New England Peptide)
β-catenin short– KSYLD(pS)GIH(pS)GATTAPRRASY (synthesized from Max Planck Institute of Biochemistry Core Facility)
β-catenin medium– KAWQQQSYLD(pS)GIH(pS)GATTTAPRRASY (synthesized from New England Peptide)
β-catenin long– KAAVSHWQQQSYLD(pS)GIH(pS)GATTAPRRASY (synthesized from Max Planck Institute of Biochemistry Core Facility)
β-catenin for sortasing– GGGGYLD(pS)GIH(pS)GATTAPRRASY (synthesized from Max Planck Institute of Biochemistry Core Facility)

Peptides used substrate priming ubiquitylation assays:
IκBα – KKERLLDDRHD(pS)GLD(pS)MKDEE
CyE – KAMLSEQNRASPLPSGLL(pT)PPQ(pS)GRRASY

Peptide used in competition experiment which is a Ubiquitin non-modifiable substrate analog:
IκBα – RRERLLDDRHD(pS)GLD(pS)MRDEE (synthesized from Max Planck Institute of Biochemistry Core Facility)

Peptides used in cryo-EM experiments
-For structure representing neddylated CRL1 β-TRCP –UBE2D~UB–IκBα substrate:
IκBα – CKKERLLDDRHD(pS)GLD(pS)MKDEEDYKDDDDK (synthesized from Max Planck Institute of Biochemistry Core Facility)
-For cryo EM of unnneddylated and neddylated CRL1 β-TRCP– IκBα:
IκBα – KKERLLDDRHD(pS)GLD(pS)MKDEE

2.3 Expression of His-TEV-UB(1-75)-MESNa

His-TEV-UB(1-75) was cloned into a pTYB1 vector (New England BioLabs) and transformed into BL21(DE3) RIL for expression. Cells were grown in TB media at 37 °C to OD 600 = 0.8 and then induced with 0.5 mM IPTG, shaking overnight at 16°C. Cells were then harvested and resuspended in resuspension buffer (20 mM HEPES, 50 mM NaOAc, 100 mM NaCl, 2.5 mM PMSF, pH 6.8), sonicated (8 cycles of 8 second pulses), and then centrifuged (20,000 rpm at 4°C for 30 min). Ni-NTA resin (1 mL resin per liter of broth) was equilibrated with the resuspension buffer and the spun down lysate was incubated at 4°C on a roller at 30 rpm for 1 hour. The incubated resin was then transferred to a gravity column and washed 5 times with 1 column volume buffer in 20 mM HEPES, 50 mM NaOAc, 100 mM NaCl, pH 6.8. Protein was then eluted 5 times with 1 column volume in elution buffer containing 20 mM HEPES, 50 mM NaOAc, 100 mM NaCl, 300 mM Imidazole pH 6.8. Ubiquitin was cleaved from the chitin binding domain by diluting the eluted protein 10-fold in volume with 20 mM HEPES, 50 mM NaOAc, 100 mM NaCl, 100 mM sodium 2-mercaptoethanesulfonate (Sigma Aldrich) pH 6.8. This solution was incubated at room temperature overnight rolling at 30 rpm. UB-MESNa was finally purified by size-exclusion chromatography equilibrated with buffer containing 12.5 mM HEPES, 25 mM NaCl, pH 6.5.

Sequence of His-TEV-UB(1-75)-chitin binding domain:

MGSSHHHHHHENLYFQGSGGMQIFVKTLTGKTITLEVEPSDTIENVKAKIQD
KEGIPPDQQRLIFAGKQLEDGRTLSDYNIQKESTLHLVLRLRGCFAKGTNVL
MADGSIECIENIEVGNKVMGKDGRPREVIKLPRGRETMYSVVQKSQHRAH
KSDSSREVPELLKFTCNATHELVVRTPRSVRRLSRTIKGVEYFEVITFEMGQ
KKAPDG

2.4 Generating UBE2D-UB-substrate intermediate proxy

***generation of the stable UBE2D-UB-susbtrate intermediate proxy was done in collaboration with Dr. David Krist**

Native chemical ligation to make UB(1-75)-Cys-IκBα

His-UB(1-75)-MESNa (200 μM final concentration) was mixed with IκBα peptide (H-CKKERLLDDRHD(pS)GLD(pS)MKDEEDYKDDDDK-OH, synthesized at the Max-Planck Institute of Biochemistry core facility) (1000 μM final concentration) in 50 mM NaPO4, 50 mM NaCl, pH 6.5. The reaction was incubated at 30 rpm rocking in room temperature, and after 1 hr, TCEP was added to final concentration of 1 mM. After incubating for an additional 1 hr at room temperature, the reaction was quenched by adding NaPO4 pH 8.0 to a final concentration of 45 mM. The solution was then incubated with Ni-NTA resin (~300 μL of resin for a 1 mL reaction) at 30 rpm for 1 hr at 4°C. The reaction was transferred to a gravity column, and the resin was then washed 6 column volumes with 50 mM NaPO4, 50 mM NaCl, 1 mM β-mercaptoethanol, pH 8.0. Reaction was then eluted with 50 mM NaPO4, 50 mM NaCl, 1 mM β-mercaptoethanol, 300 mM imidazole, pH 8.0, and the elution fractions were subject to SDS-PAGE and nanodrop for analysis.

Connecting UBE2D Cys85 to UB(1-75)-Cys-IκBα via a disulfide bond

In order to utilize the catalytic cysteine of UBE2D to react with UB-Cys-IκBα, all other cysteines required mutating to non-reactive amino acids. ~50 different structurally guided mutational combinations to remove 3 other non-catalytic cysteines combining UBE2D2 and UBE2D3 were made and tested by activity assays to ensure proper activity and validity of UBE2D. UBE2D C21I C107A C111D, the top candidate mutant out of the optimization, was purified and then immediately used for disulfide formation. After size exclusion chromatography, the protein was concentrated (Amicon, EMD Millipore) to 600 μM. 200 μL of protein were separately desalted (2 x Zeba, 0.5 mL column, 7K MWCO, ThermoFisher) to 20 mM HEPES, 250 mM NaCl, 5 mM EDTA pH 7. Eluates from the desalting columns were combined and immediately added with 34 μL of 10 mM 5,5'-dithiobis-(2-Nitrobenzoic acid) (SigmaAldrich, dissolved in 50 mM NaPO4 pH 7.5). Reaction was mixed thoroughly by pipetting before incubating at room temperature for 30 minutes. The reaction was then desalted (2 x Zeba, 0.5 mL column, 7K MWCO,

ThermoFisher) to 20 mM HEPES pH 7, 250 mM NaCl, 5 mM EDTA and simultaneously UB(1-75)-Cys-IκBα (500 µL at 100 µM) was also desalted (1 x Zeba, 2 mL column, 7K MWCO, ThermoFisher) to the same buffer. UBE2D and UB components were then immediately combined, mixed, and incubated at room temperature for 30 minutes, and the sample centrifugated for 5 minutes to remove any aggregation, and was subject to size exclusion chromatography equilibrated with buffer 20 mM HEPES, 250 mM NaCl, 5 mM EDTA pH 7.

2.5 Cryo-EM sample preparation, data collection, and structure determination

For the structure determination of the neddylated CUL1-RBX1-SKP1-β-TRCP-UB-UBE2D-IκBα complex, neddylated CUL1-RBX1-SKP1-β-TRCP were mixed first to pre-form a stable CRL1 β-TRCP complex. Then 1.5-fold excess of intermediate proxy (UB-UBE2D-IκBα) was added to the preformed neddylated CUL1-RBX1-SKP1-β-TRCP, incubated for 30 minutes on ice, and purified by size exclusion chromatography in 25 mM HEPES 150 mM NaCl pH 7.5. Peak fractions of the complex were examined by SDS-PAGE, concentrated and crosslinked with a gradient of glutaraldehyde overnight by GraFix (Kastner et al., 2008). GraFix'ed sample was harvested with 200 µL volume fractions, and the fraction concentrations were measured by Bradford assay. Selected peak fractions were buffer exchanged away from glycerol using Zeba Desalt Spin Columns (0.5 mL column, 7K MWCO, ThermoFisher). 3µL of the sample measured at 0.08mg/ml were applied to manually graphene oxide coated Quantifoil R2/1 holey carbon grids (Quantifoil) (Palovcak et al., 2018) and was plunged frozen by Vitrobot Mark IV in liquid ethane.

Electron Microscopy

Samples were initially screened on a FEI Talos Arctica at 200kV using a Falcon II direct detector in linear mode. For each complex combination, around 800 movies were recorded at 1.997Å/pixel with a nominal magnification of 73,000x overnight. A total dose of ~60 e-/Å2 were collected over 40 frames, with a defocus range of -1.5µm to -3.5µm. For each screening dataset, optimal grids were saved in preparation for high resolution datasets. Once a screening dataset had proven to provide reconstructions reaching subnanometer resolution, grids from the same session were taken to the Titan Krios for High resolution data collection.

High resolution cryo-EM data were collected on a FEI Titan Krios electron microscope at 300kV with a Quantum-LS energy filter, using a K2 Summit (Gatan) direct detector in counting mode. 9112 Images were recorded at 1.06Å/pixel with a nominal magnification of 130,000x with active beam tilt to accelerate data collection, with 2 shots per hole and a 5 x 5 hole collection schematic. A total dose of 70.2 e-/Å2 were fractionated over 60 frames, with a defocus range of -1.2µm to -3.6µm.

Data Processing

Frames were motion-corrected using RELION-3.0 (Zivanov et al., 2018) with dose weighing, and each micrograph was manually inspected to discard suboptimal micrographs for further processing. CTF was estimated using CTFFIND, and particles were picked with Gautomatch (K. Zhang, MRC Laboratory of Molecular Biology, Cambridge). 2D classification was performed in RELION-3.0, and the classified particles were used to generate a 3D ab initio model using sxviper.py from SPARX (Hohn et al., 2007). The initial 3D model from sxviper.py was imported to RELION-3.0 as a template for further 3D classification, and 3D refinement. Once screening datasets from the Talos Arctica were fully processed, an optimized 2D template was generated from the screening data to utilize for picking particles from the high resolution dataset, as well as the initial 3D model. Final post-processing was performed together with particle polishing using frames 2-25.

Protein Identification and model building:

***Structural model building was performed in collaboration with Dr. J Rajan Prabu**

Final 3D reconstruction displayed clear main chain and side chain densities, that enabled us to model and refine the atomic coordinates of the ubiquitylation complex. Previously determined components from X-ray crystallography derived structures (taken from PDB ID 1LDJ, 1P22, 4P5O, 4V3L) (Buetow et al., 2015; Scott et al., 2014; Wu et al., 2003; Zheng et al., 2002b) were manually placed as a whole or in parts. Components were manually fitted to the density, and also rigid body fitted using USCF Chimera (Pettersen et al., 2004). The resultant parts of the structure were combined into a singular PDB in coot, and was subject to rigid body refinements in which each protein/domain was allowed to move independently. Further iterative manual model building and real space refinements were performed until good geometry and map-to-model correlation was established. Model building was done using COOT (Afonine et al., 2018; Emsley et al., 2010) was used for real space refinement.

2.5 Biochemical assays

Lysine discharge assays monitor intrinsic activity of E2~UB ('~' indicates thioester bond formation between E2 and UB) to discharge its thioester linked ubiquitin onto free lysine in solution in the presence or absence of E3 ligases that would catalyze its discharge. 9 μM of UBE2D~UB thioester was initially formed by incubating 10 μM UBE2D, 15 μM UB, and 0.2 μM UBA1 in 50 mM HEPES, 50 mM NaCl, 2.5 mM $MgCl_2$ 1.5 mM ATP pH 7.5. The reaction was incubated at room temperature for 15 minutes, and quenched with 50mM EDTA. The preformed thioester was subject to 5 mM free lysine in the presence or absence of NEDD8–CUL1-RBX1, harboring a RBX1 N98R mutation which adds a canonical 'linchpin arginine' to catalyze the discharge of ubiquitin in order to monitor the E3 catalyzed activity in a relatively short timeframe. The reaction was initiated by adding E2~UB onto a mixture containing 5 mM free lysine with either no E3, 0.5 μM CUL1-RBX1 (N98R, and an additional K720R mutant to prevent automodification of CUL1 by ubiquitin at its neddylation site), or 0.5 μM NEDD8–CUL1-RBX1. After each timepoint, reactions were quenched by adding 2xSDS-PAGE sample buffer. Assays were run on SDS-PAGE and visualized by Coomassie-blue staining.

Ubiquitylation of IκBα by neddylated CRL1β-TRCP via UBE2D3 was monitored using a pulse-chase format that specifically detects CRL1 β-TRCP dependent ubiquitin modification from UBE2D to IκBα. The pulse was generated by creating a thioester linked UBE2D~UB intermediate by incubating 10 μM UBE2D, 15 μM fluorescently labeled UB, and 0.2 μM UBA1 in 50 mM Tris, 50 mM NaCl, 2.5 mM $MgCl_2$, 1.5 mM ATP pH 7.5 in room temperature for 10 minutes. The pulse was quenched by adding 50 mM EDTA on ice for 5 minutes, then was further diluted to 100 nM E2~UB in buffer containing 25 mM MES, 150 mM NaCl, pH 6.5 to be ready for mixing with the chase reaction. The chase reaction consisted of 400 nM NEDD8–CUL1-RBX1-SKP1-β-TRCP, and 1 μM phosphorylated IκBα peptide in 25 mM MES 150 mM NaCl pH 6.5 on ice. The diluted pulse was mixed with the chase at a 1:1 ratio on ice to start the reaction so that final reaction concentrations were at 50 nM UBE2D~UB thioester and 200 nM neddylated CRL1 β-TRCP to catalyze substrate ubiquitylation. Samples were taken each time point, quenched with 2xSDS-PAGE sample buffer, run on SDS-PAGE, and scanned on a Amersham Typhoon (GE) detecting fluorescence of fluorescently labeled ubiquitin. To probe for effects by unneddylated CRLs,

NEDD8 modification site Lys of CUL1 or CUL4 were mutated to Arg (CUL1 K720R, CUL4A K705R) to avoid ubiquitylation of the NEDD8 modification site and influencing activity.

Ubiquitylation of phosphorylated CyE (pCyE) probing variations of CUL1-RBX1 was monitored similarly as above, but in concentrations at 100 nM UBE2D~UB, 250 nM NEDD8–CUL1-RBX1-SKP1-FBXW7 (263-C, truncation to make it a monomeric form), and 2.5 μM pCyE in 25 mM HEPES 150 mM NaCl pH 7.5 at room temperature. Effects of UBE2D mutants were monitored at 100 nM UBE2D~UB, 500 nM NEDD8–CUL1-RBX1-SKP1-FBXW7(263-C), 2.5 μM pCyE.

Ubiquitylation of IKZF ZF2 was monitored in a similar format as the assays above but at concentrations of 400 nM UBE2D~UB, 500 nM NEDD8–CUL4-RBX1-DDB1-CRBN, 5 μM Pomalidomide, and 2.5 μM IKZF ZF2 in 25 mM HEPES 150 mM NaCl pH 7.5 in room temperature. Effects of Ubiquitylated CUL4-RBX1 were probed in 100 nM UBE2D~UB, 250 nM UB–CUL4-RBX1-DDB1-CRBN, 2.5 μM Pomalidomide, and 1.25 μM IKZF ZF2.

Ubiquitylated CUL1 and CUL4A were generated by using an identity swap at ubiquitin residue 72 for E1 specificity, thus using UB R72A allowed loading via APPBP1-UBA3, further modifying CUL1/4 by UBE2M. Due to the inefficiency of UB ligation to CUL4A by APPBP1-UBA3 and UBE2M, a higher pH at 8.8 was necessitated to drive the reaction to completion. NEDD8 I44A required a compensatory mutant on UBE2M (Y130L), discovered from previous studies (Scott et al., 2014), to enable modification on CUL1 K720.

Generation of isopeptide linked UBE2D–UB

A stable mimic of UBE2D~UB thioester was created by mimicking the thioester bond with an isopeptide bond by introducing a Cys85Lys (catalytic cysteine to lysine) mutant to prevent hydrolysis of the thioester bound UB. 200 μM UBE2D C>K, 200 μM UB, 1 μM UBA1 in 50 mM Tris, 50 mM NaCl, 10 mM $MgCl_2$, 5 mM ATP pH 9.0 in 30°C for 16 hours and 37°C for another 6 hours. Reaction was further purified on size exclusion chromatography in buffer containing 25 mM HEPES, 150 mM NaCl, 1 mM DTT, and fractions were examined by SDS-PAGE and Coomassie-blue staining. Pure fractions were concentrated and frozen in small aliquots for the experiments.

Generation of Ubiquitylated β-catenin fusion via Sortase reaction

A mimic of a ubiquitylated β-catenin was generated by fusing ubiquitin with a C-terminal addition of the sortase motif LPETGG with a GGGG–β-catenin peptide. Reaction was incubated with concentrations of 50 μM UB LPETGG, 300 μM GGGG-β-catenin peptide, and 10μM His-Sortase A for 10 minutes in 50 mM Tris 150 mM NaCl 10 mM $CaCl_2$ pH 8.0 on ice. Sortase A was further removed by retention on nickel resin, and the reaction was purified by size exclusion chromatography in 25 mM HEPES 150 mM NaCl 1 mM DTT pH 7.5.

Sequence of Ubiquitin harboring the sortase motif:
MQIFVKTLTGKTITLEVEPSDTIENVKAKIQDKEGIPPDQQRLIFAGKQLEDGRTLSDY
NIQKESTLHLVLRLRGSGSGSLPETGG

2.6 Competition pulse-chase assay

Competition ubiquitylation assays were carried out similarly as described for biochemical assays monitoring ubiquitylation of IκBα by CRL1 β-TRCP via UBE2D3 with certain modifications. The pulse reaction involved formation of a thioester linked UBE2D~UB intermediate by incubating 10 μM UBE2D, 15 μM unlabeled UB, and 0.2 μM UBA1 in a buffer containing 50 mM Tris, 50 mM NaCl, 2.5 mM $MgCl_2$, and 1.5 mM ATP, pH 7.6 at room temperature for 5 minutes. The pulse reaction was quenched by the addition of 50 mM EDTA final and placed on ice for 5 minutes, then further diluted to 100nM in a buffer containing 25 mM MES, and 150mM NaCl, pH 6.5. The chase reaction was also assembled at room temperature for 5 minutes, and consisted of 200 nM NEDD8–CUL1-RBX1, 200 nM SKP1-β-TRCP, 1 μM fluorescein-labeled phosphorylated IκBα peptide, and 1 μM of competitor in a buffer consisting of 25 mM MES, and 150mM NaCl, pH 6.5. The order of addition for the chase reaction was buffer, neddylated CUL1-RBX1, SKP1-β-TRCP, phosphorylated IκBα peptide, and then either competitor (phosphorylated IκBα peptide without a target lysine site, E2~UB isopeptide, or the stable UBE2D-UB-substrate conjugate mimic) or buffer. the E3-substrate mixes were further incubated on ice for an additional 5 minutes to achieve equilibrium. Reactions were initiated on ice by the addition of an equal volume of pulse reaction to the E3-substrate mix, resulting in final reaction concentrations that were 50 nM E2~UB, 100 nM E3, and 500 nM substrate with or without equimolar competitor. Samples were taken at each indicated time points and quenched with 2xSDS-PAGE sample buffer. Assay was examined by SDS-PAGE, and subsequently scanned on an Amersham Typhoon (GE) to detect the fluorescence of the fluorescein-labeled phosphorylated IκBα peptide.

2.7 Kinetics

*All kinetics experiments were performed in collaboration with Dr. Spencer Hill at the laboratory of Dr. Kleiger at University of Nevada Las Vegas.

3 Results

NEDD8 activation of CRL1 β-TRCP-IκBα

As we sought out to monitor the effects of NEDD8 modification in ubiquitylation, kinetics of ubiquitin priming with or without NEDD8 provided striking effects. Kinetic parameters determined by rapid quench-flow methods for CRL1 β-TRCP and UBE2D-catalyzed ubiquitylation of model substrates (phosphopeptides derived from β-catenin and IκBα, harboring single acceptor lysines) showed that NEDD8 activated CRL massively stimulates the ubiquitylation reaction, by a near 2000-fold overall (comparing kobs/Km, **Figure 3.1**).

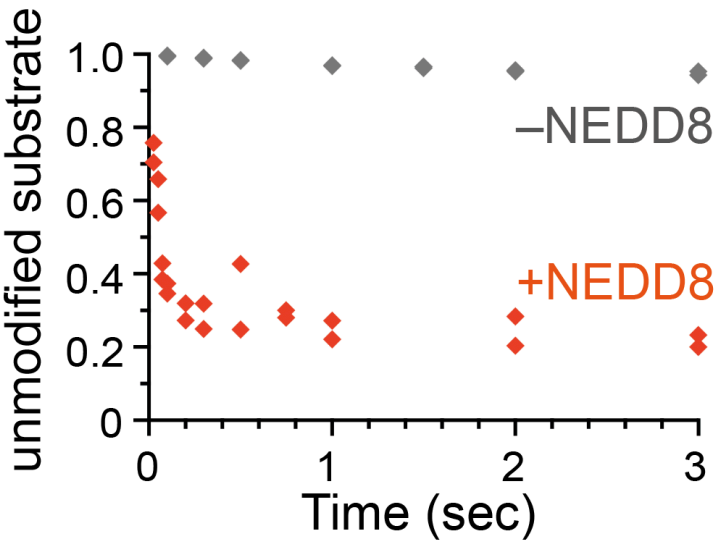

Figure 3.1: Kinetic effects of neddylated CRL on substrate priming
Effect of CUL1 neddylation on CRL1 β-TRCP-catalyzed UB transfer from E2 UBE2D3 to a radiolabeled β-catenin-derived substrate peptide. The plot shows non-ubiquitylated substrate remaining during pre-steady-state rapid quench-flow ubiquitylation reactions with saturating UBE2D3 and either neddylated or unneddylated CRL1 β-TRCP. Within the timeframe shown, neddylated CRL substantially ubiquitylates the substrate and depletes the amount of unmodified substrate, whereas unneddylated CRL only minorly depletes the unmodified substrate.

Performing experiments under conditions allowing multiple UBE2D turnover events enabled probing for effects on the first ubiquitin conjugation step (priming) versus the formation of subsequent ubiquitin molecules building processive polyubiquitin chains (extending). Quantifying individual rates for linkage of successive UBs during polyubiquitylation showed that NEDD8 activates both UBE2D-catalyzed "priming", whereby the first ubiquitin is ligated directly onto the substrate, and subsequent ubiquitin chain elongation. The effects of NEDD8 are also highlighted in a qualitative assay in a pulse-chase format, whereby the assay follows ubiquitin conjugation only from UBE2D~UB thioester to substrate, that exclusively monitors substrate priming (**Figure 3.2**). These assays were performed in attenuated conditions with lower temperature on ice and lower pH at 6.5, in order to monitor the reaction efficiency in a non-kinetic environment to assess qualitative effects, as kinetics has shown that the reaction to be extremely fast. Indeed, without attenuating the reaction, neddylated CRL mediated ubiquitin transfer was already saturating at 7 seconds, which does not allow comparative assessment with mutants harboring defects that are potentially very minor.

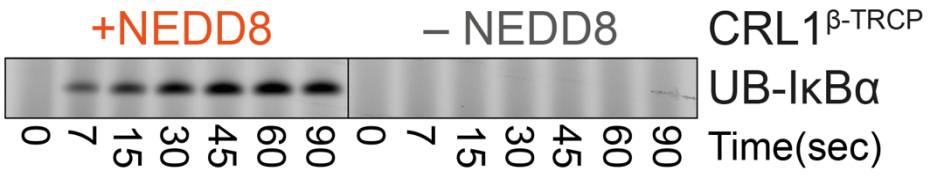

Figure 3.2: Qualitative effects of neddylated CRL on substrate priming
SDS-PAGE detecting fluorescently labeled ubiquitin transferred from UBE2D~UB directly to IκBα-derived substrate in a qualitative assay for substrate priming. While neddylated CRL shows robust ubiquitylation of substrate IκBα peptide starting at 7 seconds, unneddylated CRL shows essentially no activity in these timepoints.

Such rapid substrate priming is difficult to rationalize by prior structural models. At one extreme, CUL1-RBX1 crystal structures showed that the RING domain of RBX1 is fixed by interactions with CUL1's WHB domain (Zheng et al., 2002b). This conformation allows CAND1 binding while excluding substrate receptor complexes such as SKP1-F-box proteins to a cullin (Goldenberg et al., 2004). When modeling a RING-docked UBE2D~UB intermediate, this would place the catalytic site of UBE2D and the C-terminal tail of ubiquitin

over 50Å apart from the F-box protein-bound substrate ("~" refers to thioester bond and "–" refers to isopeptide bond). A more recent structure of a NEDD8-modified C-terminal portion of CUL5 showed rather multiple conformations of the NEDD8-linked WHB and RBX1 RING domains, demonstrating the potential for these alternative conformations to allow a more flexible range of E2~UB for substrate ubiquitylation (Duda et al., 2008). However, while potential hints were provided by these previous studies, it has remained unknown whether CRLs adopt a specific conformation during ubiquitylation, or if the RBX1 RING and CUL1 WHB domains – with or without NEDD8 - are inherently dynamic. While X-ray crystallography provides high-resolution data yet with limited conformational information, cryo-EM allows monitoring numerous energetically stable conformations even at lower resolution. Thus, we obtained cryo EM data for both unneddylated and neddylated monomeric versions of CRL1 β-TRCP bound to the phosphodegron portion of the IκBα substrate (**Figure 3.3**).

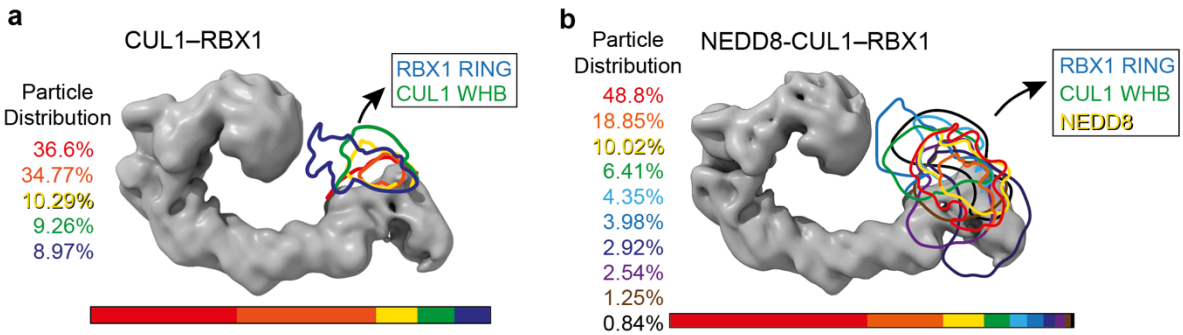

Figure 3.3: Cryo-EM reconstructions of unneddylated CRL β-TRCP and neddylated β-TRCP.

a, Cryo-EM map of unneddylated CRL β-TRCP with density representation of the substrate scaffolding region. Data generated several 3D classes, whereby the density for RBX1 RING and CUL1 WHB domains appeared with different orientations. The corresponding densities for each class are highlighted in colored outlines, along with its respective particle distribution of each class. **b,** same as in a, but with neddylated CRL β-TRCP. Compared to the classes shown in unneddylated CRL β-TRCP, neddylated CRL β-TRCP shows a much diverse population of classes with a wider range of motion and variability of the RBX1 RING, CUL1 WHB, and its conjugated NEDD8 densities.

Reconstructions, refined to 4.8 and 6.7 Å overall resolution for unneddylated and neddylated substrate-bound CRL1 β-TRCP, show two regions with distinct structural properties. A "substrate scaffolding module" bridging substrate with RBX1 displays well-resolved density readily fit with crystal structures of substrate-bound SKP1-β-TRCP and the portion of CUL1-RBX1 comprising CUL1's N-terminal domain (NTD) and C/R domain (**Figure 3.4**).

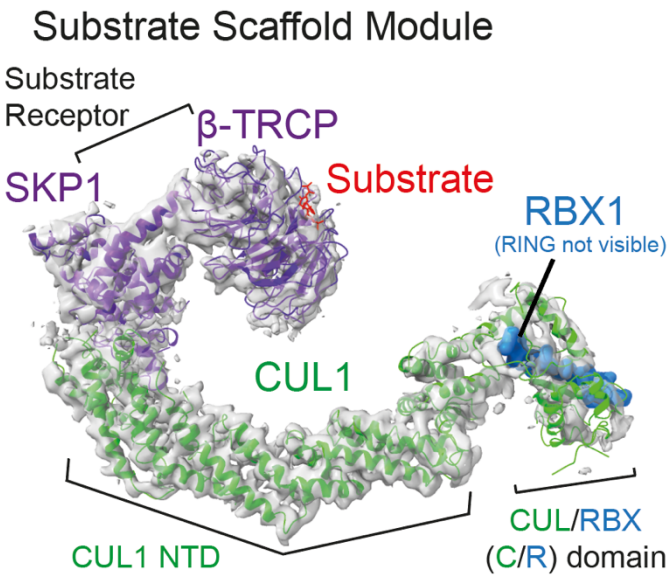

Figure 3.4: Substrate Scaffolding Module of unneddylated CRL β-TRCP.
Cryo-EM density of CRL β-TRCP with previous crystal structures of CUL1-RBX1 (PDB ID 1LDK) and SKP1-β-TRCP (PDB ID 1P22) fitted into the density. The RBX1 RING and CUL1 WHB domain are masked out during this 3D reconstruction to provide a more heterogeneous signal for the substrate-scaffold module. The substrate scaffolding module, which consists of the substrate receptor complex SKP1-β-TRCP bound to CUL1's N-terminal domain (NTD), and CUL1's C-terminal domain which harbors the catalytic RING RBX1, whereby RBX1's N-terminal β-strand forms an intertwined β-sheet with CUL1's C-terminal domain (CTD), to form the C/R domain.

The resultant model superimposes well with that based on docking overlapping regions of the subcomplex structures (Tang et al., 2007; Wu et al., 2003; Zheng et al., 2002b). By contrast, density for RBX1's RING and CUL1's WHB domains are relatively lacking in some classes of the unneddylated complex and in a focused refinement at 4.7 Å resolution. Moreover, when these domains and the CUL1-linked NEDD8 are detectable, they are visualized collectively only at low contour and in varying positions in different classes (**Figure 3.3**). It seems likely that these domains sample multiple orientations, yet it is difficult to conceptualize how seemingly uncoordinated, nanometer-scale motions of RBX1-activated UBE2D and a flexibly tethered substrate could lead to productive ubiquitylation.

Determining the cryo-EM structure representing a CRL catalyzing substrate ubiquitylation

Considering that the substrate priming reaction likely involves avid interactions in the fleeting intermediate when UBE2D's active site, ubiquitin's C-terminus, and the substrate are simultaneously linked, a method to chemically adjoin surrogates for these entities at a single atom with near-native geometry was necessary to generate a stable mimic of ubiquitylation (**Figure 3.5**).

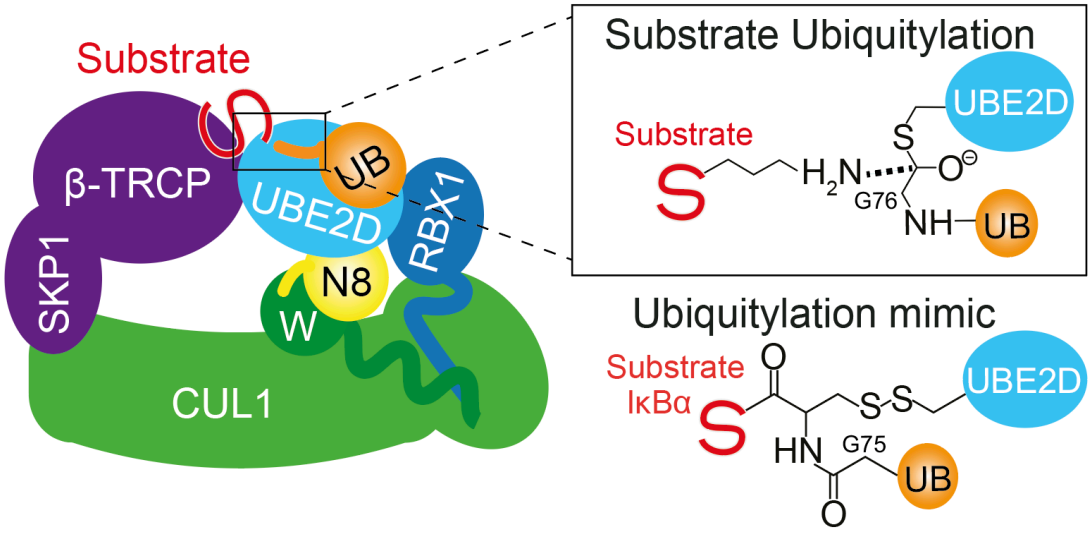

Figure 3.5: Chemical mimic of substrate ubiquitylation
During the native ubiquitylation intermediate, chemical entities are thought to be immobilized in a transient manner for only an extremely short period of time. In order to visualize the fleeting intermediate, chemical methods adjoining surrogates for the active site of UBE2D, the C-terminus of ubiquitin, and the ubiquitin acceptor site on the IκBα derived substrate peptide were designed to create a stable proxy to utilize for structural studies.

Our strategy for trapping the transient neddylated CRL E2~UB–substrate complex required that the E2 UBE2D contains only a single cysteine at the active site to utilize cysteine based chemistry. UBE2D contains three additional cysteines (Cys21, Cys107, Cys111) apart from the catalytic cysteine. Canonical cysteine replacements to either serine or alanine while retaining the catalytic cysteine severely compromised the intrinsic activity of

E2. After examining the structural locations of these cysteines, we presumed that these Ser/Ala mutations hindered formation of the active UBE2D~UB conformation (Pruneda et al., 2012; Yunus and Lima, 2006). We devised a systematic approach to identify suitable mutation combinations that qualitatively maintain wild-type level activity dependent on neddylated CRLs to provide near-native conditions (**Figure 3.6a**). Structural analysis showed that Cys21 and Cys107 are in close proximity facing towards the core of the E2, such that mutation of both residues to Ala may generate a destabilizing cavity which would potentially disrupt the structural integrity of the enzyme. Combining UBE2D2 Cys107Ala with Cys21 mutated to Ile, Leu or Val to compensate for the reduced hydrophobic volume led to the identification of Cys21Ile Cys107Ala as a suitable version for testing all other possible replacements for Cys111. Including 17 different Cys111 mutants from the basis of Cys21Ile and Cys107Ala, a total of 48 different versions of UBE2D were tested to identify the Cys21Ile Cys107Ala Cys111Asp mutant suitable for chemical trapping at the remaining active site Cysteine.

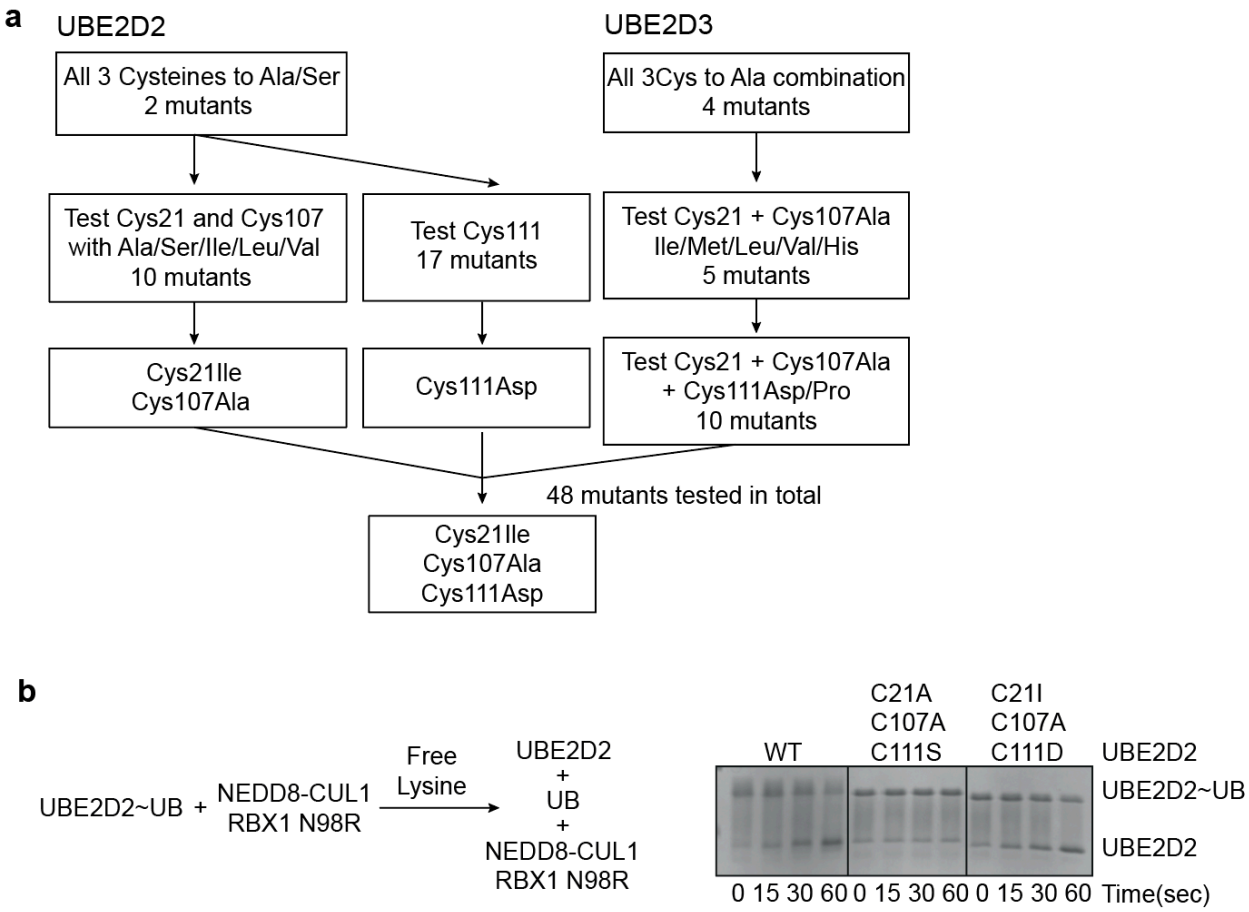

Figure 3.6: Designing UBE2D mutants for ubiquitylation mimic.

a, Strategy table to find mutant combinations of non-catalytic cysteines of UBE2D2 or UBE2D3 to retain wild-type like activity while only keeping the catalytic cysteine for cysteine based chemistry. **b**, Left, schematic of pulse-chase assay testing intrinsic activation of thioester-linked UBE2D~UB intermediates onto free lysine in a neddylated CRL dependent manner. Bottom, example assay described showing that Ser/Ala mutations of noncatalytic cysteines were defective in intrinsic E2 activity (Cys21Ala Cys107Ala Cys111Ser), while the optimized mutant (Cys21Ile Cys107Ala Cys111Asp) retains wild-type like activity.

With an assay monitoring RING-dependent discharge of ubiquitin from UBE2D to free lysine, RBX1 RING-dependent activity is limited in this assay due to sequence constraints imposed by the requirements for binding to partners other than UBE2D (Scott et al., 2014). Nonetheless, substrate-independent activation of UBE2D~UB can be readily examined using CUL1-RBX1 harboring a hyperactive RBX1 Asn98Arg mutant, or the so-called the canonical "linchpin" residue (Scott et al., 2014), along with high enzyme and lysine concentrations (**Figure 3.7**). UBE2D~UB was pre-formed in a pulse reaction, and this was subbsequently mixed with neddylated CUL1–RBX1 (together with RBX1 Asn98Arg mutant) and free lysine to start the reaction. Ubiquitin discharge onto free lysine was monitored at indicated timepoints by Coomassie-stained SDS-PAGE as shown in representative gel demonstrating that standard Ser/Ala mutations of noncatalytic cysteines compromised intrinsic E2 activity (Cys21Ala Cys107Ala Cys111Ser), while the optimized mutant (Cys21Ile Cys107Ala Cys111Asp) retains wild-type like activity (**Figure 3.6b**). A similar approach was used for UBE2D3 to identify similar mutants retaining wild-type like activity.

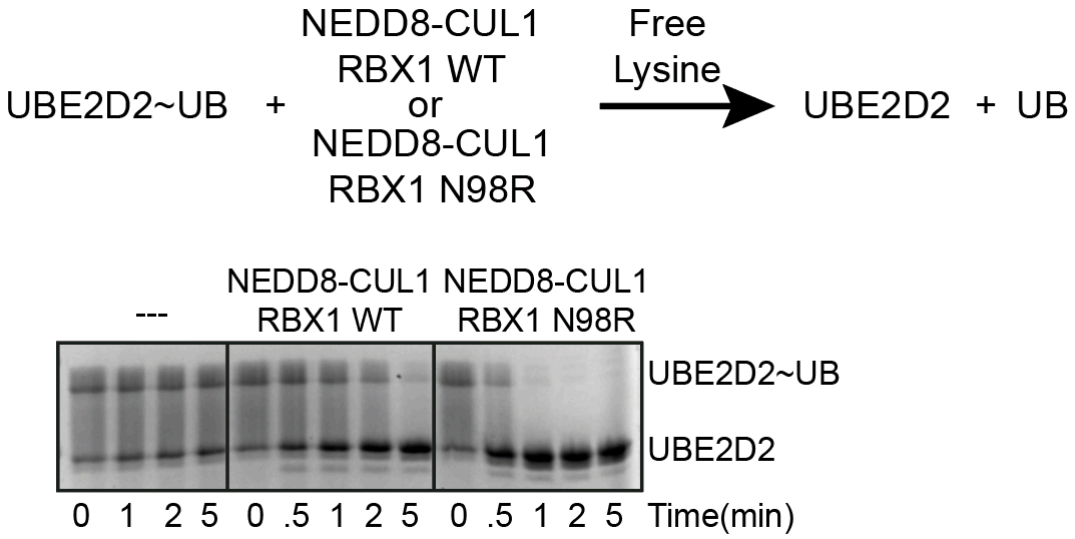

Figure 3.7: Hyperactive RBX1 mutant activity.

RBX1's Asn98Arg mutation increases intrinsic activity of ubiquitin discharge from UBE2D~UB onto free lysine. While wild-type neddylated CUL1-RBX1 shows robust ubiquitin discharge starting at 5 minutes, harboring the Asn98Arg mutation allows similar activity at 30 seconds.

After generating the stable mimic of ubiquitylation connecting UBE2D~UB-phosphorylated IκBα using the mutant UBE2D with wild-type like activity, these intermediate "traps" were also tested in neddylated CRL dependent ubiquitylation assays to ensure that each components were maximally engaging the active protein complex with avidity as designed. Based on the hypothesis that its simultaneous occupation of these binding sites for UBE2D~UB and the substrate receptor should allow potent inhibition of substrate ubiquitylation, we were able to completely abolish substrate targeting by incubating the ubiquitylation reaction with the stable mimic competitor, thus indicating that the designed proxy was properly engaging each binding site.

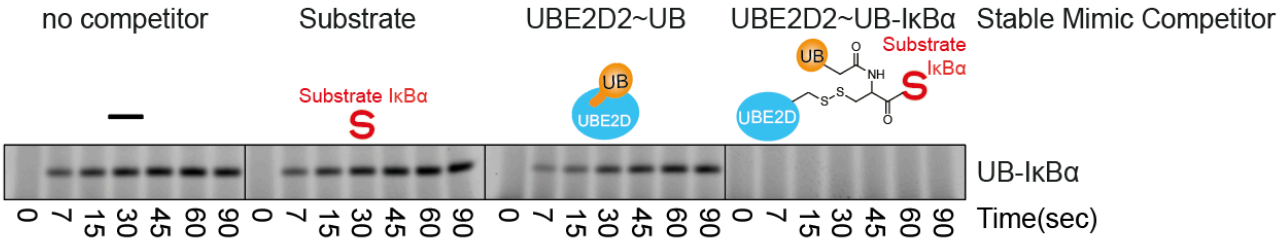

Figure 3.8: Stable ubiquitylation mimic inhibits substrate ubiquitylation activity. Ubiquitylation of peptide substrate derived from phosphorylated IκBα by UBE2D and neddylated CRL β-TRCP was monitored in the absence or presence of free substrate phosphorylated IκBα harboring no targetable lysine residue, isopeptide linked UBE2D–UB that mimics thioester linked UBE2D~UB, and the stable ubiquitylation mimic connecting UBE2D~UB-phosphorylated IκBα. Only in the presence of the stable mimic incorporating all three components fully inhibited substrate ubiquitylation.

Several complexes with the stable mimics were screened by cryo-EM to know which combination of protein complex and stable mimic were viable for high resolution structure studies. Comparing previously established stable mimic methods (Streich and Lima, 2016), along with monomeric or dimeric β-TRCP complexes, and UBE2D2 or UBE2D3, with or without an additional canonical linchpin, we were able to obtain high resolution data for our proxy for UBE2D2~UB–IκBα substrate intermediate bound to a hyperactive version of neddylated CRL1 β-TRCP incorporating mutations designed to increase homogeneity optimally for cryo-EM (**Figure 3.9, Figure 3.10, Table 1**).

IκBα–UB~UBE2D crosslink (C21I C107A C111D)	UBE2D2 2x2way XL	UBE2D3 3way XL	UBE2D3 3way XL	UBE2D2 3way XL	UBE2D2 3way XL	none	none
Substrate Receptor	β-TRCP2	β-TRCP1 175-C	β-TRCP1 175-C	β-TRCP1 175-C	β-TRCP1 175-C	β-TRCP1 175-C	β-TRCP1 175-C
RBX1	WT	WT	N98R	N98R	N98R	WT	WT
NEDD8	yes	yes	yes	yes	yes	no	yes
SKP1	WT	ΔΔ	ΔΔ	ΔΔ	ΔΔ	WT	WT
	EMDB-10578	EMDB-10579	EMDB-10580	EMDB-10581	EMDB-10585 PDB 6TTU	EMDB-10582	EMDB-10583
Data collection and processing							
Microscope	Krios	Arctica	Arctica	Arctica	Krios	Glacios	Glacios
Magnification	105,000	92,000	73,000	73,000	130,000	36,000	22,000
Voltage (kV)	300	200	200	200	300	200	200
Electron exposure (e–/Å^2)	56	61.3	60.8	70	70.2	60	59
Defocus range (μm)	-1.2 ~ -3.6	-1.5 ~ -3.5	-1.5 ~ -3.5	-1.5 ~ -3.5	-1.2 ~ -3.3	-1.2 ~ -3.3	-1.2 ~ -3.3
Pixel size (Å)	1.34	1.612	1.997	1.997	1.06	1.181	1.885
Symmetry imposed	C2	C1	C1	C1	C1	C1	C1
Initial particle images (no.)	2,575,161	464,344	601,121	459,011	1,661,870	2,051,804	1,666,293
Final particle images (no.)	33,738	47,246	107,311	40,835	106,257	262,116	349,803
Map resolution (Å)	9.3	8.6	9.4	8.4	3.72	4.64	6.7
FSC threshold	(0.143)	(0.143)	(0.143)	(0.143)	(0.143)	(0.143)	(0.143)
Map resolution range (Å)	-	-	-	-	3.46 ~ 6.0	-	-
Refinement							
Initial model used (PDB code)					1LDJ 1P22 4P5O 4V3L		
Model resolution (Å)					3.7		
FSC threshold					(0.143)		
Map sharpening *B* factor (Å^2)	-578.9	-1159	-1272	-983.5	-94.2	-199	-338
Model composition							
Non-hydrogen atoms					13034		
Protein residues					1616		
Ligands					3(ZN)		
B factors (Å^2)							
Protein					91		
Ligand					224		
R.m.s. deviations							
Bond lengths (Å)					0.011		
Bond angles (°)					1.043		
Validation							
MolProbity score					2.37		
Clashscore					16.31		
Poor rotamers (%)					0.21		
Ramachandran plot							
Favored (%)					85.12		
Allowed (%)					14.88		
Disallowed (%)					0		

Table 1: Cryo-EM statistics on validation, refinement, data collection, and database codes

a UBE2D2 + CRL1$^{\beta\text{-TRCP2}}$ WT

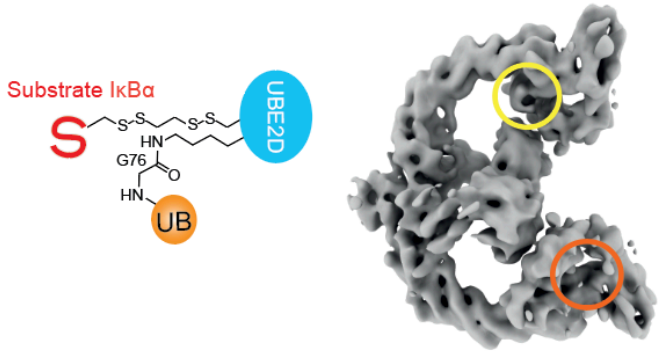

b UBE2D3 + CRL1$^{\beta\text{-TRCP1}\Delta D}$

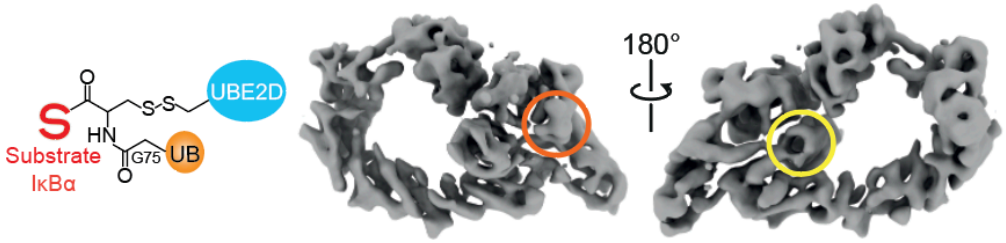

c UBE2D3 + CRL1$^{\beta\text{-TRCP1}\Delta D}$ + canonical linchpin

d UBE2D2 + CRL1$^{\beta\text{-TRCP1}\Delta D}$ + canonical linchpin

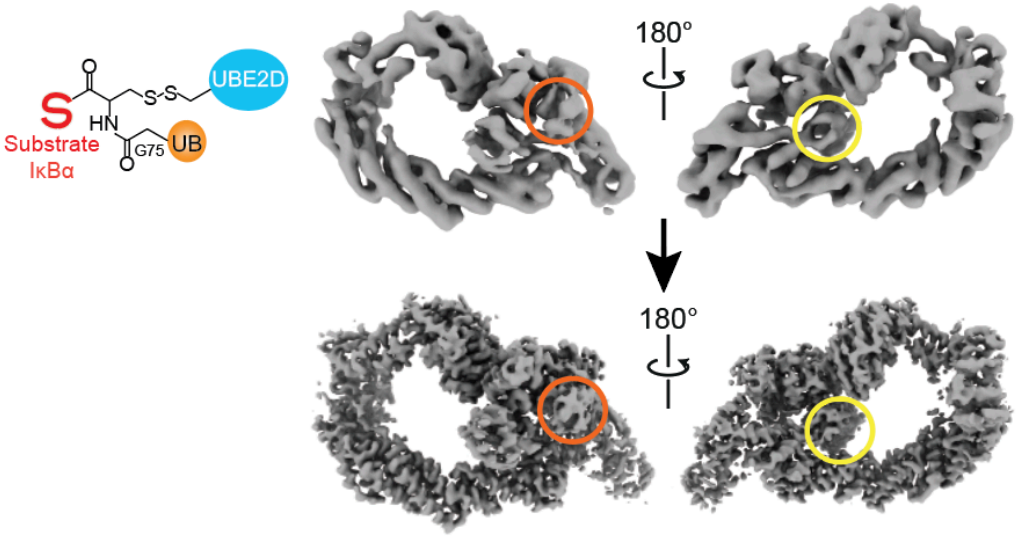

Figure 3.9: Cryo-EM screening of stable mimic.

a, Cryo-EM reconstruction of neddylated CRL1 β-TRCP2 (with full-length, dimeric β-TRCP2) bound to a mimic of the UBE2D2~UB–IκBα generated by adapting the method used previously to visualize non-canonical lysine Sumoylation (Streich and Lima, 2016). Ubiquitin is isopeptide-bonded to a UBE2D Leu119Lys residue substitution, which covalently connects the ubiquitin's c-terminus to residue in close proximity to the catalytic cysteine, thus mimicking a UBE2D~UB thioester. Then the catalytic cysteine available was disulfide-linked to the substrate peptide harboring a cysteine residue. This EM map visualizes the catalytic architecture of dimeric CRL1 β-TRCP2 and its conjugated NEDD8 (encircled in yellow) which is contacting the backside of UBE2D. However, the donor UB (absent from region circled in orange) was not visible, presumably due to the method used to generate this mimic of the catalytic intermediate, in which the UB and substrate are not both simultaneously linked to the UBE2D catalytic Cys, thus allowing more freedom of ubiquitin to be flexible. Variations between the two protomers of the dimer also exacerbated sample heterogeneity, thus not yielding high resolution reconstructions.

b, Cryo-EM reconstruction of neddylated CRL1 β-TRCP1ΔDimer (truncation of β-TRCP1 N-terminal region from residues 175 to the C-terminus that prevents dimer formation) bound to our newly devised proxy for the UBE2D3~UB–IκBα intermediate. Both the NEDD8 (encircled in yellow) and donor UB (encircled in orange) were fully visible. **c,** To increase cryo-EM sample homogeneity, we incorporated RBX1 Asn98Arg (linchpin hyperactive mutation) that represents a compromise for its many different catalytic activities achieved with various E2 enzymes, and regulators of CRLs including the inhibitor GLMN (Duda et al., 2012). **d,** Cryo-EM reconstructions of neddylated CRL1 β-TRCP1ΔDimer with RBX1 Asn98Arg bound to our newly devised proxies for the UBE2D2~UB–IκBα intermediate. This combination was pursued for high resolution microscopy which yielded a final 3D reconstruction refined to 3.7Å resolution shown below. Clear density for both ubiquitin (circled in orange) and NEDD8 (circled in yellow) are presented.

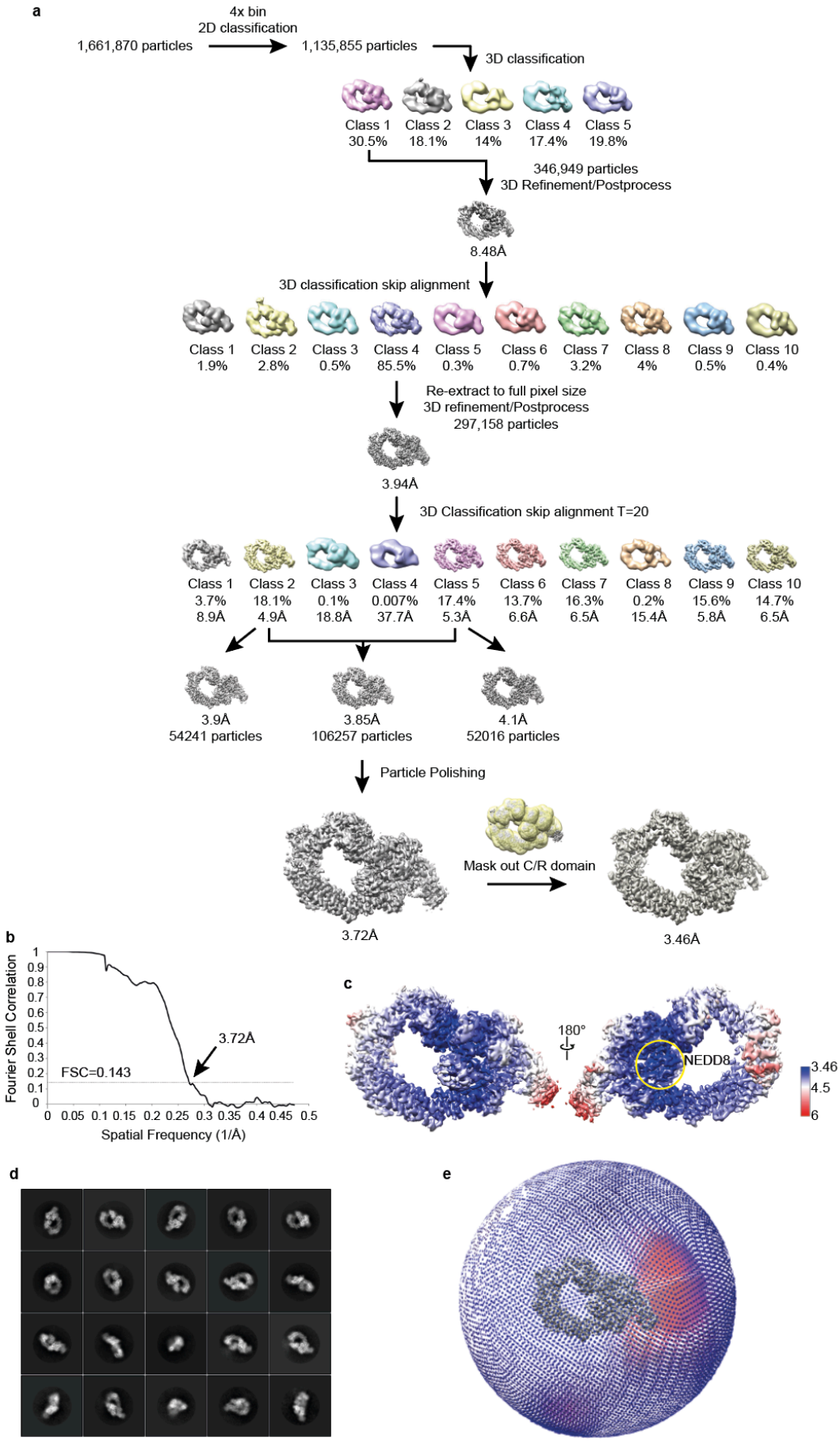
a
4x bin
2D classification
1,661,870 particles
1,135,855 particles
3D classification
Class 1
30.5%
Class 2
18.1%
Class 3
14%
Class 4
17.4%
Class 5
19.8%
346,949 particles
3D Refinement/Postprocess
8.48Å
3D classification skip alignment
Class 1
1.9%
Class 2
2.8%
Class 3
0.5%
Class 4
85.5%
Class 5
0.3%
Class 6
0.7%
Class 7
3.2%
Class 8
4%
Class 9
0.5%
Class 10
0.4%
Re-extract to full pixel size
3D refinement/Postprocess
297,158 particles
3.94Å
3D Classification skip alignment T=20
Class 1
3.7%
8.9Å
Class 2
18.1%
4.9Å
Class 3
0.1%
18.8Å
Class 4
0.007%
37.7Å
Class 5
17.4%
5.3Å
Class 6
13.7%
6.6Å
Class 7
16.3%
6.5Å
Class 8
0.2%
15.4Å
Class 9
15.6%
5.8Å
Class 10
14.7%
6.5Å
3.9Å
54241 particles
3.85Å
106257 particles
4.1Å
52016 particles
Particle Polishing
3.72Å
Mask out C/R domain
3.46Å
b
Fourier Shell Correlation
FSC=0.143
3.72Å
Spatial Frequency (1/Å)
c
180°
NEDD8
3.46
4.5
6
d
e

Figure 3.10: Cryo-EM processing schematic.

a, Cryo-EM processing schematic to yield high resolution structure of neddylated CRL1 β-TRCP1ΔDimer with the ubiquitylation mimic trap. Iterative 2D and 3D classifications and 3D refinements lead to a map of 3.7Å global resolution. Data was processed by RELION. **b,** Gold standard Fourier Shell Correlation curve showing reconstruction of 3.7Å resolution with a 0.143 cutoff. **c,** Map colored by local resolution. Note the highest resolution region is at the center of the map where NEDD8 is located, circled in yellow. **d,** 2D representations of the particles used for final 3D reconstruction. **e,** Angular distribution of the particles used for final 3D reconstruction.

High resolution reconstruction showed clear density revealing all domains, organized within three functional modules. 1) CUL1 and SKP1-β-TRCP formed the previously shown "substrate scaffolding module", 2) RBX1's RING, UBE2D and its linked UB form the "catalytic module", and 3) CUL1's WHB and its linked NEDD8 interact non-covalently in an "activation module" (**Figure 3.11**). The structure shows that NEDD8 positions the catalytic module relative to the substrate scaffolding module while entirely encircled through extensive interfaces throughout the complex. Indeed, NEDD8's central role is highlighted by its corresponding most ordered EM density of the complex (**Figure 3.10c**).

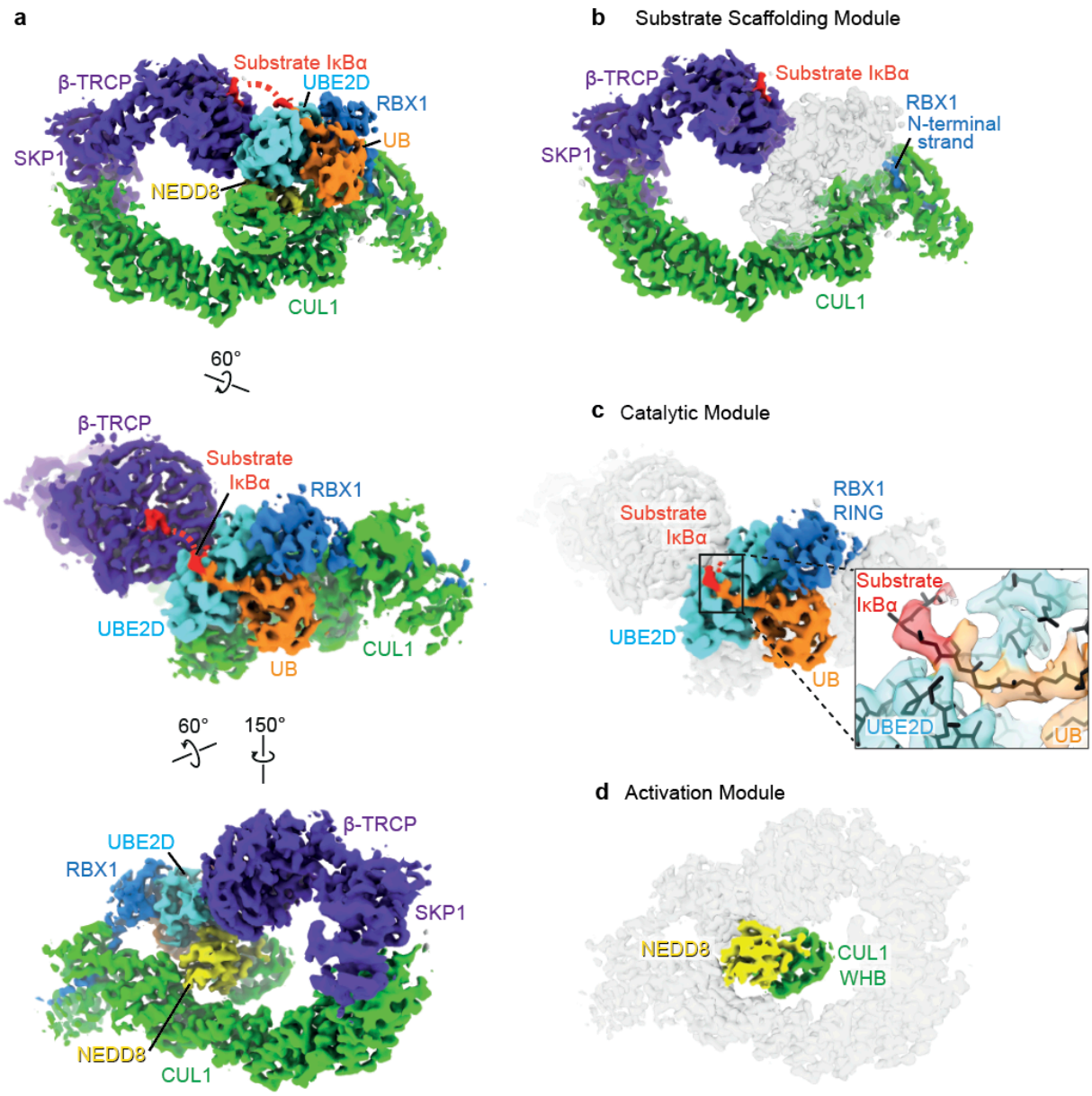

Figure 3.11: Cryo-EM structure of neddylated CRL1 β-TRCP-mediated ubiquitin transfer from to IκBα substrate.

a, Cryo-EM structure representing the neddylated CRL1 β-TRCP-UBE2D~ubiquitin-IκBα substrate intermediate. UBE2D~ubiquitin is activated and juxtaposed with the substrate IκBα peptide. The structure reveals 3 functional modules. **b,** The substrate scaffolding module recruits the substrate via β-TRCP connecting it to the intermolecular cullin-RBX (C/R) domain. **c,** The catalytic module comprises of the noncovalent interactions between RBX1's RING domain, UBE2D, and ubiquitin linked to its active site, which together forms the active "closed" conformation. The inset shows a closeup of the region where the catalytic cysteine of UBE2D, ubiquitin's C-terminus, and the substrate acceptor site adjoins. **d,** The

activation module consists of noncovalent interactions between NEDD8 and the covalently-linked CUL1 WHB domain. Together they locate at the center of the complex harboring numerous interactions to mediate efficient ubiquitylation.

The unprecedented cullin-RING arrangement in our complex representing the neddylated CRL1 β-TRCP–UBE2D~UB–substrate intermediate positions and activates the catalytic center adjacent to the substrate recruited by its substrate receptor. The close proximity in which the catalytic components are adjoined by the activation module explains how rapid ubiquitylation of substrate can be achieved during the priming reaction, and catalyzed by NEDD8. The ≈22 Å distance between IκBα's β-TRCP-bound phosphodegron and the UBE2D~UB active site is compatible with the spacing between this motif and a potential acceptor lysines in many substrates of β-TRCP (**Figure 3.12**) (Low et al., 2014).

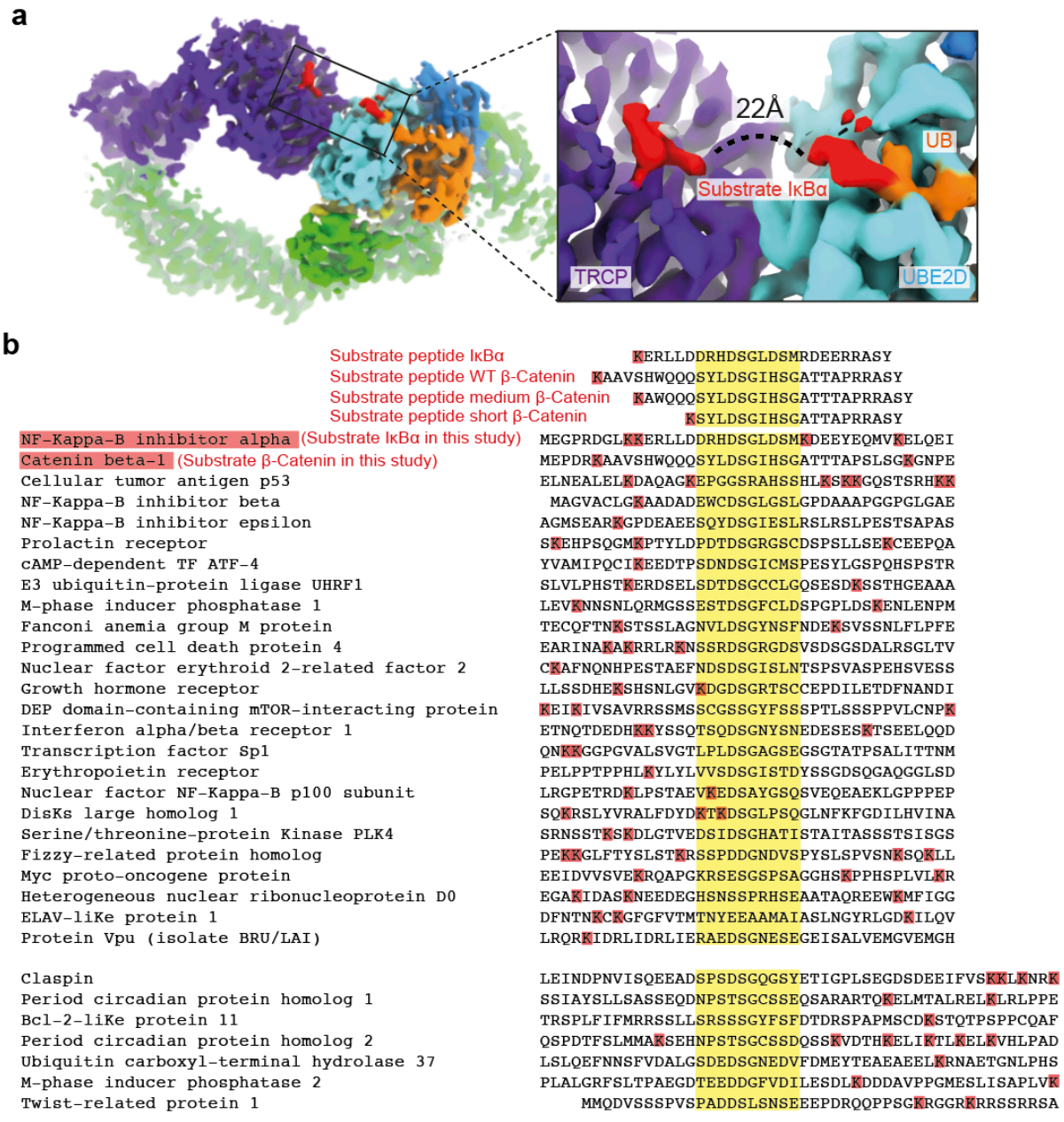

Figure 3.12: Geometry between the phosphodegron and acceptor of substrates.

a, Cryo-EM density highlighting the relative position of the substrate degron and UBE2D~UB active site. The ~22Å distance between UBE2D~UB active site and the phosphodegron of β-TRCP-bound substrate IκBα requires at least 6 connecting amino acids in a substrate. **b,** Sequence alignment for several reported β-TRCP substrates, highlighting the phosphodegron sequence in yellow and all neighboring lysines in red which are potential sites for ubiquitylation. Also shown above are sequences of peptide substrates with a single acceptor Lys that were used in kinetic analyses. These peptide sequences were derived from

phosphorylated IκBα, and from phosphorylated β-catenin with varying lengths between the phosphodegron and the acceptor lysine: WT β-catenin peptide, “medium” β-catenin peptide which harbors a lysine residue at the position corresponding to the lysine of IκBα, and “short” β-catenin peptide with a lysine positioned 5 residues upstream of the N-terminal phosphoserine in the degron. The “short” β-catenin peptide would be too short to bridge the structurally-observed distance between the phosphodegron binding site on β-TRCP and UBE2D catalytic cysteine in the ubiquitylation active site.

The structurally-observed catalytic architecture predicts: 1) peptide substrates with sufficient residue length between the phosphodegron and acceptor lysine to span across ≈22Å should be rapidly primed in a neddylated CRL-dependent manner; 2) peptide substrates with too few residues (4 or less residues) in the spacer to span this gap should be geometrically impaired for priming by neddylated CRL1 β-TRCP and UBE2D. Indeed, the shorter β-catenin peptide was heavily impaired in substrate priming (**Figure 3.13**). However, an addition of ubiquitin could satisfy the geometric constraints and enable further polyubiquitylation, as high molecular weight polyubiquitylated products appeared rapidly.

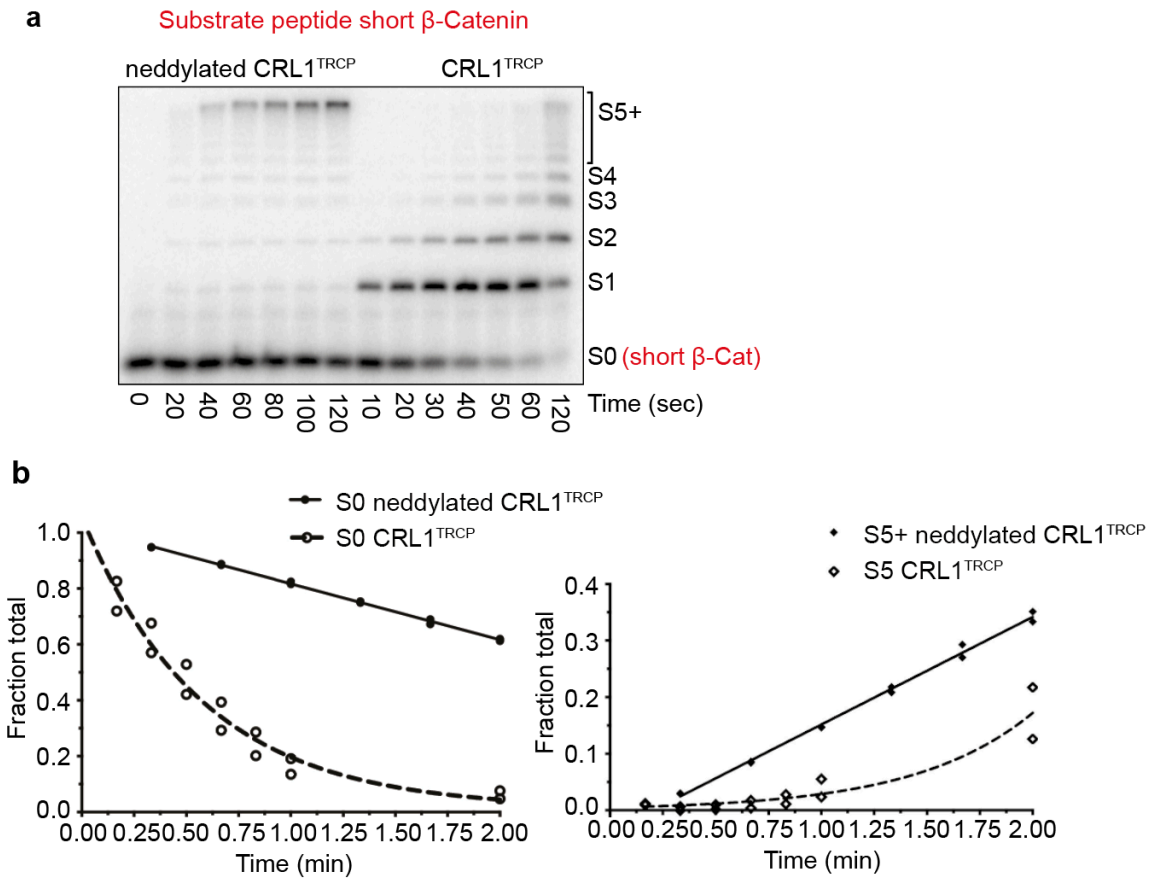

Figure 3.13: Impact of substrate geometry in ubiquitylation.

a, Autoradiogram of SDS-PAGE gel showing products of ubiquitylation reactions under multiple turnover conditions by either neddylated or unneddylated CRL1 β-TRCP. The autoradiogram detects radiolabeled short β-catenin peptide substrate. The amount of short β-catenin peptide modified by neddylated CRL1 β-TRCP and UBE2D in this assay is too low for quantification of kinetic parameters, yet, once a small proportion of this substrate is modified, it is heavily polyubiquitylated. **b,** Plots fitting the consumption of non-ubiquitylated short β-catenin peptide substrate (S0) compared to formation of polyubiquitin chains with 5 or more UBs (S5+) from reactions as shown in panel a.

The catalytic module

In the catalytic module, RBX1 RING binds UBE2D and its linked ubiquitin in the canonical RING-activated "closed" conformation, where the noncovalent interactions between UBE2D and ubiquitin allosterically activate the thioester bond. Compared to the isolated RING-UBE2D~UB structures (Dou et al., 2012b; Plechanovova et al., 2012; Pruneda et al., 2012), additional density corresponding to the substrate intermediate traverses a potential target's trajectory to the ubiquitylation active site (**Figure 3.14**). The chemical trap superimposes with consensus acceptors visualized in active sites of sumoylation and neddylation intermediates, where neighboring aromatic side-chains guide the acceptor lysine target (Scott et al., 2014; Yunus and Lima, 2006). However, UBE2D's myriad substrates neither conform to a specific motif, nor do they display specific side-chains that guide lysine acceptors into the catalytic center. Instead, in the neddylated CRL1 β-TRCP–UBE2D~UB–substrate complex, density from backbone atoms of the substrate preceding the chemical proxy for the acceptor lysine occupies the locations that correspond to the aromatic guides seen in sumoylation and neddylation intermediates (**Figure 3.14 inset**). It is possible that the polypeptide backbone assistance in projecting the target lysine into the active site may contribute to UBE2D's ability to ubiquitylate a broader range of substrates (Brzovic and Klevit, 2006).

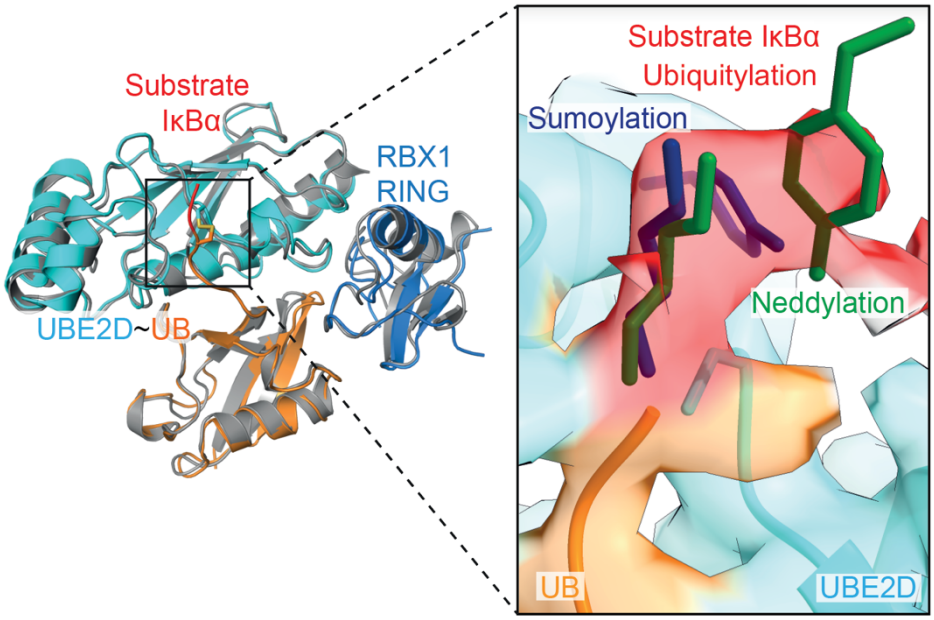

Figure 3.14: Catalytic module of substrate ubiquitylation

Superposition of the catalytic module from the structure representing the neddylated CRL1 β-TRCP-UBE2D~UB- IκBα intermediate matches well with a prior structure of an isolated RING-E2~UB complex (grey, PDB ID 4AP4) (Dou et al., 2012b; Plechanovova et al., 2012; Pruneda et al., 2012). The superposition also highlights that the new structure representing active ubiquitylation shows the density for the covalently-linked proxy from the IκBα substrate's acceptor juxtaposed at the active site shown in red. In the inset, the density (red) for this is shown along with relative positions of the sumoylation (blue) and neddylation (green) acceptor lysines and their aromatic guide residues (Scott et al., 2014; Yunus and Lima, 2006).

The activation module

The activation module, located at the heart of the complex, enables NEDD8 to choreograph the substrate scaffolding and catalytic module. The module itself is an unprecedented globular unit comprised of NEDD8 and its covalently linked CUL1 WHB domain. NEDD8's hydrophobic patch that involves residues Ile36/Leu71/Leu73 and the C-terminal tail form a groove embracing the hydrophobic face of the isopeptide-bound CUL1 helix (**Figure 3.15**). At the center of this hydrophobic interface, NEDD8's Gln40 contacts CUL1 backbone atoms, the isopeptide bond, and NEDD8's C-terminal tail in a buried polar interaction typical of those organizing apolar interfaces (Lumb and Kim, 1995). This provides an explanation for how enteropathogenic bacterial effectors such as Cif catalyzes Gln40 deamidation impair CRL1-dependent ubiquitylation (Cui et al., 2010; Jubelin et al., 2010; Morikawa et al., 2010; Yu et al., 2015). The resultant negative charge by deamidation would shatter the CUL1-NEDD8 interface. Indeed, ubiquitylation of IκBα by neddylated CRL1 β-TRCP with a NEDD8 Q40E mutation was severely impaired in substrate priming, underscoring the interface formation of the activation module by NEDD8 and CUL1 WHB (**Figure 3.16**).

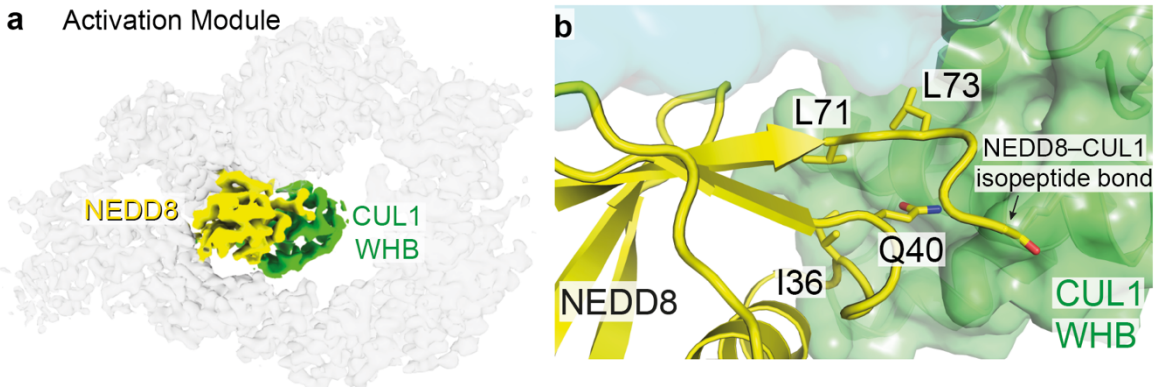

Figure 3.15: Activation module

a, The activation module density shown at the center of the entire structure representing neddylated CRL1 β-TRCP-UBE2D~UB- IκBα intermediate. **b,** Close-up of NEDD8's buried polar residue including Gln40 and the hydrophobic patch involving Ile36/Leu71/Leu73. NEDD is covalently linked to CUL1's WHB domain at its lysine 720 residue by a isopeptide linkage. At the center of the activation module, NEDD8's Gln40 faces directly towards CUL1's WHB domain.

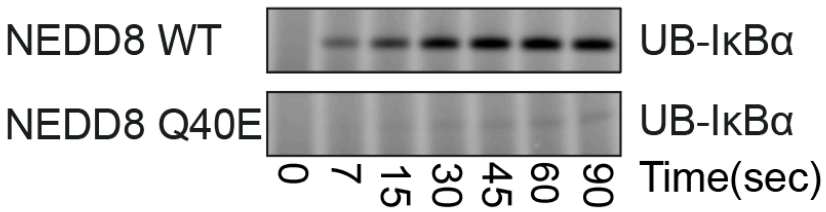

Figure 3.16: NEDD8 Gln40 deamidation

Mutating NEDD8's Gln40 to Glu, which mimics the deamidation effects caused by bacterial effectors that hijack cullin-RING ligases, causes several defects in ubiquitylating substrate IκBα by neddylated CRL1 β-TRCP and UBE2D.

NEDD8 Loop-in and Loop-out

NEDD8 and ubiquitin both contain a common Leu8-containing β1/β2-loop. While previously not well characterized, the Leu8 loop seemingly had conformational correlation according to its bound locations. When NEDD8 or ubiquitin was bound at the donor site linked to the catalytic cysteine of E2 enzymes, the Leu8 loop normally adopts the "Loop-in" conformation. However, a recent study showed that ubiquitin can also bind to the backside of UBE2D, adopting an alternative "Loop-out" conformation (Buetow et al., 2015). Comparing the conformation of NEDD8 and ubiquitin from the structure representing neddylated CRL1 β-TRCP-UBE2D~UB- IκBα intermediate, we could also see the same correlation previously seen (**Figure 3.17**).

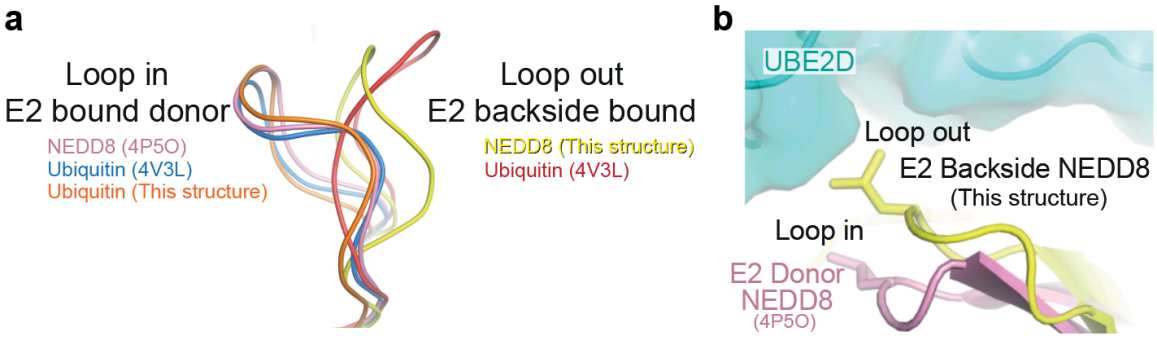

Figure 3.17: NEDD8 and ubiquitin adopts "loop-in" and "loop-out" conformations. **a,** Comparison of the β1/β2-loop conformations of various NEDD8 and UB structures from this study and previous structures. While NEDD8 and UB can adopt both "loop-in" and "loop-out" conformations, NEDD8 and UB at the donor site linked to the E2 active site in RING activated complexes adopt the "loop-in" conformation. Those that are bound to UBE2D backside adopt "loop-out" conformations. **b,** Close-up of UBE2D and NEDD8 showing role of the NEDD8 loop-out conformation for sensing UBE2D's backside, in comparison to NEDD8 bound at the donor site adopting the loop-in conformation (PDB ID 4P5O).

NEDD8's noncovalent interactions with CUL1's WHB domain sculpt its fold and surface properties by requiring the formation of a "Loop-out" orientation of the NEDD8 Leu8-containing β1/β2-loop. In the alternative "Loop-in" conformation, which was previously observed in the structure representing CUL1 neddylation in action, NEDD8's

Leu8 filling the Ile36 hydrophobic patch would preclude interactions with CUL1's WHB domain.

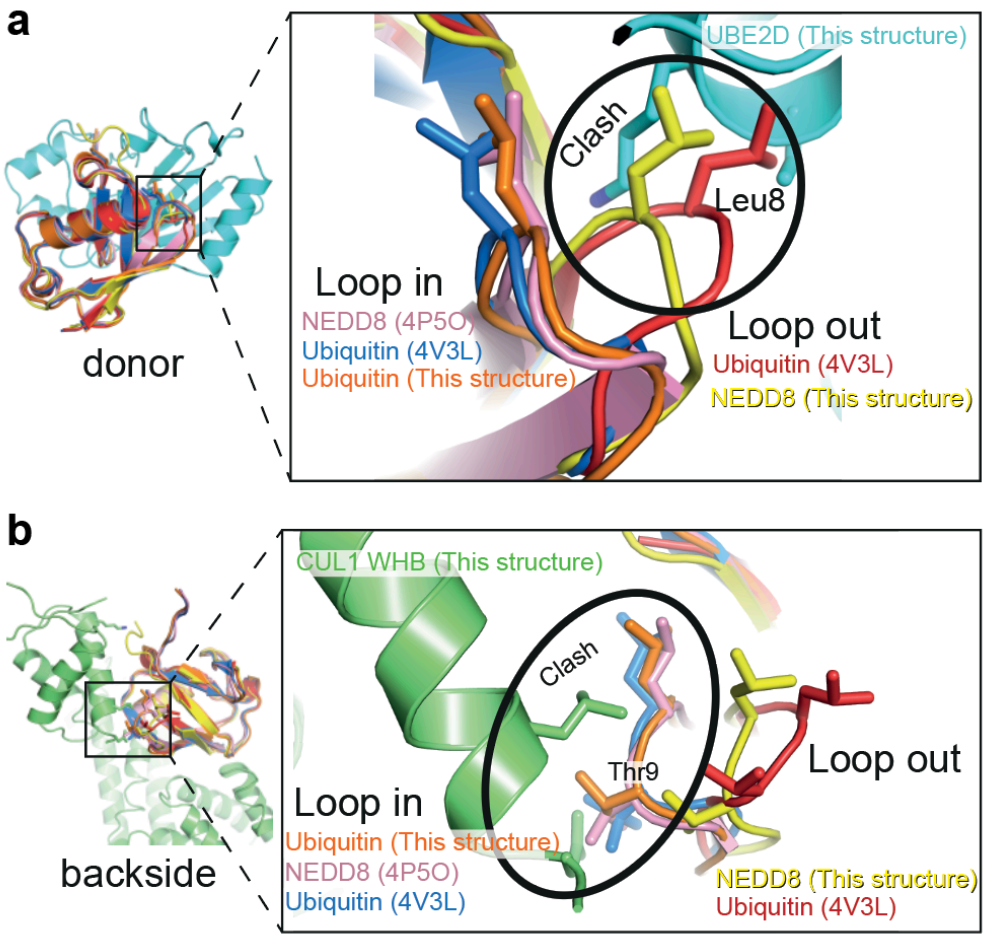

Figure 3.18: NEDD8 and Ubiquitin's Leu8 loop conformation by location.
a, When NEDD8 and Ubiquitin are located at the donor site, only the "loop-in" conformation is compatible, as the "loop-out" conformation clashes with the central helix of E2, in this case UBE2D. **b,** When NEDD8 and Ubiquitin are located at the backside of UBE2D, only the "loop-out" conformation is compatible as the "loop-in" conformation clashes with the isopeptide linked CUL1's WHB domain.

Interactions between the activation and catalytic modules

Although it has been perceived that different conformations of UB and UB-like proteins influence protein-protein interactions, UB-binding domains selecting between "Loop-in" or "Loop-out" orientations of the Leu8-containing β1/β2-loop has been largely unknown as to how these conformations might simultaneously impact multiple interactions (Hospenthal et al., 2013). Our data shows in the context of a fully assembled complex of ubiquitylation in action that NEDD8 must adopt the Loop-out conformation to both form the activation module and to engage the catalytic module via the backside of UBE2D. NEDD8's conformation apparently serves as a coincidence detector, coupling noncovalent binding to its linked CUL1 WHB domain and to the catalytic module (**Figure 3.17-18**).

NEDD8's hydrophobic patch involving Ile44 binds the "backside" of UBE2D, which centers around residue Ser22 that is located at the complete opposite side from the ubiquitylation active site (**Figure 3.19**). The structure of ubiquitylation by β-TRCP finally solves the mystery of how neddylation can assist CRL1 β-TRCP recruit UBE2D in cells (Kawakami et al., 2001). Previous CRL structures were unable to explain how NEDD8 can be simultaneously linked to a cullin and also bind the backside of UBE2D that is engaging the RBX1 (Duda et al., 2008; Sakata et al., 2007; Zheng et al., 2002b). Indeed, when mutating key residues at the interface between the activation module and the catalytic module, ubiquitylation activity is severely hampered in the attenuated pulse-chase format assay (**Figure 3.19**).

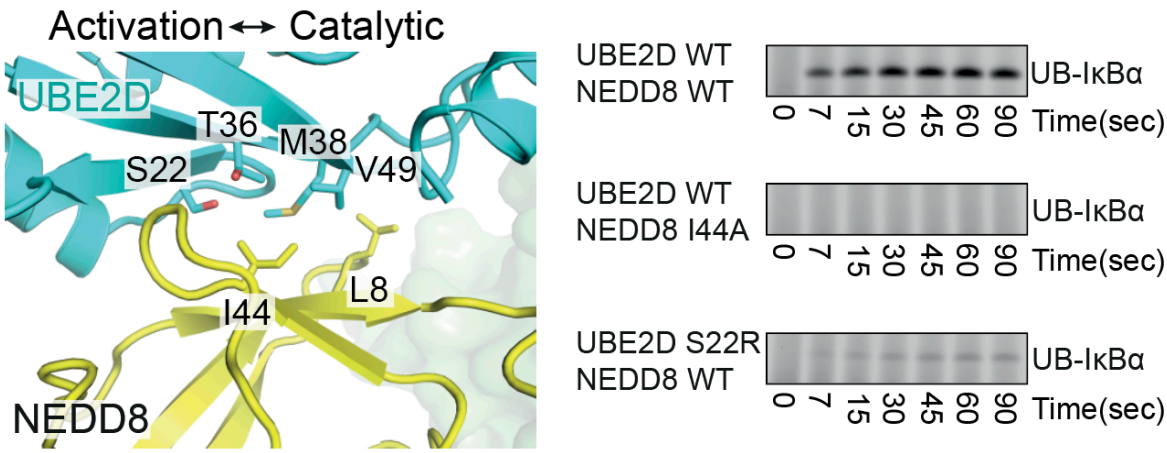

Figure 3.19: Interface between NEDD8 hydrophobic patch and UBE2D backside. Close-up at the interface between NEDD8 and UBE2D backside showing key residues involved in the interaction. Effects of mutations from either NEDD8 Ile44Ala or UBE2D Ser22Arg, which would disrupt the interface between the catalytic module and the activation module, are shown by substrate-priming assays on the right in comparison to wild-type activity at indicated timepoints.

The contacts shown in the structure representing neddylated CRL1 β-TRCP-UBE2D~UB-IκBα intermediate between NEDD8 and the catalytic module resemble to those previously described for either free NEDD8 or ubiquitin binding to UBE2D, which were thought to somehow allosterically activate the intrinsic reactivity of a UBE2D~UB intermediate (Brzovic et al., 2006; Buetow et al., 2015; Ozkan et al., 2005; Sakata et al., 2007). Although this is often tested by monitoring RING-dependent discharge of UB from UBE2D to free lysine, CRL-dependent activity is limited in this assay due to sequence requirements for RBX1 RING binding to many partners in addition to UBE2D (Duda et al., 2012; Scott et al., 2016; Yunus and Lima, 2006). Nonetheless, using a previously-described hyperactive mutant (Scott et al., 2014), along with high enzyme and lysine concentrations, we found that the substrate-independent ubiquitin transferase activity is impaired by UBE2D mutations that would disrupt interactions with its covalently-linked UB, the RING domain or NEDD8, and the by the NEDD8 Q40E mutation disrupting the activation module (**Figure 3.20-23**). Thus, the architecture observed in the neddylated CRL1 β-TRCP–UBE2D~UB–substrate intermediate structure may well contribute to both stimulating reactivity of the UBE2D~UB intermediate as well as positioning the catalytic center in proximity of the β-TRCP-bound substrate for efficient ubiquitylation.

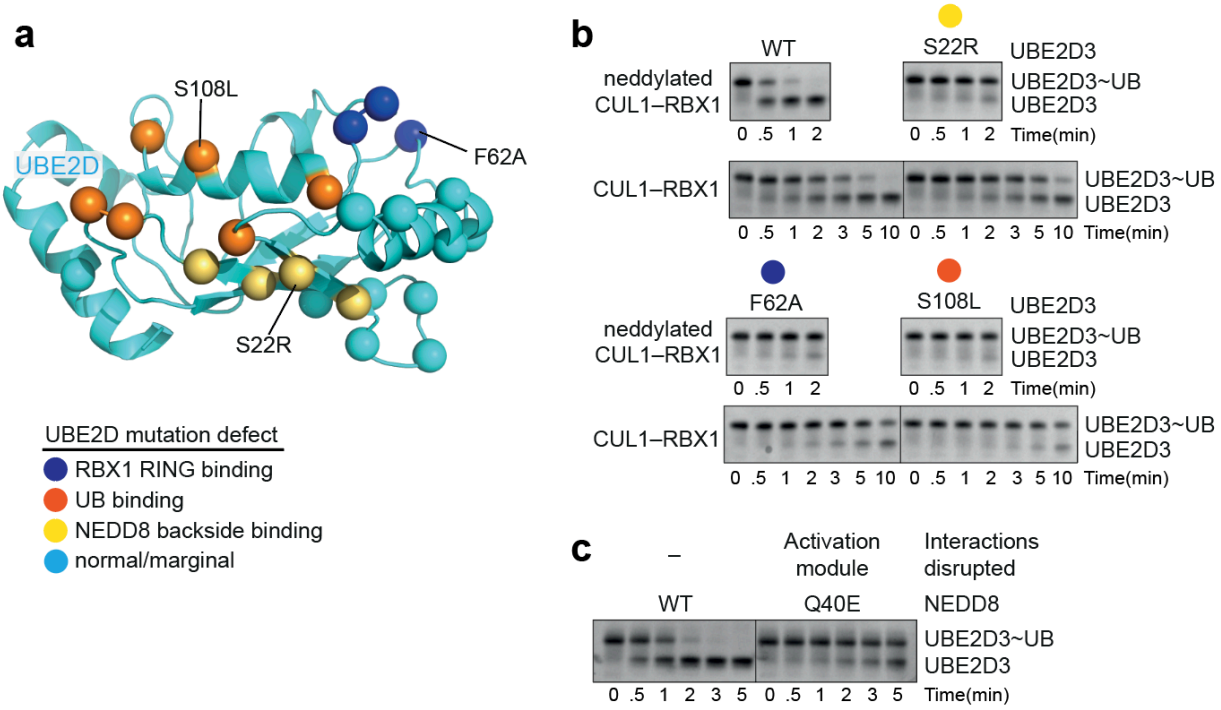

Figure 3.20: Key interfaces residues mediated by the catalytic module

a, Locations of mutations shown as spheres on UBE2D from the structure representing neddylated CRL1 β-TRCP-UBE2D~UB-IκBα intermediate, colored by effects and locations on UBE2D~UB discharge to free lysine. Mutations with marginal or no effect are shown in cyan, whereas those with major effects are color coded accordingly. Mutations causing major defects in the RBX1 RING-binding site are in blue, the interaction surface with the donor ubiquitin in orange, and the interaction surface with NEDD8 backside binding in yellow. **b,** Reactions monitoring substrate-independent discharge of ubiquitin from a preformed UBE2D~UB thioester to free lysine, in presence of either neddylated or unneddylated CUL1-RBX1 harboring the Asn98Arg mutation, shown in coommassie-stained SDS-PAGE. **c,** Same as in **b** except testing effect of NEDD8 Gln40Glu mutation, which disrupts the activation module itself.

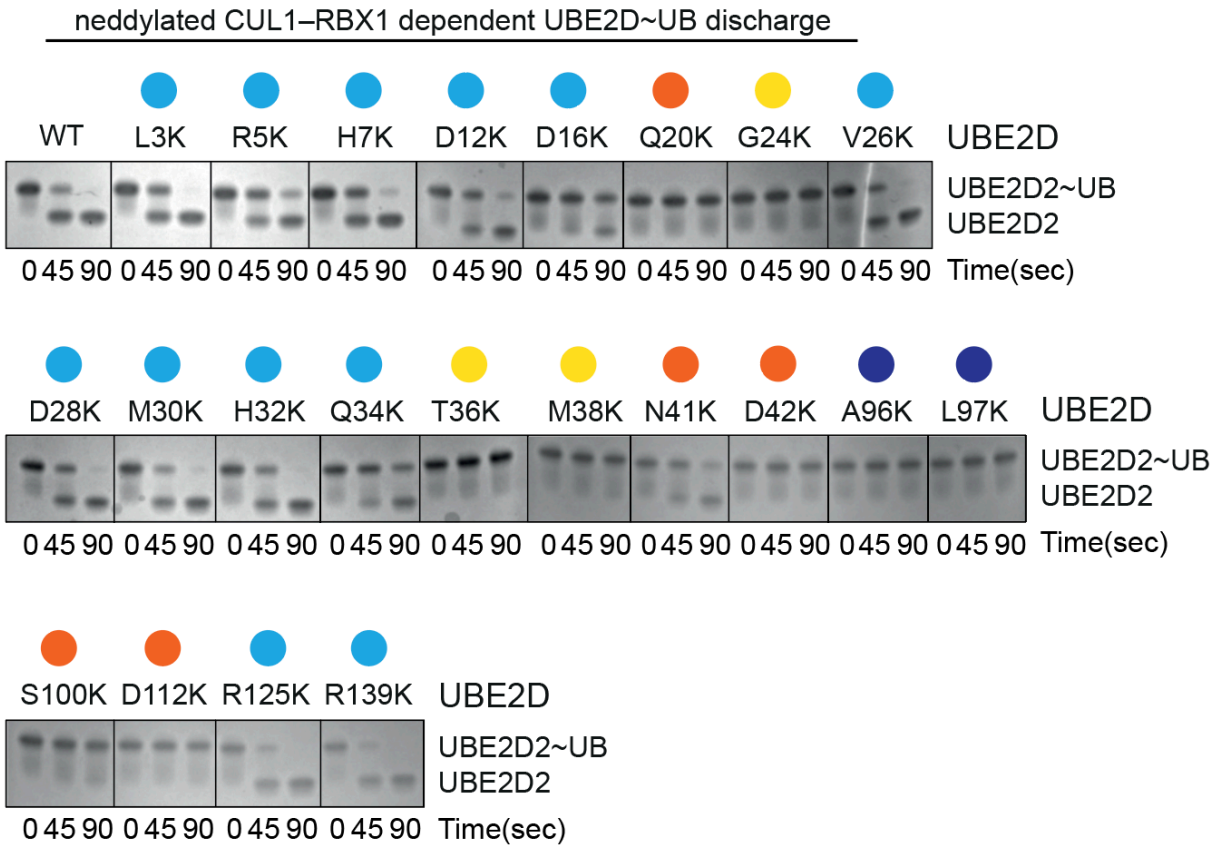

Figure 3.21: Neddylated CUL1-RBX1 N98R dependent UBE2D~UB discharge with various UBE2D2 mutants

Reactions monitoring substrate-independent discharge of ubiquitin from preformed UBE2D~UB thioester variants with indicated mutations of UBE2D2 to free lysine as in Figure 3.20, in presence of neddylated CUL1-RBX1 harboring the Asn98Arg mutation, shown in coommassie-stained SDS-PAGE. Each mutant is marked by color codes that indicate specific defects based on the structure representing neddylated CRL1 β-TRCP-UBE2D~UB-IκBα intermediate shown as in Figure 3.20a.

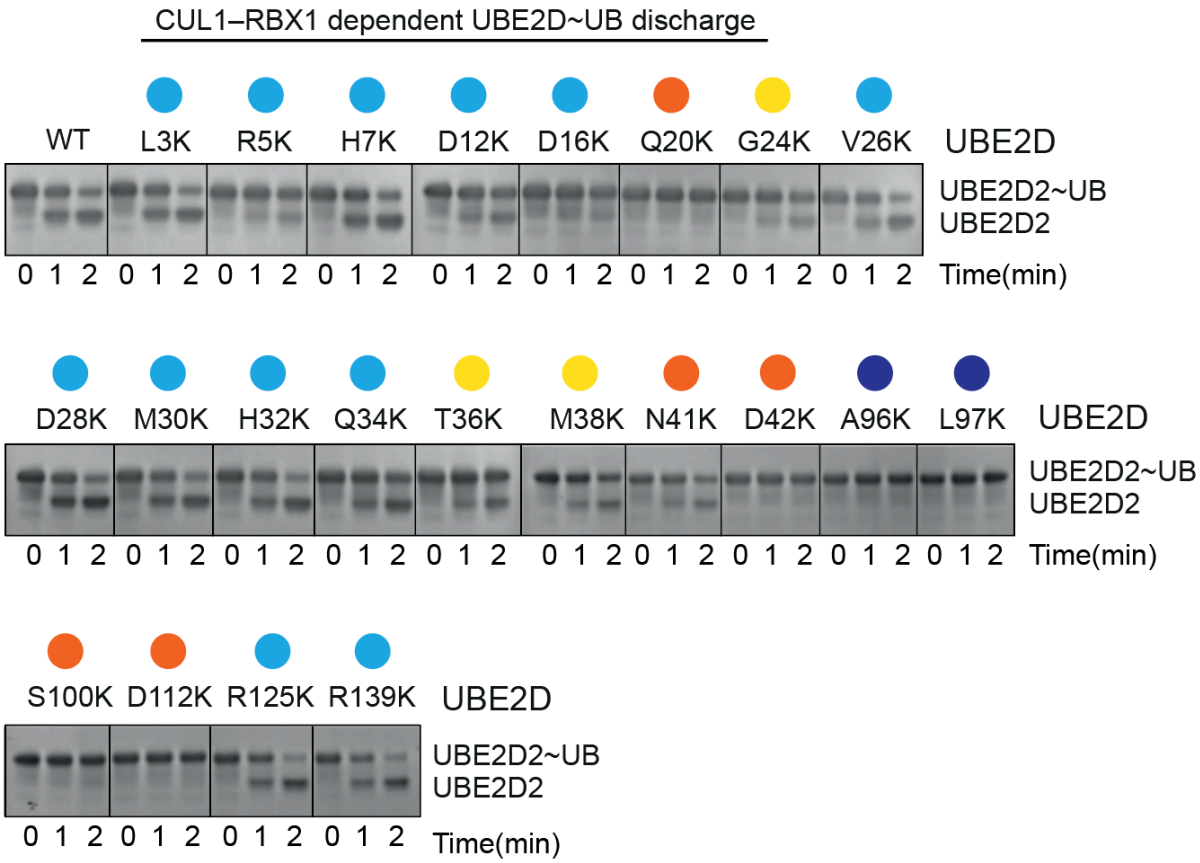

Figure 3.22: Unneddylated CUL1-RBX1 N98R dependent UBE2D~UB discharge with various UBE2D2 mutants

Reactions monitoring substrate-independent discharge of ubiquitin from preformed UBE2D~UB thioester variants with indicated mutations of UBE2D2 to free lysine as in Figure 3.20, in presence of unneddylated CUL1-RBX1 harboring the Asn98Arg mutation, shown in coommassie-stained SDS-PAGE. Each mutant is marked by color codes that indicate specific defects based on the structure representing neddylated CRL1 β-TRCP-UBE2D~UB-IκBα intermediate shown as in Figure 3.20.

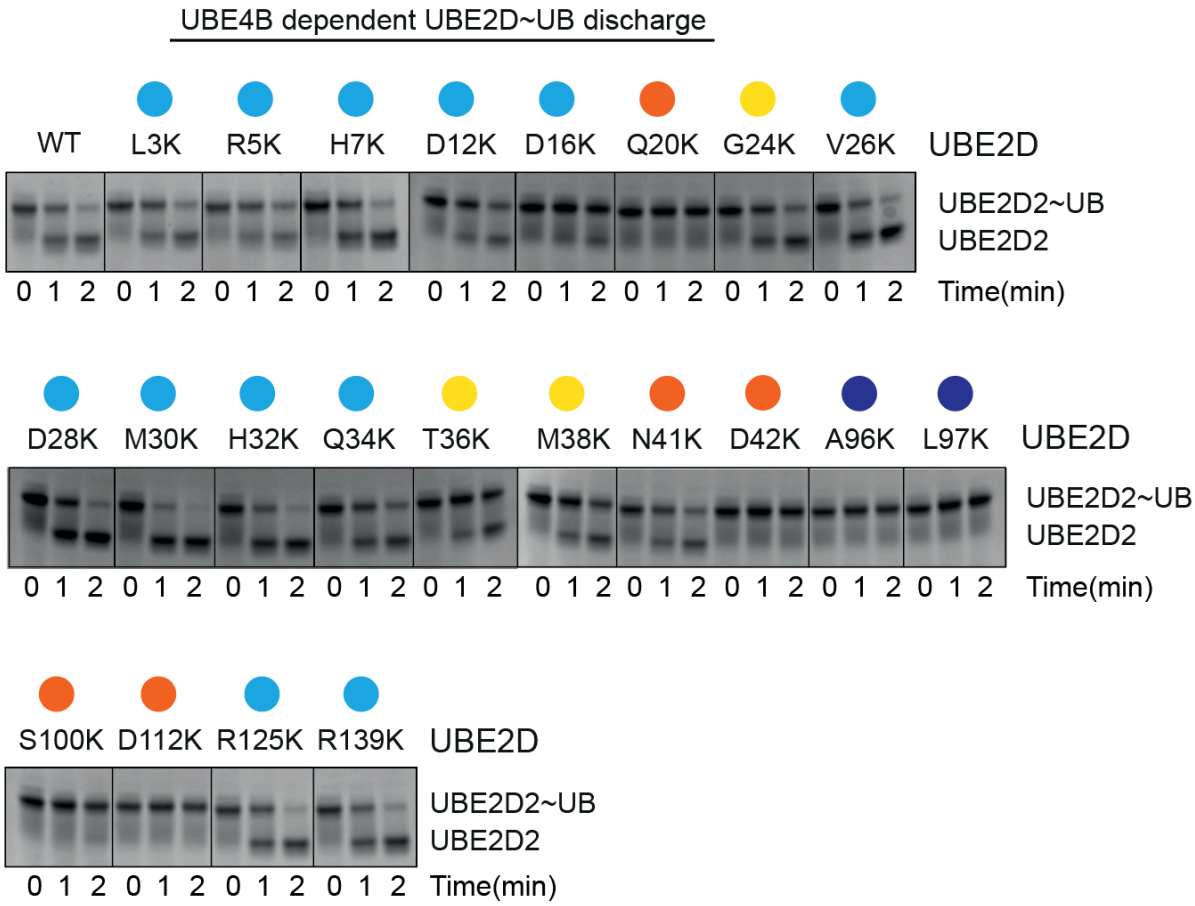

Figure 3.23: UBE4B dependent UBE2D~UB discharge with various UBE2D2 mutants
Reactions monitoring substrate-independent discharge of ubiquitin from preformed UBE2D~UB thioester variants with indicated mutations of UBE2D2 to free lysine as in Figure 3.20, in presence of UBE4B, a U-box RING E3 to show effects of these mutations in the absence of the CRL architecture. Assays are shown in coommassie-stained SDS-PAGE. Each mutant is marked by color codes that indicate specific defects based on the structure representing neddylated CRL1 β-TRCP-UBE2D~UB-IκBα intermediate shown as in Figure 3.20a.

Interactions between activation and substrate scaffolding modules

NEDD8, located at the heart of the active CRL architecture, also binds the substrate scaffolding module, through its residues involving Leu2, Lys4, Glu14, Asp16, Arg25, Arg29, Glu32, Gly63 and Gly64 that is nestled in a complementary concave surface of CUL1 (**Figure 3.24**). Notably, while NEDD8 and UB share ~58% sequence homology, these indicated residues of NEDD8, which are at the interface of CUL1's scaffolding module, differ in UB, accounting for nearly one-third of the variations between them (**Figure 3.25**). Moreover, their UB counterparts would be predicted to repel CUL1. Replacing NEDD8 with UB Arg72Ala that is competent for ligation to CUL1 by allowing ubiquitin to utilize NEDD8's E1 enzyme, or with a version swapping six key interface residues for those in UB, substantially impaired substrate priming in our assay, rationalizing a need for NEDD8 as a distinctive UB-like protein (**Figure 3.26-27**).

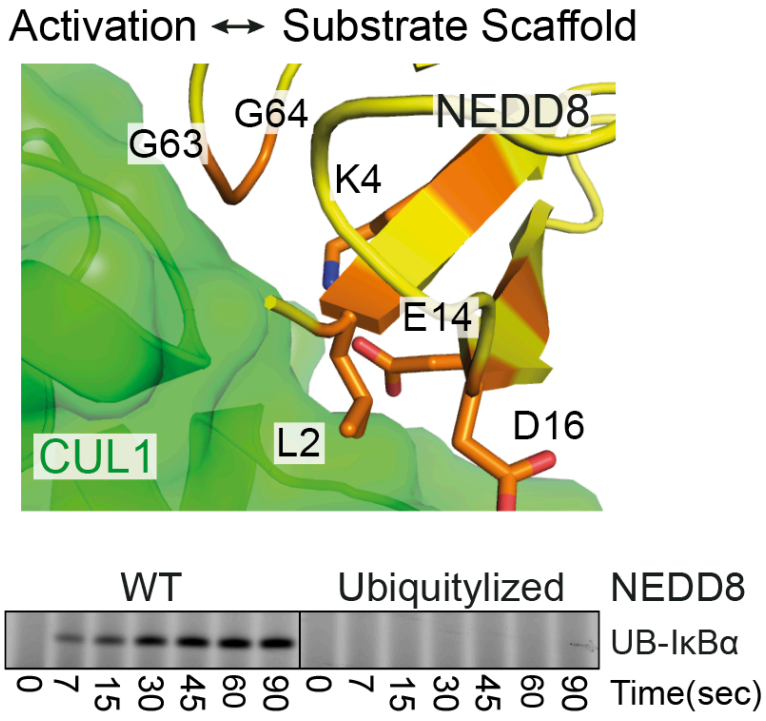

Figure 3.24: Interface between NEDD8 and CUL1 scaffold

Close-up of the interface between substrate scaffolding module and NEDD8 highlighting the NEDD8 residues that differ in comparison with ubiquitin, with effects of CUL1 modification by a "Ubiquitylized" NEDD8 mutant with six residues swapped for UB counterparts (Leu2Gln Lys4Phe Glu14Thr Asp16Glu Gly63Lys Gly64Glu) shown on the bottom in ubiquitylating substrate IκBα.

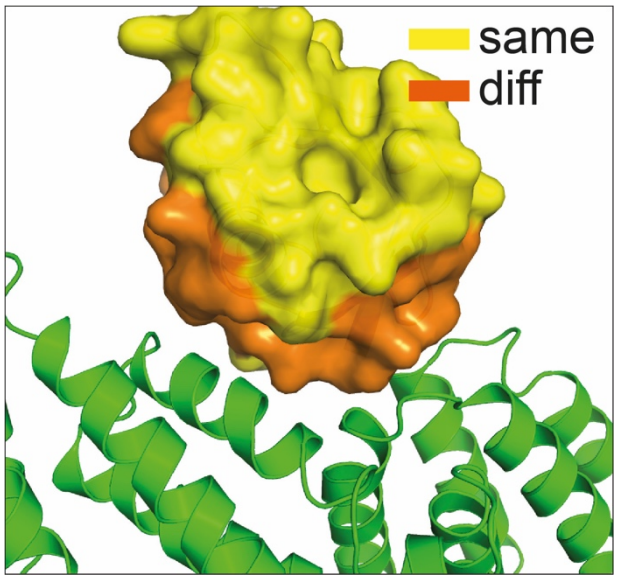

Figure 3.25: Residue conservation between NEDD8 and Ubiquitin

Surface representation of NEDD8 shown at the interface of the scaffolding module, colored by conservation of sequence between NEDD8 and ubiquitin. Parts that are colored in yellow have same residues with ubiquitin, whereas the parts colored in orange are residues that differ between NEDD8 and ubiquitin. Notably, the parts that are colored in orange, which differ between NEDD8 and ubiquitin, face CUL1's scaffolding module. This explains why a ubiquitylated CRL cannot function the same way as a neddylated CRL.

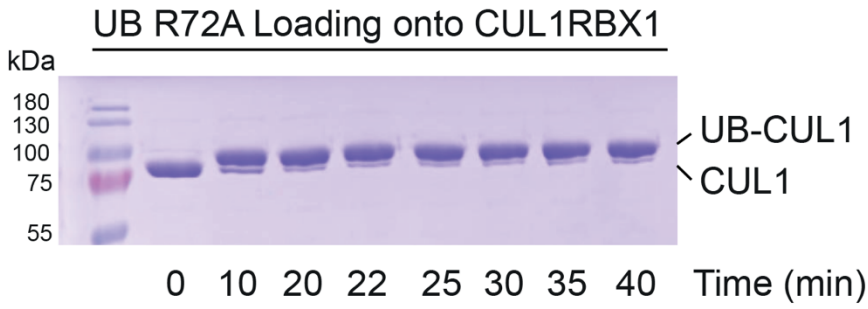

Figure 3.26: Generating Ubiquitylated CUL1-RBX1

In order to create a ubiquitylated CUL1-RBX1, Ubiquitin requires a Arg72Ala mutation to allow engaging it's C-terminal tail through the NEDD8 E1, APPBP1-UBA3. With the mutation, ubiquitin is readily loaded onto CUL1-RBX1 with slightly longer timepoints in comparison to NEDD8.

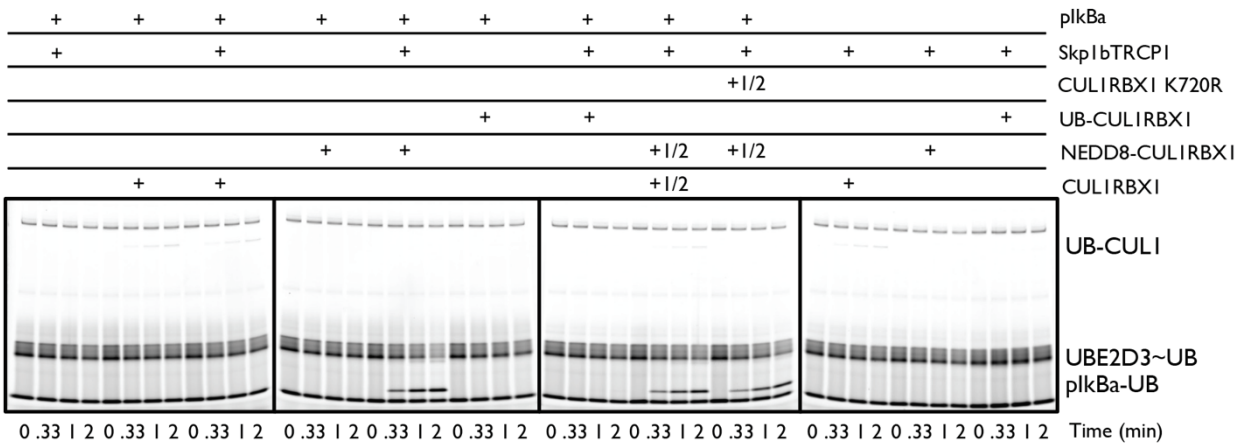

Figure 3.27: Ubiquitylation activity assay comparing Ubiquitylated CRL, neddylated CRL, and unneddylated CRL.

Substrate priming pulse-chase assay showing IκBα ubiquitylation mediated by CRL1 β-TRCP comparing ubiquitylated CUL1, neddylated CRL, and unneddylated CUL1. Unneddylated CRL harbors a Lys720Arg mutation to prevent ubiquitylation of its neddylation site. While neddylated CRL1 β-TRCP efficiently ubiquitylates substrate IκBα, ubiquitylated or unneddylated CRL1 β-TRCP does not seem to target substrate in these conditions.

Interactions between catalytic and substrate scaffolding modules

The catalytic module abuts both CUL1-RBX1 and substrate-receptor side of the substrate scaffolding module. At one end, RBX1's RING stacks on RBX1's C/R domain Trp35 side-chain. This is consistent with complex effects reported for an RBX1 Trp35Ala mutation, reducing UBE2D-mediated substrate priming while enabling polyubiquitylation by neddylated CUL1 (Scott et al., 2014). While RBX1 RING adopts multiple orientations according to its stages of functionality, Trp35 side-chain remains the same orientation, further emphasizing its function as a pivot point of the RING domain (**Figure 3.28-29**). At the other end of the catalytic module, UBE2D's curved β-sheet complements β-TRCP's propeller domain (**Figure 3.30**). UBE2D's His32 forms hydrogen bonds with backbone atoms from the loop following β-TRCP's blade-2. Accordingly, a UBE2D His32Ala mutant presents a mild defect in our substrate priming assay. Notably, a parallel role of UBE2D's His32 was previously observed in PRC-dependent histone H2A monoubiquitylation, suggesting common roles in some pathways employing this E2 ubiquitin carrying enzyme (McGinty et al., 2014).

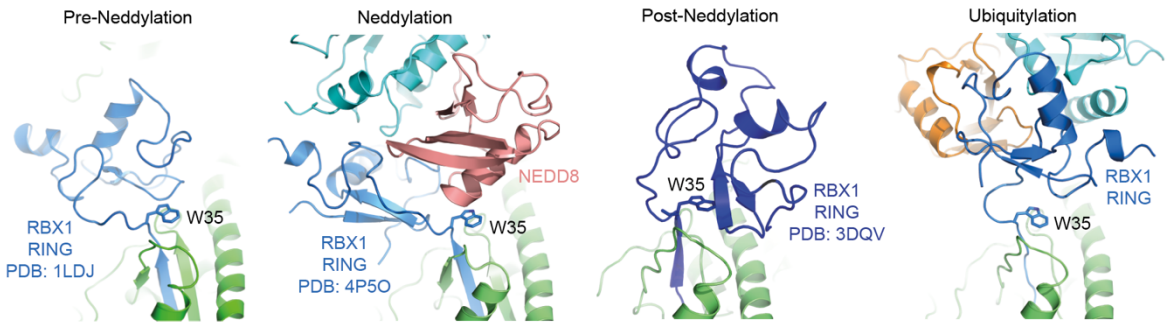

Figure 3.28: Conformational changes of RBX1 ring during neddylation and ubiquitylation.

Comparison of relative RBX1 RING domain locations in different CRL complexes after superposition of the C/R domains from the crystal structures of CUL1-RBX1 (PDB ID 1LDJ, "Pre-Neddylation", the structure representing the "Neddylation" reaction (PDB ID 4P5O), and the structure of a neddylated CUL5-RBX1 (PDB ID 3DQV, "Post-Neddylation", which revealed the potential for neddylated CUL WHB and RBX1 RING domain with dramatic conformational changes), and the structure representing "active ubiquitylation" presented here showing how the neddylated CUL1 WHB domain and RBX1 RING are harnessed in a

catalytic architecture. RBX1's Trp35 is highlighted in all structures to show it serving as a multifunctional platform for the different orientations of the RBX1 RING domain.

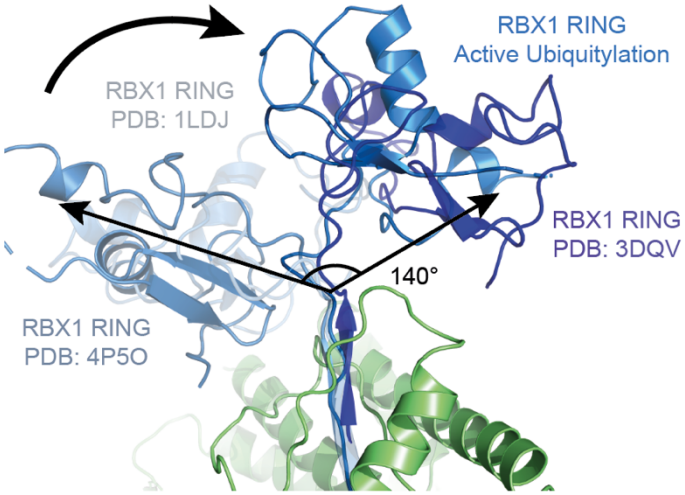

Figure 3.29: Dynamic orientations of the RBX1 RING domain.
Superposition of the structures of different CRL complexes shown in Figure 3.28, highlighting relative RING positions that differ significantly between each step.

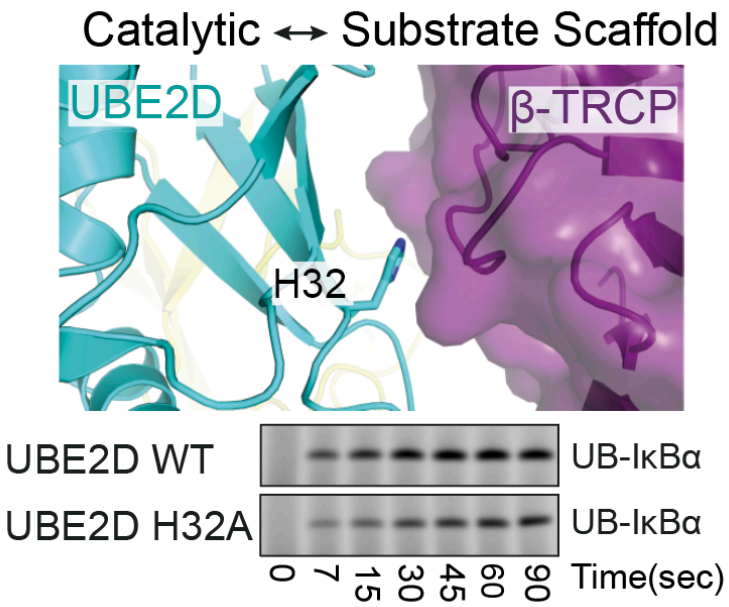

Figure 3.30: Interface between the catalytic module and the substrate scaffolding module.

Zoom-in of the interface between UBE2D and β-TRCP, whereby residue His32 of UBE2D makes a minor contact with β-TRCP. When mutating His32 to Ala, an extremely minor defect can be observed in the pulse-chase format of ubiquitylation. However, when combined with other mutations at different interfaces, it shows severe defects in kinetics (data not shown).

Dynamics of the CUL1 WHB domain

CUL1's WHB domain has been shown to also adopt various orientations in the structure of a neddylated CUL1 (Duda et al., 2008). Also in the structure representing "active ubiquitylation", the WHB domain samples yet another orientation to juxtapose its covalently linked NEDD8 to present the activation module (**Figure 3.31**). However, not only was the conformation substantially different, the domain itself was projecting a further distance that was not achievable while maintaining the helical structure of the connecting helix 29. Indeed, the cryo-EM density showed only patchy density of helix 29 which hinted that the rod-like helix29 no longer exists as a helix. It seems that CUL1's helix 29 dissolves into a flexible tether, which would also rationalize the previously observed proteolytic sensitivity of this region in a neddylated CUL1-RBX1 complex (**Figure 3.32**) (Duda et al., 2008).

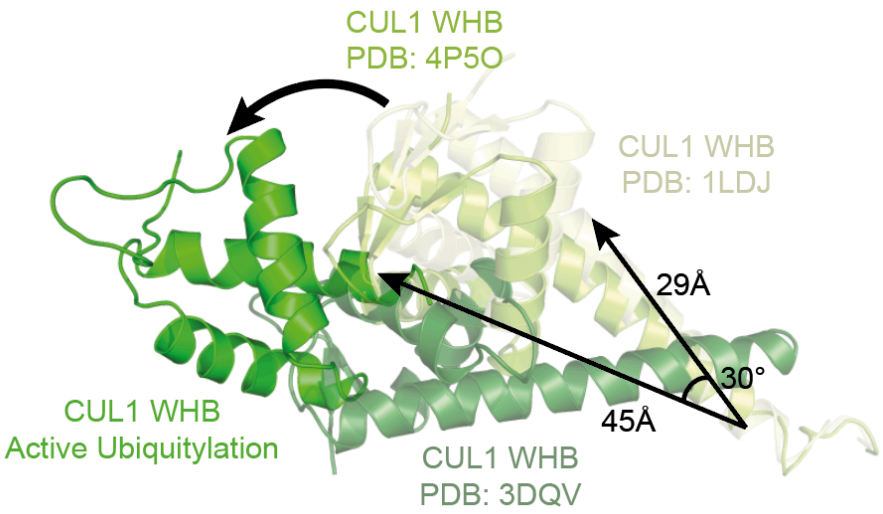

Figure 3.31: Dynamic orientation of CUL1 WHB domain.
CUL1's WHB domain is shown in multiple orientations from structures of CUL1. CUL1-RBX1 alone, CUL1 during neddylation, CUL1 post-neddylation, and CUL1 during active ubiquitylation all adopt different orientations of CUL1 WHB.

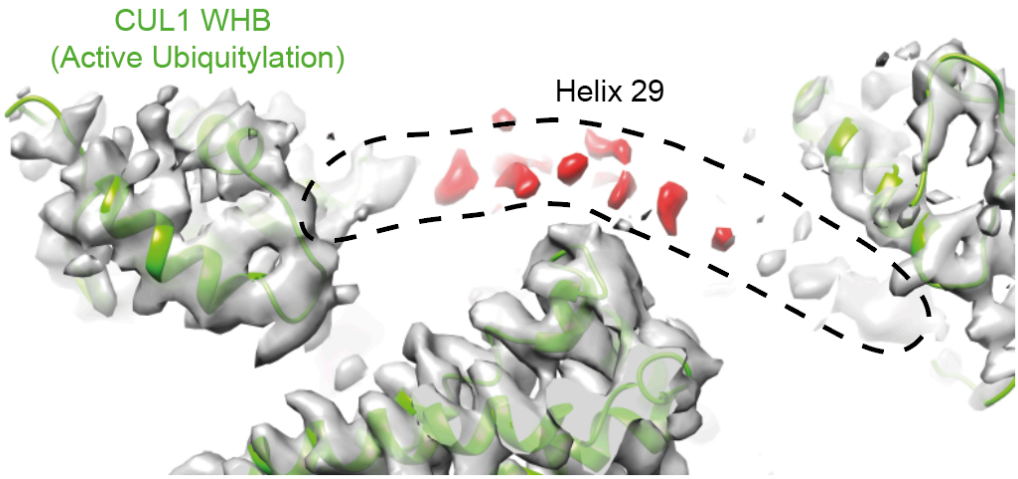

Figure 3.32: CUL1 Helix 29's flexibility to juxtapose the WHB domain.

In the structure of "active ubiquitylation", the ensuing helix 29 from the CUL1 WHB domain seems to have melt to orient the activation module harboring CUL1's WHB domain and its linked NEDD8. Shown here is the cryo-EM density of this region, where highlighted in red with dotted lines indicates the patchy density of CUL1 helix 29 shown.

Potential Mechanism of other CRLs

Conservation of WHB domain residues mediating interactions with NEDD8 suggests that similar mechanistic principles may apply to some other CRLs (**Figure 3.33**). Although future studies will be required to visualize the precise structural basis for NEDD8 activation of substrate priming by other CRLs, sequence alignment of WHB domains of CUL1, CUL2, CUL3, CUL4A, CUL4B and CUL5 showed significant conservation of residues except CUL5. While CUL2, CUL3, CUL4A, and CUL4B showed potential to adopt the configuration of the activation module shown in the neddylated CRL1 β-TRCP–UBE2D~UB–substrate intermediate complex, CUL5 contained a residue that would disrupt this conformation hinting that CUL5 could potentially adopt a different conformation. Indeed the structure of CUL5 covalently modified with NEDD8 showed a different conformation utilizing the Ile36 hydrophobic patch to interact with the WHB domain instead of the Ile44 hydrophobic patch (Duda et al., 2008).

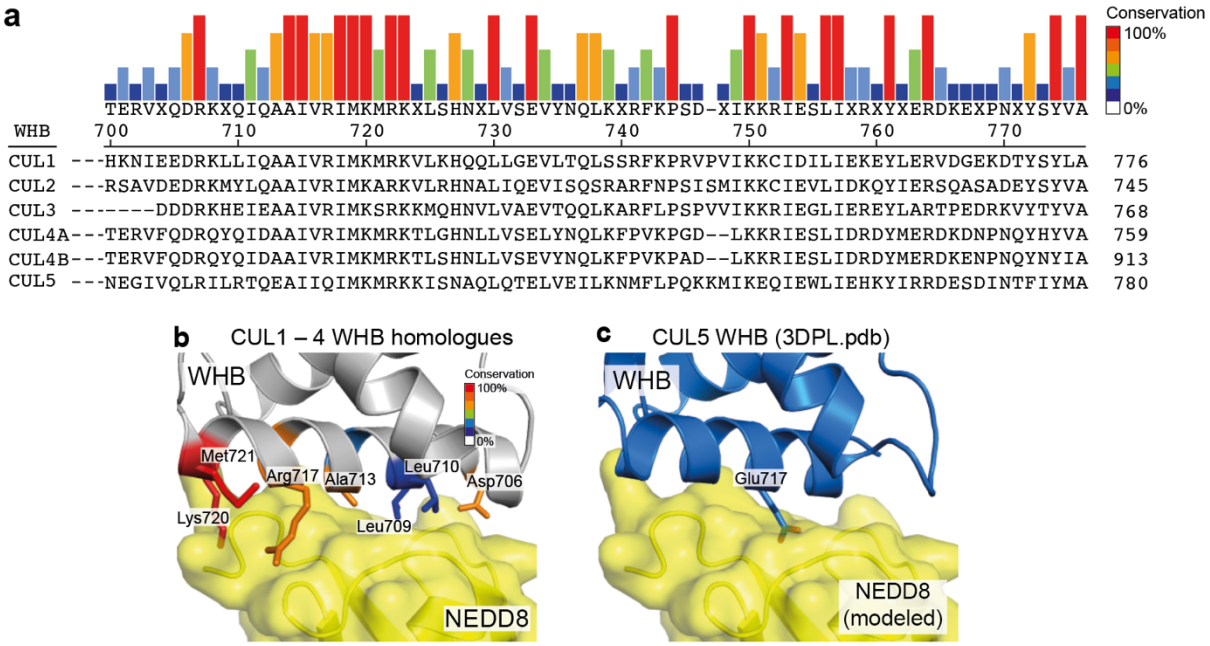

Figure 3.33: Conservation of CUL WHB domains.

a, Sequence alignment of the WHB domains of CUL1, CUL2, CUL3, CUL4A, CUL4B, and CUL5. The WHB domain shares substantial parts of the sequence throughout different cullins, while CUL5 shared the least amount of conservation. **b,** Activation module interface between NEDD8 (yellow) and its linked CUL1 WHB domain(grey). Key CUL1 residues at

the interface are shown in sticks and colored by conservation. **c,** Distinct features of CUL5, modeled by superposition of its WHB domain (blue, PDB ID 3DPL) with CUL1's bound to NEDD8. CUL5 Glu717 could potentially interfere with binding to NEDD8 in the configuration of the activation module, which hints that CUL5 could adopt a potentially different structural mechanism.

As other CRLs seem to have potential for sharing similar mechanistic principles by its sequence conservation by the WHB domain, other substrate receptors of CUL1 and a different CRL (CUL4) were tested to understand if the mechanism found in the structure representing neddylated CRL1 β-TRCP-UBE2D~UB-IκBα intermediate can be applied in a more global manner. We therefore tested another F-box protein CRL1 FBXW7 to monitor priming its substrate phosphorylated cyclin E peptide (pCyE) (**Figure 3.34**). Indeed, when using UBE2D mutants that are at essential interfaces such as the backside of UBE2D (Ser22Arg), which was a core factor mediating interactions with the activation module, or mutants that either prevent binding to RBX1 RING (Phe62Ala) or preventing ubiquitin binding to the core helix of UBE2D (Ser108Leu) all impaired UBE2D mediated priming by neddylated CRL FBXW7, while again His32Ala mutant showed a minor to no visible defect in this assay format. Moreover, when various mutants of neddylated CRL1 that disrupt the activation module (Gln40Glu), inhibit NEDD8 interaction with the backside of UBE2D, replacing NEDD8 by ubiquitin, or using unneddylated CRL all impaired priming of pCyE to various degrees. Although CRL1 FBXW7 might share similar principles in UBE2D mediated priming, it is also known that FBXW7 utilizes another ubiquitin carrying enzyme, ARIH1, to ubiquitylate its substrates (Scott et al., 2016). It is possible that the interfaces that form in the mechanism of ARIH1 mediated ubiquitylation of FBXW7 substrates might also emerge to be essential.

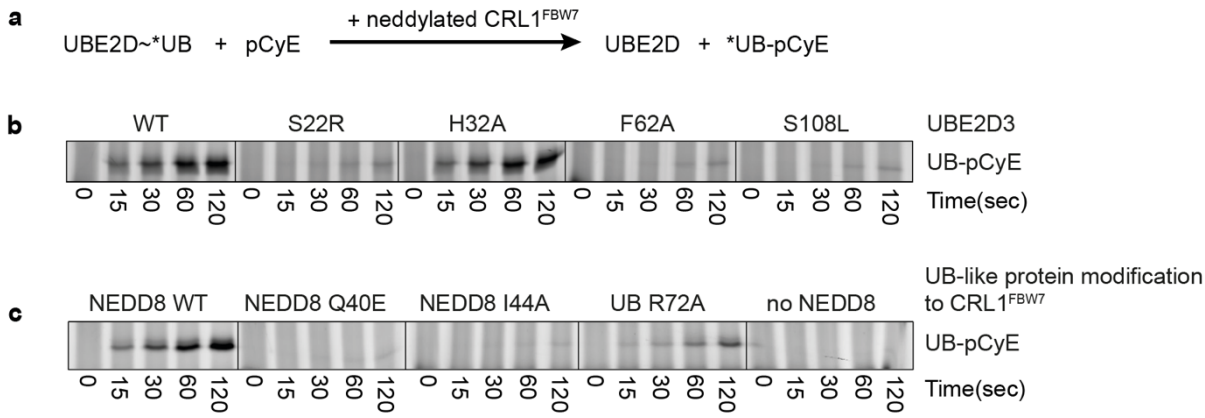

Figure 3.34: Priming by neddylated CRL1 FBXW7 and UBE2D.

a, Schematic of the pulse-chase assay for testing effects of mutations in neddylated CRL1 FBW7 with UBE2D on substrate priming. Assay monitors transfer of fluorescent ubiquitin (*UB) from UBE2D~UB thioester to peptide substrate derived from phosphorylated Cyclin E (pCyE). **b,** Fluorescence scan detecting ubiquitin transfer to the pCyE substrate by neddylated CRL1 FBXW7 with the indicated mutants of UBE2D. **c,** Fluorescence scan detecting ubiquitin transfer to the pCyE substrate by UBE2D and variants of neddylated, ubiquitylated, or unneddylated CRL1 FBXW7.

These principles were shown with similar properties when testing CRL4 CRBN mediated priming of IKZF zinc finger 2, which utilizes a FDA-approved immunomodulatory drug pomalidomide (Sievers et al., 2018a; Sievers et al., 2018b) (**Figure 3.35**). First, in the absence of the molecular glue pomalidomide, which is responsible to recruiting IKZF ZF2 to the substrate receptor CRBN, IKZF was not ubiquitylated at all. When UBE2D's backside binding was disrupted, the priming efficiency massively decreased, while His32Ala again had minor to no visible effect, in conjunction with how β-TRCP or FBXW7 mediates priming by UBE2D. Furthermore, replacing NEDD8 with ubiquitin, or NEDD8 with mutants disrupting the activation module, backside binding, or having no NEDD8 all impaired IKZF priming with varying degrees. Although the exact mechanism behind each different CRLs cannot be concluded without structural or further biochemical characterization, we can make the assumption that the interfaces seen from the structure representing neddylated CRL1 β-

TRCP-UBE2D~UB-IκBα intermediate seem to share similar importance in other CRLs as well.

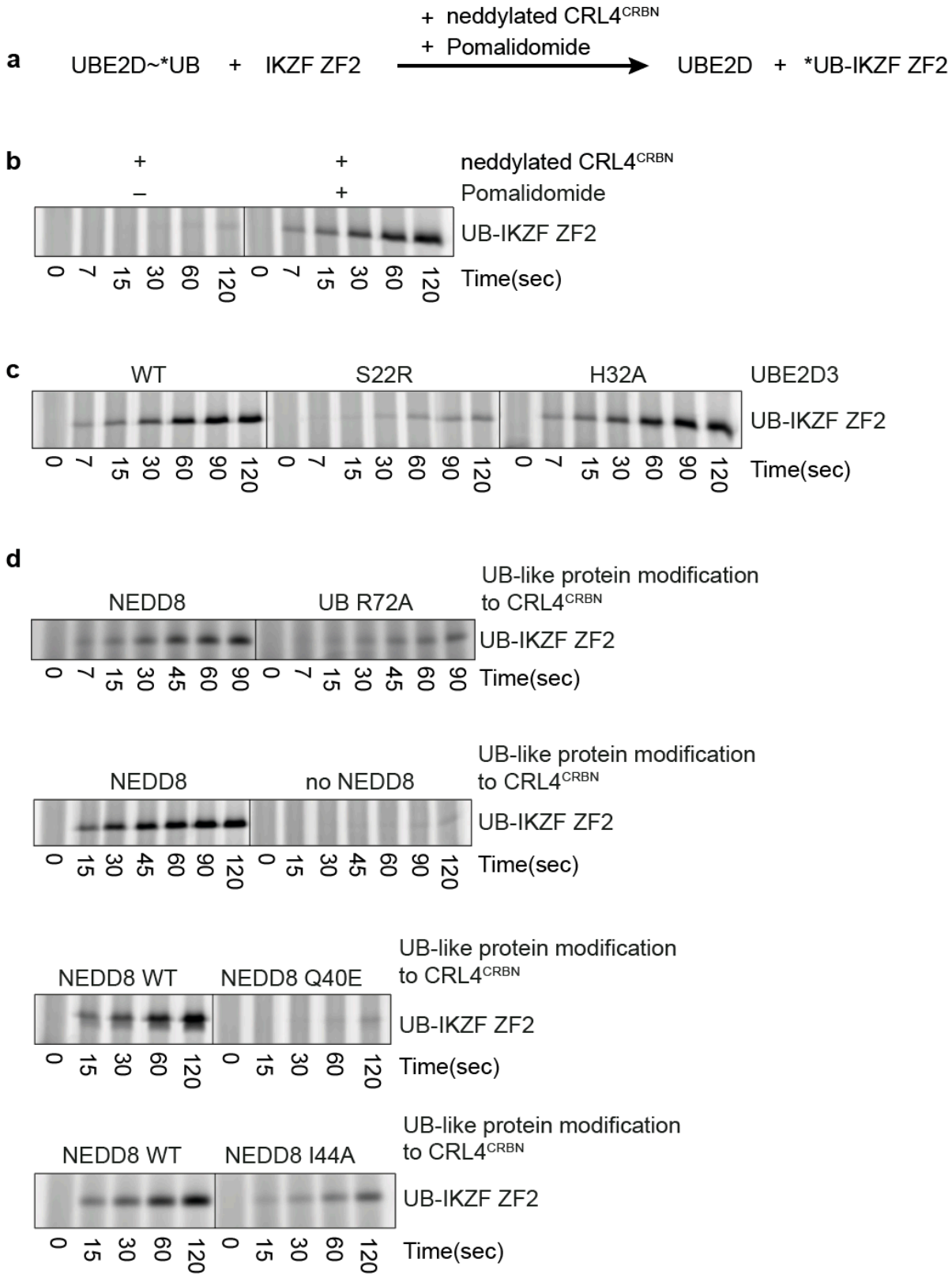
a
UBE2D~*UB + IKZF ZF2
+ neddylated CRL4CRBN
+ Pomalidomide
UBE2D + *UB-IKZF ZF2
b
neddylated CRL4CRBN
Pomalidomide
UB-IKZF ZF2
Time(sec)
0 7 15 30 60 120 0 7 15 30 60 120
c
WT
S22R
H32A
UBE2D3
UB-IKZF ZF2
Time(sec)
0 7 15 30 60 90 120 0 7 15 30 60 90 120 0 7 15 30 60 90 120
d
NEDD8
UB R72A
UB-like protein modification to CRL4CRBN
UB-IKZF ZF2
Time(sec)
0 7 15 30 45 60 90 0 7 15 30 45 60 90
NEDD8
no NEDD8
UB-like protein modification to CRL4CRBN
UB-IKZF ZF2
Time(sec)
0 15 30 45 60 90 120 0 15 30 45 60 90 120
NEDD8 WT
NEDD8 Q40E
UB-like protein modification to CRL4CRBN
UB-IKZF ZF2
Time(sec)
0 15 30 60 120 0 15 30 60 120
NEDD8 WT
NEDD8 I44A
UB-like protein modification to CRL4CRBN
UB-IKZF ZF2
Time(sec)
0 15 30 60 120 0 15 30 60 120

Figure 3.35: Priming of CRL4 CRBN substrate mediated by UBE2D.

a, Schematic of pulse-chase assay to test the effects of mutations in neddylated CRL4 CRBN or UBE2D on substrate priming. The assay monitors fluorescently labeled ubiquitin transfer from UBE2D to the IKZF1/3 ZF2 substrate in the presence of the immunomodulatory drug molecular glue pomalidomide. **b,** Fluorescence scan of assay validating the pomalidomide-dependence in ubiquitylating IKZF by CRL4 CRBN. **c,** Fluorescence scan detecting ubiquitin transfer to the IKZF substrate by CRL4 CRBN, pomalidomide and the indicated variants of UBE2D. **d,** Fluorescence scan detecting ubiquitin transfer to the IKZF substrate by UBE2D and the indicated variants of neddylated, ubiquitylated, or unneddylated CRL4 CRBN with pomalidomide.

4 Discussion

Our structural and biochemical data representing active ubiquitylation via a neddylated CRL1 β-TRCP–UBE2D~UB–substrate intermediate suggests a model for substrate priming that answers numerous longstanding mysteries. First, relative to prior structures, the new structures show conformational changes that enable NEDD8, the cullin, and the RBX1-bound UBE2D~UB intermediate to make numerous interactions to activate UBE2D and synergistically place its catalytic center adjacent to the recruited substrate by β-TRCP. This structurally observed configuration adjoining these catalytic components in proximity explains how a neddylated CRL1 β-TRCP and UBE2D can rapidly ubiquitylate its substrates. Second, perplexing biochemical features of neddylated CRL that were incompatible with prior structures are now rationally explicable, such as NEDD8-stimulated crosslinking between a CRL1 β-TRCP-bound phosphopeptide and UBE2D (Saha and Deshaies, 2008); NEDD8 binding to the backside of RBX1 RING-bound UBE2D while simultaneously connected to the CUL1 WHB domain (Duda et al., 2008; Sakata et al., 2007; Zheng et al., 2002b); and catastrophic effects on CRL mediated ubiquitylation by bacterial effector protein catalyzed deamidation of NEDD8's Gln40 (Cui et al., 2010; Jubelin et al., 2010; Morikawa et al., 2010). Third, despite the striking ~60% sequence identity between NEDD8 and ubiquitin, six residues differing between them would induce a clash with cullin residues contacting NEDD8 in the catalytic architecture, and are responsible for the majority of the defect caused by replacing NEDD8 with ubiquitin on a cullin. Thus, we can now explain the function and requirement for this distinct UB-like protein to activate CRLs, and why a ubiquitin cannot replace NEDD8, even with the striking similarity in the structure and sequence.

We speculate that this catalytic configuration is formed in a series of steps where the range of options and conformations progressively narrows down similar to a progression down a free energy funnel. In the absence of other factors, neddylated CRL1 β-TRCP regions display distinct dynamic properties. While the substrate scaffolding module robustly bridges the substrate with the C/R domain, RBX1's RING and CUL1's WHB domains with or without a linked NEDD8 are relatively dynamic, and at an extreme may be substantially waving around. These mobile entities are ultimately harnessed in the neddylated CRL1 β-TRCP–UBE2D~UB–substrate intermediate for ubiquitylation. During this process, the

requirement of the large number of protein-protein interactions and conformational changes suggest that there could be multiple options to achieve the catalytic architecture. It seems equally plausible that the UBE2D~UB intermediate would first encounter RBX1's RING domain or NEDD8, either of which would raise the effective concentration for the other interaction. Likewise, noncovalent-binding between NEDD8 and its linked WHB domain, or with UBE2D's backside, would stabilize NEDD8's Loop-out conformation favoring the other interaction as well.

Because ubiquitylation does occur with mutant substrates or enzymes, albeit at substantially lower rates, at this point we cannot exclude the possibility that UB could be transferred from RING- and NEDD8-bound UBE2D in various orientations relative to the substrate-scaffolding module. However, when the thioester bond is both in the RING-activated configuration and adjacent to substrate, as shown in the cryo-EM structure, this would accelerate the rate in which the presumably random exploration of three-dimensional space by a substrate lysine would narrow down to a productive engagement with the active site. Accordingly, blunting any singular contribution to the structurally-observed catalytic architecture increases the relative importance of other contacts – even the ones with minimal impact, when assessed in combination.

CRL1 β-TRCP and UBE2D seem to be optimized for UB priming of peptide-like substrates: consistent with the structure representing the neddylated CRL1 β-TRCP–UBE2D~UB–substrate intermediate, the rate of substrate priming is substantially greater than linkage of subsequent UBs, and structure-based mutations drastically impair priming. Meanwhile, the limited effect of the mutations on linkage of subsequent UBs raises the possibility that different forms of ubiquitylation involve alternative, presently elusive, catalytic architectures. One question for future studies is if in scenarios where formation of the NEDD8-dependent catalytic architecture is compromised, for example for substrates with too short a spacer between degron and acceptor lysine to span the distance between β-TRCP and the active site, can substrate-linked UBs bind UBE2D's backside to serve some roles normally established by NEDD8 and thereby drive processive polyubiquitylation despite low efficiency of substrate priming?

In addition to UBE2D, CRLs can employ a range of other UB-carrying enzymes – from ARIH-family RBR E3s to other E2s (Kelsall et al., 2013; Scott et al., 2016; Wu et al., 2010). Although which of these contribute to ubiquitylation of most cellular targets remains uncharacterized, where best understood, it seems different UB-carrying enzymes mediate substrate priming and UB-chain extension. As examples, CRL1 β-TRCP and CRL4 CRBN/immunomodulatory drug-dependent ubiquitylation of their IκBα and IKZF substrates are thought to employ UBE2D-family E2s for substrate priming and UBE2R-family E2s or UBE2G1, respectively, for extending K48-linked polyUB chains (Hill et al., 2019; Huttenhain et al., 2019; Lu et al., 2018; Wu et al., 2010). In contrast, some CRLs preferentially employ ARIH-family RBR E3s to mediate substrate priming in vitro (Scott et al., 2016), and to promote cellular substrate degradation (Huttenhain et al., 2019). Despite enzymological differences, CRL activation of partner UB-carrying enzymes commonly depends on neddylation (Duda et al., 2008; Lu et al., 2018; Read et al., 2000; Saha and Deshaies, 2008; Scott et al., 2016; Yamoah et al., 2008).

Moreover, besides activating ubiquitylation, some neddylated CRLs bind UBXD7, which in turn recruits the AAA-ATPase p97 to further regulate ubiquitylated substrates (Alexandru et al., 2008; den Besten et al., 2012). Although future studies will be required to determine the structural mechanisms underlying these other forms of neddylated CRL-catalyzed ubiquitylation and regulation, it seems likely that the capacity for NEDD8 and the CUL WHB and RBX1 RING domains to adopt multiple relative orientations and conformations enables partner enzymes to achieve distinct architectures specifying their particular catalytic activities, much like neddylated CRL1 β-TRCP and the thioester-linked UBE2D~UB intermediate interact through multiple surfaces to achieve the configuration specifying substrate priming. Furthermore, it seems likely that the conformational dynamics of the unneddylated CUL1 WHB and RBX1 RING domains would enable inactive CRLs to adopt the different conformations coordinating cycles of neddylation/deneddylation with CAND1-driven substrate receptor assembly and disassembly (Cavadini et al., 2016; Faull et al., 2019; Fischer et al., 2011; Goldenberg et al., 2004; Liu et al., 2018; Mosadeghi et al., 2016; Scott et al., 2014; Zheng et al., 2002b). Thus, the diverse nature of interactions and conformations determining robust and rapid substrate priming, revealed by the structure of active ubiquitylation from the neddylated CRL1 β-TRCP–UBE2D~UB–substrate intermediate, provides a mechanism by which shared elements of the cullin-RING ligase can

be transformed by different protein partners to allow interconversion between distinct CRL assemblies meeting the cellular demand for ubiquitylation.

References

Afonine, P.V., Poon, B.K., Read, R.J., Sobolev, O.V., Terwilliger, T.C., Urzhumtsev, A., and Adams, P.D. (2018). Real-space refinement in PHENIX for cryo-EM and crystallography. Acta Crystallogr D Struct Biol *74*, 531-544.

Alexandru, G., Graumann, J., Smith, G.T., Kolawa, N.J., Fang, R., and Deshaies, R.J. (2008). UBXD7 binds multiple ubiquitin ligases and implicates p97 in HIF1alpha turnover. Cell *134*, 804-816.

Bai, C., Sen, P., Hofmann, K., Ma, L., Goebl, M., Harper, J.W., and Elledge, S.J. (1996). SKP1 connects cell cycle regulators to the ubiquitin proteolysis machinery through a novel motif, the F-box. Cell *86*, 263-274.

Bekes, M., Langley, D.R., and Crews, C.M. (2022). PROTAC targeted protein degraders: the past is prologue. Nat Rev Drug Discov *21*, 181-200.

Bornstein, G., Ganoth, D., and Hershko, A. (2006). Regulation of neddylation and deneddylation of cullin1 in SCFSkp2 ubiquitin ligase by F-box protein and substrate. Proc Natl Acad Sci U S A *103*, 11515-11520.

Branigan, E., Carlos Penedo, J., and Hay, R.T. (2020). Ubiquitin transfer by a RING E3 ligase occurs from a closed E2~ubiquitin conformation. Nat Commun *11*, 2846.

Brown, N.G., VanderLinden, R., Watson, E.R., Qiao, R., Grace, C.R., Yamaguchi, M., Weissmann, F., Frye, J.J., Dube, P., Ei Cho, S.*, et al.* (2015). RING E3 mechanism for ubiquitin ligation to a disordered substrate visualized for human anaphase-promoting complex. Proc Natl Acad Sci U S A *112*, 5272-5279.

Brown, N.G., VanderLinden, R., Watson, E.R., Weissmann, F., Ordureau, A., Wu, K.P., Zhang, W., Yu, S., Mercredi, P.Y., Harrison, J.S.*, et al.* (2016). Dual RING E3 Architectures Regulate Multiubiquitination and Ubiquitin Chain Elongation by APC/C. Cell *165*, 1440-1453.

Brzovic, P.S., and Klevit, R.E. (2006). Ubiquitin transfer from the E2 perspective: why is UbcH5 so promiscuous? Cell Cycle *5*, 2867-2873.

Brzovic, P.S., Lissounov, A., Christensen, D.E., Hoyt, D.W., and Klevit, R.E. (2006). A UbcH5/ubiquitin noncovalent complex is required for processive BRCA1-directed ubiquitination. Mol Cell *21*, 873-880.

Buetow, L., Gabrielsen, M., Anthony, N.G., Dou, H., Patel, A., Aitkenhead, H., Sibbet, G.J., Smith, B.O., and Huang, D.T. (2015). Activation of a primed RING E3-E2-ubiquitin complex by non-covalent ubiquitin. Mol Cell *58*, 297-310.

Buetow, L., and Huang, D.T. (2016). Structural insights into the catalysis and regulation of E3 ubiquitin ligases. Nat Rev Mol Cell Biol *17*, 626-642.

Cappadocia, L., and Lima, C.D. (2018). Ubiquitin-like Protein Conjugation: Structures, Chemistry, and Mechanism. Chem Rev *118*, 889-918.

Cavadini, S., Fischer, E.S., Bunker, R.D., Potenza, A., Lingaraju, G.M., Goldie, K.N., Mohamed, W.I., Faty, M., Petzold, G., Beckwith, R.E*., et al.* (2016). Cullin-RING ubiquitin E3 ligase regulation by the COP9 signalosome. Nature *531*, 598-603.

Cope, G.A., Suh, G.S., Aravind, L., Schwarz, S.E., Zipursky, S.L., Koonin, E.V., and Deshaies, R.J. (2002). Role of predicted metalloprotease motif of Jab1/Csn5 in cleavage of Nedd8 from Cul1. Science *298*, 608-611.

Cui, J., Yao, Q., Li, S., Ding, X., Lu, Q., Mao, H., Liu, L., Zheng, N., Chen, S., and Shao, F. (2010). Glutamine deamidation and dysfunction of ubiquitin/NEDD8 induced by a bacterial effector family. Science *329*, 1215-1218.

den Besten, W., Verma, R., Kleiger, G., Oania, R.S., and Deshaies, R.J. (2012). NEDD8 links cullin-RING ubiquitin ligase function to the p97 pathway. Nat Struct Mol Biol *19*, 511-516, S511.

Dou, H., Buetow, L., Hock, A., Sibbet, G.J., Vousden, K.H., and Huang, D.T. (2012a). Structural basis for autoinhibition and phosphorylation-dependent activation of c-Cbl. Nat Struct Mol Biol *19*, 184-192.

Dou, H., Buetow, L., Sibbet, G.J., Cameron, K., and Huang, D.T. (2012b). BIRC7-E2 ubiquitin conjugate structure reveals the mechanism of ubiquitin transfer by a RING dimer. Nat Struct Mol Biol *19*, 876-883.

Dou, H., Buetow, L., Sibbet, G.J., Cameron, K., and Huang, D.T. (2013). Essentiality of a non-RING element in priming donor ubiquitin for catalysis by a monomeric E3. Nat Struct Mol Biol *20*, 982-986.

Duda, D.M., Borg, L.A., Scott, D.C., Hunt, H.W., Hammel, M., and Schulman, B.A. (2008). Structural insights into NEDD8 activation of cullin-RING ligases: conformational control of conjugation. Cell *134*, 995-1006.

Duda, D.M., Olszewski, J.L., Tron, A.E., Hammel, M., Lambert, L.J., Waddell, M.B., Mittag, T., DeCaprio, J.A., and Schulman, B.A. (2012). Structure of a glomulin-RBX1-CUL1

complex: inhibition of a RING E3 ligase through masking of its E2-binding surface. Mol Cell *47*, 371-382.

Emsley, P., Lohkamp, B., Scott, W.G., and Cowtan, K. (2010). Features and development of Coot. Acta Crystallogr D Biol Crystallogr *66*, 486-501.

Enchev, R.I., Scott, D.C., da Fonseca, P.C., Schreiber, A., Monda, J.K., Schulman, B.A., Peter, M., and Morris, E.P. (2012). Structural basis for a reciprocal regulation between SCF and CSN. Cell Rep *2*, 616-627.

Faull, S.V., Lau, A.M.C., Martens, C., Ahdash, Z., Hansen, K., Yebenes, H., Schmidt, C., Beuron, F., Cronin, N.B., Morris, E.P.*, et al.* (2019). Structural basis of Cullin 2 RING E3 ligase regulation by the COP9 signalosome. Nat Commun *10*, 3814.

Fischer, E.S., Scrima, A., Bohm, K., Matsumoto, S., Lingaraju, G.M., Faty, M., Yasuda, T., Cavadini, S., Wakasugi, M., Hanaoka, F.*, et al.* (2011). The molecular basis of CRL4DDB2/CSA ubiquitin ligase architecture, targeting, and activation. Cell *147*, 1024-1039.

Frescas, D., and Pagano, M. (2008). Deregulated proteolysis by the F-box proteins SKP2 and beta-TrCP: tipping the scales of cancer. Nat Rev Cancer *8*, 438-449.

Goldenberg, S.J., Cascio, T.C., Shumway, S.D., Garbutt, K.C., Liu, J., Xiong, Y., and Zheng, N. (2004). Structure of the Cand1-Cul1-Roc1 complex reveals regulatory mechanisms for the assembly of the multisubunit cullin-dependent ubiquitin ligases. Cell *119*, 517-528.

Hao, B., Oehlmann, S., Sowa, M.E., Harper, J.W., and Pavletich, N.P. (2007). Structure of a Fbw7-Skp1-cyclin E complex: multisite-phosphorylated substrate recognition by SCF ubiquitin ligases. Mol Cell *26*, 131-143.

Hart, M., Concordet, J.P., Lassot, I., Albert, I., del los Santos, R., Durand, H., Perret, C., Rubinfeld, B., Margottin, F., Benarous, R.*, et al.* (1999). The F-box protein beta-TrCP associates with phosphorylated beta-catenin and regulates its activity in the cell. Curr Biol *9*, 207-210.

Hill, S., Reichermeier, K., Scott, D.C., Samentar, L., Coulombe-Huntington, J., Izzi, L., Tang, X., Ibarra, R., Bertomeu, T., Moradian, A.*, et al.* (2019). Robust cullin-RING ligase function is established by a multiplicity of poly-ubiquitylation pathways. Elife *8*.

Hohn, M., Tang, G., Goodyear, G., Baldwin, P.R., Huang, Z., Penczek, P.A., Yang, C., Glaeser, R.M., Adams, P.D., and Ludtke, S.J. (2007). SPARX, a new environment for Cryo-EM image processing. J Struct Biol *157*, 47-55.

Hospenthal, M.K., Freund, S.M., and Komander, D. (2013). Assembly, analysis and architecture of atypical ubiquitin chains. Nat Struct Mol Biol *20*, 555-565.

Huttenhain, R., Xu, J., Burton, L.A., Gordon, D.E., Hultquist, J.F., Johnson, J.R., Satkamp, L., Hiatt, J., Rhee, D.Y., Baek, K.*, et al.* (2019). ARIH2 Is a Vif-Dependent Regulator of CUL5-Mediated APOBEC3G Degradation in HIV Infection. Cell Host Microbe *26*, 86-99 e87.

Jiang, J., and Struhl, G. (1998). Regulation of the Hedgehog and Wingless signalling pathways by the F-box/WD40-repeat protein Slimb. Nature *391*, 493-496.

Jin, J., Cardozo, T., Lovering, R.C., Elledge, S.J., Pagano, M., and Harper, J.W. (2004). Systematic analysis and nomenclature of mammalian F-box proteins. Genes Dev *18*, 2573-2580.

Jubelin, G., Taieb, F., Duda, D.M., Hsu, Y., Samba-Louaka, A., Nobe, R., Penary, M., Watrin, C., Nougayrede, J.P., Schulman, B.A.*, et al.* (2010). Pathogenic bacteria target NEDD8-conjugated cullins to hijack host-cell signaling pathways. PLoS Pathog *6*, e1001128.

Kamadurai, H.B., Qiu, Y., Deng, A., Harrison, J.S., Macdonald, C., Actis, M., Rodrigues, P., Miller, D.J., Souphron, J., Lewis, S.M.*, et al.* (2013). Mechanism of ubiquitin ligation and lysine prioritization by a HECT E3. Elife *2*, e00828.

Kamadurai, H.B., Souphron, J., Scott, D.C., Duda, D.M., Miller, D.J., Stringer, D., Piper, R.C., and Schulman, B.A. (2009). Insights into ubiquitin transfer cascades from a structure of a UbcH5B approximately ubiquitin-HECT(NEDD4L) complex. Mol Cell *36*, 1095-1102.

Kastner, B., Fischer, N., Golas, M.M., Sander, B., Dube, P., Boehringer, D., Hartmuth, K., Deckert, J., Hauer, F., Wolf, E.*, et al.* (2008). GraFix: sample preparation for single-particle electron cryomicroscopy. Nat Methods *5*, 53-55.

Kawakami, T., Chiba, T., Suzuki, T., Iwai, K., Yamanaka, K., Minato, N., Suzuki, H., Shimbara, N., Hidaka, Y., Osaka, F.*, et al.* (2001). NEDD8 recruits E2-ubiquitin to SCF E3 ligase. EMBO J *20*, 4003-4012.

Kelsall, I.R., Duda, D.M., Olszewski, J.L., Hofmann, K., Knebel, A., Langevin, F., Wood, N., Wightman, M., Schulman, B.A., and Alpi, A.F. (2013). TRIAD1 and HHARI bind to and are activated by distinct neddylated Cullin-RING ligase complexes. EMBO J *32*, 2848-2860.

Kirkin, V., and Dikic, I. (2007). Role of ubiquitin- and Ubl-binding proteins in cell signaling. Curr Opin Cell Biol *19*, 199-205.

Kleiger, G., Saha, A., Lewis, S., Kuhlman, B., and Deshaies, R.J. (2009). Rapid E2-E3 assembly and disassembly enable processive ubiquitylation of cullin-RING ubiquitin ligase substrates. Cell *139*, 957-968.

Kung, W.W., Ramachandran, S., Makukhin, N., Bruno, E., and Ciulli, A. (2019). Structural insights into substrate recognition by the SOCS2 E3 ubiquitin ligase. Nat Commun *10*, 2534.

Latres, E., Chiaur, D.S., and Pagano, M. (1999). The human F box protein beta-Trcp associates with the Cul1/Skp1 complex and regulates the stability of beta-catenin. Oncogene *18*, 849-854.

Lee, J., and Zhou, P. (2007). DCAFs, the missing link of the CUL4-DDB1 ubiquitin ligase. Mol Cell *26*, 775-780.

Liu, J., Furukawa, M., Matsumoto, T., and Xiong, Y. (2002). NEDD8 modification of CUL1 dissociates p120(CAND1), an inhibitor of CUL1-SKP1 binding and SCF ligases. Mol Cell *10*, 1511-1518.

Liu, X., Reitsma, J.M., Mamrosh, J.L., Zhang, Y., Straube, R., and Deshaies, R.J. (2018). Cand1-Mediated Adaptive Exchange Mechanism Enables Variation in F-Box Protein Expression. Mol Cell *69*, 773-786 e776.

Low, T.Y., Peng, M., Magliozzi, R., Mohammed, S., Guardavaccaro, D., and Heck, A.J. (2014). A systems-wide screen identifies substrates of the SCFbetaTrCP ubiquitin ligase. Sci Signal *7*, rs8.

Lu, G., Weng, S., Matyskiela, M., Zheng, X., Fang, W., Wood, S., Surka, C., Mizukoshi, R., Lu, C.C., Mendy, D.*, et al.* (2018). UBE2G1 governs the destruction of cereblon neomorphic substrates. Elife *7*.

Lumb, K.J., and Kim, P.S. (1995). A buried polar interaction imparts structural uniqueness in a designed heterodimeric coiled coil. Biochemistry *34*, 8642-8648.

Lyapina, S., Cope, G., Shevchenko, A., Serino, G., Tsuge, T., Zhou, C., Wolf, D.A., Wei, N., Shevchenko, A., and Deshaies, R.J. (2001). Promotion of NEDD-CUL1 conjugate cleavage by COP9 signalosome. Science *292*, 1382-1385.

Lydeard, J.R., Schulman, B.A., and Harper, J.W. (2013). Building and remodelling Cullin-RING E3 ubiquitin ligases. EMBO Rep *14*, 1050-1061.

Mabbitt, P.D., Loreto, A., Dery, M.A., Fletcher, A.J., Stanley, M., Pao, K.C., Wood, N.T., Coleman, M.P., and Virdee, S. (2020). Structural basis for RING-Cys-Relay E3 ligase activity and its role in axon integrity. Nat Chem Biol *16*, 1227-1236.

Margottin, F., Bour, S.P., Durand, H., Selig, L., Benichou, S., Richard, V., Thomas, D., Strebel, K., and Benarous, R. (1998). A novel human WD protein, h-beta TrCp, that interacts with HIV-1 Vpu connects CD4 to the ER degradation pathway through an F-box motif. Mol Cell *1*, 565-574.

Martinez-Zapien, D., Ruiz, F.X., Poirson, J., Mitschler, A., Ramirez, J., Forster, A., Cousido-Siah, A., Masson, M., Vande Pol, S., Podjarny, A.*, et al.* (2016). Structure of the E6/E6AP/p53 complex required for HPV-mediated degradation of p53. Nature *529*, 541-545.

McGinty, R.K., Henrici, R.C., and Tan, S. (2014). Crystal structure of the PRC1 ubiquitylation module bound to the nucleosome. Nature *514*, 591-596.

Monda, J.K., Scott, D.C., Miller, D.J., Lydeard, J., King, D., Harper, J.W., Bennett, E.J., and Schulman, B.A. (2013). Structural conservation of distinctive N-terminal acetylation-dependent interactions across a family of mammalian NEDD8 ligation enzymes. Structure *21*, 42-53.

Morikawa, H., Kim, M., Mimuro, H., Punginelli, C., Koyama, T., Nagai, S., Miyawaki, A., Iwai, K., and Sasakawa, C. (2010). The bacterial effector Cif interferes with SCF ubiquitin ligase function by inhibiting deneddylation of Cullin1. Biochem Biophys Res Commun *401*, 268-274.

Mosadeghi, R., Reichermeier, K.M., Winkler, M., Schreiber, A., Reitsma, J.M., Zhang, Y., Stengel, F., Cao, J., Kim, M., Sweredoski, M.J.*, et al.* (2016). Structural and kinetic analysis of the COP9-Signalosome activation and the cullin-RING ubiquitin ligase deneddylation cycle. Elife *5*.

Orian, A., Gonen, H., Bercovich, B., Fajerman, I., Eytan, E., Israel, A., Mercurio, F., Iwai, K., Schwartz, A.L., and Ciechanover, A. (2000). SCF(beta)(-TrCP) ubiquitin ligase-mediated processing of NF-kappaB p105 requires phosphorylation of its C-terminus by IkappaB kinase. EMBO J *19*, 2580-2591.

Ozkan, E., Yu, H., and Deisenhofer, J. (2005). Mechanistic insight into the allosteric activation of a ubiquitin-conjugating enzyme by RING-type ubiquitin ligases. Proc Natl Acad Sci U S A *102*, 18890-18895.

Palovcak, E., Wang, F., Zheng, S.Q., Yu, Z., Li, S., Betegon, M., Bulkley, D., Agard, D.A., and Cheng, Y. (2018). A simple and robust procedure for preparing graphene-oxide cryo-EM grids. J Struct Biol *204*, 80-84.

Pettersen, E.F., Goddard, T.D., Huang, C.C., Couch, G.S., Greenblatt, D.M., Meng, E.C., and Ferrin, T.E. (2004). UCSF Chimera--a visualization system for exploratory research and analysis. J Comput Chem *25*, 1605-1612.

Pierce, N.W., Lee, J.E., Liu, X., Sweredoski, M.J., Graham, R.L., Larimore, E.A., Rome, M., Zheng, N., Clurman, B.E., Hess, S.*, et al.* (2013). Cand1 promotes assembly of new SCF complexes through dynamic exchange of F box proteins. Cell *153*, 206-215.

Plechanovova, A., Jaffray, E.G., Tatham, M.H., Naismith, J.H., and Hay, R.T. (2012). Structure of a RING E3 ligase and ubiquitin-loaded E2 primed for catalysis. Nature *489*, 115-120.

Pruneda, J.N., Littlefield, P.J., Soss, S.E., Nordquist, K.A., Chazin, W.J., Brzovic, P.S., and Klevit, R.E. (2012). Structure of an E3:E2~Ub complex reveals an allosteric mechanism shared among RING/U-box ligases. Mol Cell *47*, 933-942.

Read, M.A., Brownell, J.E., Gladysheva, T.B., Hottelet, M., Parent, L.A., Coggins, M.B., Pierce, J.W., Podust, V.N., Luo, R.S., Chau, V.*, et al.* (2000). Nedd8 modification of cul-1 activates SCF(beta(TrCP))-dependent ubiquitination of IkappaBalpha. Mol Cell Biol *20*, 2326-2333.

Reichermeier, K.M., Straube, R., Reitsma, J.M., Sweredoski, M.J., Rose, C.M., Moradian, A., den Besten, W., Hinkle, T., Verschueren, E., Petzold, G.*, et al.* (2020). PIKES Analysis Reveals Response to Degraders and Key Regulatory Mechanisms of the CRL4 Network. Mol Cell *77*, 1092-1106 e1099.

Reitsma, J.M., Liu, X., Reichermeier, K.M., Moradian, A., Sweredoski, M.J., Hess, S., and Deshaies, R.J. (2017). Composition and Regulation of the Cellular Repertoire of SCF Ubiquitin Ligases. Cell *171*, 1326-1339 e1314.

Reverter, D., and Lima, C.D. (2005). Insights into E3 ligase activity revealed by a SUMO-RanGAP1-Ubc9-Nup358 complex. Nature *435*, 687-692.

Rusnac, D.V., Lin, H.C., Canzani, D., Tien, K.X., Hinds, T.R., Tsue, A.F., Bush, M.F., Yen, H.S., and Zheng, N. (2018). Recognition of the Diglycine C-End Degron by CRL2(KLHDC2) Ubiquitin Ligase. Mol Cell *72*, 813-822 e814.

Saha, A., and Deshaies, R.J. (2008). Multimodal activation of the ubiquitin ligase SCF by Nedd8 conjugation. Mol Cell *32*, 21-31.

Saha, A., Lewis, S., Kleiger, G., Kuhlman, B., and Deshaies, R.J. (2011). Essential role for ubiquitin-ubiquitin-conjugating enzyme interaction in ubiquitin discharge from Cdc34 to substrate. Mol Cell *42*, 75-83.

Sakata, E., Yamaguchi, Y., Miyauchi, Y., Iwai, K., Chiba, T., Saeki, Y., Matsuda, N., Tanaka, K., and Kato, K. (2007). Direct interactions between NEDD8 and ubiquitin E2 conjugating enzymes upregulate cullin-based E3 ligase activity. Nat Struct Mol Biol *14*, 167-168.

Schulman, B.A., Carrano, A.C., Jeffrey, P.D., Bowen, Z., Kinnucan, E.R., Finnin, M.S., Elledge, S.J., Harper, J.W., Pagano, M., and Pavletich, N.P. (2000). Insights into SCF ubiquitin ligases from the structure of the Skp1-Skp2 complex. Nature *408*, 381-386.

Scott, D.C., Monda, J.K., Bennett, E.J., Harper, J.W., and Schulman, B.A. (2011). N-terminal acetylation acts as an avidity enhancer within an interconnected multiprotein complex. Science *334*, 674-678.

Scott, D.C., Monda, J.K., Grace, C.R., Duda, D.M., Kriwacki, R.W., Kurz, T., and Schulman, B.A. (2010). A dual E3 mechanism for Rub1 ligation to Cdc53. Mol Cell *39*, 784-796.

Scott, D.C., Rhee, D.Y., Duda, D.M., Kelsall, I.R., Olszewski, J.L., Paulo, J.A., de Jong, A., Ovaa, H., Alpi, A.F., Harper, J.W.*, et al.* (2016). Two Distinct Types of E3 Ligases Work in Unison to Regulate Substrate Ubiquitylation. Cell *166*, 1198-1214 e1124.

Scott, D.C., Sviderskiy, V.O., Monda, J.K., Lydeard, J.R., Cho, S.E., Harper, J.W., and Schulman, B.A. (2014). Structure of a RING E3 trapped in action reveals ligation mechanism for the ubiquitin-like protein NEDD8. Cell *157*, 1671-1684.

Sievers, Q.L., Gasser, J.A., Cowley, G.S., Fischer, E.S., and Ebert, B.L. (2018a). Genome-wide screen identifies cullin-RING ligase machinery required for lenalidomide-dependent CRL4(CRBN) activity. Blood *132*, 1293-1303.

Sievers, Q.L., Petzold, G., Bunker, R.D., Renneville, A., Slabicki, M., Liddicoat, B.J., Abdulrahman, W., Mikkelsen, T., Ebert, B.L., and Thoma, N.H. (2018b). Defining the human C2H2 zinc finger degrome targeted by thalidomide analogs through CRBN. Science *362*.

Skowyra, D., Craig, K.L., Tyers, M., Elledge, S.J., and Harper, J.W. (1997). F-box proteins are receptors that recruit phosphorylated substrates to the SCF ubiquitin-ligase complex. Cell *91*, 209-219.

Soucy, T.A., Smith, P.G., Milhollen, M.A., Berger, A.J., Gavin, J.M., Adhikari, S., Brownell, J.E., Burke, K.E., Cardin, D.P., Critchley, S.*, et al.* (2009). An inhibitor of NEDD8-activating enzyme as a new approach to treat cancer. Nature *458*, 732-736.

Spencer, E., Jiang, J., and Chen, Z.J. (1999). Signal-induced ubiquitination of IkappaBalpha by the F-box protein Slimb/beta-TrCP. Genes Dev *13*, 284-294.

Stanley, D.J., Bartholomeeusen, K., Crosby, D.C., Kim, D.Y., Kwon, E., Yen, L., Cartozo, N.C., Li, M., Jager, S., Mason-Herr, J.*, et al.* (2012). Inhibition of a NEDD8 Cascade Restores Restriction of HIV by APOBEC3G. PLoS Pathog *8*, e1003085.

Streich, F.C., Jr., and Lima, C.D. (2016). Capturing a substrate in an activated RING E3/E2-SUMO complex. Nature *536*, 304-308.

Swatek, K.N., and Komander, D. (2016). Ubiquitin modifications. Cell Res *26*, 399-422.

Tang, X., Orlicky, S., Lin, Z., Willems, A., Neculai, D., Ceccarelli, D., Mercurio, F., Shilton, B.H., Sicheri, F., and Tyers, M. (2007). Suprafacial orientation of the SCFCdc4 dimer accommodates multiple geometries for substrate ubiquitination. Cell *129*, 1165-1176.

Weissmann, F., Petzold, G., VanderLinden, R., Huis In 't Veld, P.J., Brown, N.G., Lampert, F., Westermann, S., Stark, H., Schulman, B.A., and Peters, J.M. (2016). biGBac enables rapid gene assembly for the expression of large multisubunit protein complexes. Proc Natl Acad Sci U S A *113*, E2564-2569.

Willems, A.R., Schwab, M., and Tyers, M. (2004). A hitchhiker's guide to the cullin ubiquitin ligases: SCF and its kin. Biochim Biophys Acta *1695*, 133-170.

Winston, J.T., Koepp, D.M., Zhu, C., Elledge, S.J., and Harper, J.W. (1999a). A family of mammalian F-box proteins. Curr Biol *9*, 1180-1182.

Winston, J.T., Strack, P., Beer-Romero, P., Chu, C.Y., Elledge, S.J., and Harper, J.W. (1999b). The SCFbeta-TRCP-ubiquitin ligase complex associates specifically with phosphorylated destruction motifs in IkappaBalpha and beta-catenin and stimulates IkappaBalpha ubiquitination in vitro. Genes Dev *13*, 270-283.

Wright, J.D., Mace, P.D., and Day, C.L. (2016). Secondary ubiquitin-RING docking enhances Arkadia and Ark2C E3 ligase activity. Nat Struct Mol Biol *23*, 45-52.

Wu, G., Xu, G., Schulman, B.A., Jeffrey, P.D., Harper, J.W., and Pavletich, N.P. (2003). Structure of a beta-TrCP1-Skp1-beta-catenin complex: destruction motif binding and lysine specificity of the SCF(beta-TrCP1) ubiquitin ligase. Mol Cell *11*, 1445-1456.

Wu, K., Kovacev, J., and Pan, Z.Q. (2010). Priming and extending: a UbcH5/Cdc34 E2 handoff mechanism for polyubiquitination on a SCF substrate. Mol Cell *37*, 784-796.

Wu, S., Zhu, W., Nhan, T., Toth, J.I., Petroski, M.D., and Wolf, D.A. (2013). CAND1 controls in vivo dynamics of the cullin 1-RING ubiquitin ligase repertoire. Nat Commun *4*, 1642.

Yamoah, K., Oashi, T., Sarikas, A., Gazdoiu, S., Osman, R., and Pan, Z.Q. (2008). Autoinhibitory regulation of SCF-mediated ubiquitination by human cullin 1's C-terminal tail. Proc Natl Acad Sci U S A *105*, 12230-12235.

Yaron, A., Hatzubai, A., Davis, M., Lavon, I., Amit, S., Manning, A.M., Andersen, J.S., Mann, M., Mercurio, F., and Ben-Neriah, Y. (1998). Identification of the receptor component of the IkappaBalpha-ubiquitin ligase. Nature *396*, 590-594.

Yau, R., and Rape, M. (2016). The increasing complexity of the ubiquitin code. Nat Cell Biol *18*, 579-586.

Yu, C., Mao, H., Novitsky, E.J., Tang, X., Rychnovsky, S.D., Zheng, N., and Huang, L. (2015). Gln40 deamidation blocks structural reconfiguration and activation of SCF ubiquitin ligase complex by Nedd8. Nat Commun *6*, 10053.

Yunus, A.A., and Lima, C.D. (2006). Lysine activation and functional analysis of E2-mediated conjugation in the SUMO pathway. Nat Struct Mol Biol *13*, 491-499.

Zemla, A., Thomas, Y., Kedziora, S., Knebel, A., Wood, N.T., Rabut, G., and Kurz, T. (2013). CSN- and CAND1-dependent remodelling of the budding yeast SCF complex. Nat Commun *4*, 1641.

Zheng, J., Yang, X., Harrell, J.M., Ryzhikov, S., Shim, E.H., Lykke-Andersen, K., Wei, N., Sun, H., Kobayashi, R., and Zhang, H. (2002a). CAND1 binds to unneddylated CUL1 and regulates the formation of SCF ubiquitin E3 ligase complex. Mol Cell *10*, 1519-1526.

Zheng, N., Schulman, B.A., Song, L., Miller, J.J., Jeffrey, P.D., Wang, P., Chu, C., Koepp, D.M., Elledge, S.J., Pagano, M.*, et al.* (2002b). Structure of the Cul1-Rbx1-Skp1-F boxSkp2 SCF ubiquitin ligase complex. Nature *416*, 703-709.

Zivanov, J., Nakane, T., Forsberg, B.O., Kimanius, D., Hagen, W.J., Lindahl, E., and Scheres, S.H. (2018). New tools for automated high-resolution cryo-EM structure determination in RELION-3. Elife *7*.

Acknowledgements

There are not enough words to explain all the gratitude to which I owe throughout this journey. First, I would really like to thank Brenda for taking chance and giving me the opportunity to explore, learn, and develop during the past many years. Her unparalleled enthusiasm and dedication towards science has really dramatically changed how I think and approach problems that seem unsolvable and find joy in tackling these mysteries that just seemed impossible. The advice and guidance taught me to be thorough and resilient both as a scientist and as a person. Also the opportunity to experience science in different continents of the world, establishing a brand new laboratory, learning new cutting-edge technologies and also learning how to guide other people are all going to be extremely valuable groundwork for me to grow as a scientist. I will be forever grateful to all the joyful memories, the scientific development, and the opportunities I was given during the times in the Schulman lab.

The current Schulman lab exists because there was an older Schulman lab, and I would like to acknowledge our former foundation. People I have met in Memphis were truly exceptional with rigor and passion. David Miller was my first mentor who was always welcoming and helping me adapt to the new environment, teaching me all fundamental skills that I try to spread to the new members as well, on top of his endeavors making the Schulman lab run smoothly. K.P. would always be my discussion and dinner buddy in lab, sharing stories and ideas on experiments, teaching me how to approach science on a daily basis. Randy my bench buddy could listen to all my stupid ideas and could tell me if it is good or bad. We also had lots of fun moving to Germany together with David Krist, who really inspired me to always think about adjoining chemical tools to structural and biochemical experiments. Danny has been and will be my scientific goal as an experimentalist who inspires me to always try to do top quality science. Dave Duda, together with Jenny and David Y who generously shared ideas, reagents, protocols all the time, Masaya, being a force of nature doing everything with perfection, Jeremy the cloning master, Peter, good times playing tennis and grilling together, Ryan for introducing me to the world of electron microscopy, Qiu and Yumei for all the motivation and hard work, Nick for all the discussions and advice, Brian for the awesome music, Shanshan, Shein, Michael, and Sheila for always

being so kind and helpful, being able to overlap with all these amazing people was a true honor.

Of course the future of the Schulman lab are in the hands of new inspiration here in Munich. None of my science would have been possible without Sepp, the true hero making all things happen in the lab. Rajan, the mastermind behind all our computational science, and my discussion partner on any theoretical approach, guiding me on every aspect of data processing. Dawa, Kirby, and Bastian are incredible colleagues and friends who gave me the encouragement, motivation, discussions, and help every day. I get to discuss every day with Lukas sharing lab space since mid-COVID, learning new things and again testing my stupid ideas all the time, thank you for putting up with that. The cullin-RING ligase team Danny, Gary, Lukas, Linus, Sebastian, Daniel, Asia, Jiale, Ishi, Frank, with support from Maren, Lisa, and Susanne are just absolutely incredible, they force me to be a better scientist every day. Gary is the best cullin-RING ligase kineticist in my world. The GID team, the membrane team, and the autophagy team continue provide new perspective making the lab atmosphere new and diverse.

I would like to give special thanks to our past and present core facility managers, Daniel, Tillman, Mike, and Stephan. Especially Daniel and Tillman, you guys are literally the best EM managers in the world, who are so kind and generous and willing to help and teach. Thank you for making everything so easy and accessible.

Lastly, I would like to thank my parents, who constantly support me at every stage of my life unconditionally whatever decision I make. They have always been and will continue being my inspiration to pursuing a scientific career. Thank you so much.